HOKKAIDO UNIVERSITY

Title	Effects of Maternal Undernutrition on DNA Methylation, Gene Expression, and Metabolites of Fetal Thymus and Growth in Wagyu (Japanese Black) Cattle
Author(s)	PHOMVISITH, Ouanh
Degree Grantor	北海道大学
Degree Name	博士(環境科学)
Dissertation Number	甲第16187号
Issue Date	2024-12-25
DOI	https://doi.org/10.14943/doctoral.k16187
Doc URL	https://hdl.handle.net/2115/97351
Type	doctoral thesis
File Information	PHOMVISITH_Ouanh.pdf

Hokkaido University Collection of Scholarly and Academic Papers : HUSCAP

Effects of Maternal Undernutrition on DNA Methylation, Gene Expression, and Metabolites of Fetal Thymus and Growth in Wagyu (Japanese Black) Cattle

(和牛（黒毛和牛）における母牛の低栄養が胎仔胸腺の DNA メチル化、遺伝子発現、代謝産物および成長に及ぼす影響に関する研究)

Graduate School of Environmental Science, Hokkaido University

Ouanh Phomvisith

2024

Table of Contents

Titles **Page No.**

Table of Contents ..... **i**

List of Abbreviations ..... **iv**

List of Tables ..... **vii**

List of Figures ..... **ix**

Chapter 1 ..... **1**

General introduction **1**

1.1. Global issues in livestock agriculture 1

1.2. Metabolic programming in postnatal growth and beef production concept 2

1.3. Fetal development 3

1.4. Somatotropic axis 6

1.5. Immune system 8

1.6. Interaction of the somatotropic axis and immune system 15

1.7. Epigenetic modification 16

1.8. General objectives 17

Chapter 2 ..... **18**

Effects of nutrient restriction during late gestation on the physiology of cows and their offspring, and subsequent growth in neonatal calves **18**

2.1. Effects of nutritional status on hormone concentrations of the somatotropin axis and metabolites in plasma and colostrum of Japanese Black cows 18

2.1.1. Introduction 18

2.1.2. Materials and Methods 19

2.1.3. Results 25

2.1.4. Discussion 34

2.1.5. Summary 37

2.2. Effects of fetal and neonatal programming on physiological parameters and growth performance of Japanese Black calves 38

2.2.1. Introduction 38

2.2.2. Materials and Methods 39

2.2.3. Results 42

2.2.4. Discussion 49

2.2.5. Summary 52

Chapter 3 53

Effects of maternal nutrient restriction on histological structure and immunochemical properties of the Wagyu fetal thymus 53

3.1. Introduction 53

3.2. Materials and Methods 54

3.3. Results 60

3.4. Discussion 70

3.5. Summary 73

Chapter 4 74

Maternal nutrient restriction affects DNA methylation and gene expression associated with metabolism and immunopoiesis in the Wagyu fetal thymus 74

4.1. Maternal nutrient restriction influences DNA methylation linked to cellular function stability in the Wagyu fetal thymus 74

4.1.1. Introduction 74

4.1.2. Materials and Methods 75

4.1.3. Results 78

4.1.4. Discussion 86

4.1.5. Summary 89

4.2. Maternal nutrient restriction alters gene expression in thymic metabolism, stress response, and cellular defense linked to immune function 91

4.2.1. Introduction 91

4.2.2. Materials and Methods 92

4.2.3. Results 97

4.2.4. Discussion 111

4.2.5. Summary 115

Chapter 5 116

General discussion 116

Acknowledgment 131

References cited 133

List of Abbreviations

ADG: average daily weight gain

ADP: Adenosine diphosphate

ATP: adenosine triphosphate

B cell: bursa-derived cells

BCR: B cell receptor

BW: body weight

BWT: birth weight

cAMP: cyclic adenosine monophosphate

CD205: cluster of differentiation 205 or Lymphocyte antigen 75 (LY75)

CD4: cluster of differentiation 4

CD8: cluster of differentiation 8

CE-FTMS: capillary electrophoresis-Fourier transform mass spectrometry

cGMP: cyclic guanosine monophosphate

CLP: common lymphoid progenitors

CMJ: corticomedullary junction

CV: coefficient of variation

CXCL: C-X-C motif chemokine ligands

d: day

DAPI: 4′,6-diamidino-2-phenylindole

DC: dendritic cells

dl: deciliter

DM: dry matter

DN: double-negative

DNA: Deoxyribonucleic acid

DOHaD: developmental origins of health and disease

ETP: early T-cell progenitors

FADH: Flavin adenine dinucleotide hydride

FcgRIIb2: Fc fragment of IgG receptor IIb

FcRn: neonatal fragment crystallizable (Fc) receptor

FITC: Fluorescein isothiocyanate

FOXN1: Forkhead box protein N1

FOXP3: forkhead box P3

g/dl: gram per deciliter

g: gram

GH: growth hormone

GHR: growth hormone receptor

GHR-1A: growth hormone receptor family 1A

GHRH: growth hormone-releasing hormone

HC: Hassall's corpuscles

HMT: Human Metabolome Technologies

HPA: hypothalamic-pituitary-adrenal

HSC: hematopoietic stem cells

IFI16: interferon gamma inducible protein 16

IgA: immunoglobulin A

IGF-1: insulin-like growth factor 1

IGFR: insulin-like growth factor receptor

IgG: immunoglobulin G

IgM: immunoglobulin M

IL: interleukins

ILC: innate lymphoid cells

KEGG: Kyoto Encyclopedia of Genes and Genomes

kg/d: kilogram per day

kg: kilogram

KIU: Kallikrein Inhibitor Unit

m: month

mEq/l*:* milliequivalents per liter

mg: milligram

MHC: major histocompatibility complex

MJ/kg: megajoules per kilogram

ml: milliliter

mm^2: square millimeter

MPP: multipotent progenitors

NADH: Nicotinamide adenine dinucleotide

NEFA: non-esterified fatty acids

ng/ml: nanogram per milliliter

NK: natural killers

OXPHOS: Oxidative phosphorylation

PBS: Phosphate-buffered saline

pH: Potential of Hydrogen

PKG: protein kinase G

PPI: protein-protein interaction

Ras: Rat sarcoma virus

RNA: Ribonucleic acid

ROS: reactive oxygen species

rpm: revolutions per minute

rRNA: ribosomal RNA

SCF: stem cell factor

SS: somatostatin

TCR: T cell receptor

TEC: thymic epithelial cells

TG: triglyceride

Th: helper T cells

TNF: tumor necrosis factor

Treg: regulatory T cells

TSLP: thymic stromal lymphopoietin

v/v: volume per volume

w/v: weight per volume

WGBS: whole-genome bisulfite sequencing

Wnt: Wingless-related integration site

α: alpha

β: beta

δ: delta

γ: gamma

μm: micrometer

μm^2: square micrometer

List of Tables

Tables **Page No.**

Table 1. Dietary components (% on a fresh matter basis) and nutrient composition 22

Table 2. Total nutrient intake of late antepartum cows during nutritional treatments after 195-day gestation to calving 28

Table 3. Ingredient and nutrient composition of calves' diets 41

Table 4. Body weight, total milk consumption, and growth rate of Japanese Black calves 44

Table 5. Changes in body weight and body frame size of calves 46

Table 6. Comparison of overall hormone secretion and metabolite concentrations in Japanese Black calves from birth to five months of age 48

Table 7. Dietary compositions fed to the pregnant Wagyu cows during nutrient treatment period 58

Table 8. Effect of low maternal on the phenotype of the fetal thymus 62

Table 9. A comparative analysis of the areas of Hassall's corpuscles and the medulla in the fetal thymus between the CON and LOW groups 65

Table 10. Comparative analysis of the nucleus, and $CD4^+$ and $CD8^+$ T cells in the bovine fetal thymus between the CON and LOW groups 68

Table 11. DNA methylation mapping efficiency of the fetal thymus of two groups 79

Table 12. Number of differentially methylated regions for each genomic region in LOW fetal thymus 80

Table 13. Top significant pathways out of the top 20 KEGG pathways, extracted from hypo- and hypermethylated genes in the promoter, gene body, and/or UTRs 84

Table 14. Hypo- and hypermethylated genes associated with thymus growth, immunity, and protein, cholesterol, and mitochondrial metabolism 85

Table 15. Primer pairs used for quantitative PCR analysis 94

Table 16. Top significant differences ($q < 0.10$) in KEGG pathways, obtained from up- and downregulated genes in LOW and CON fetal thymuses 101

Table 17. List of genes that were both differentially methylated genes (DMGs) and differentially expressed genes (DEGs) 105

Table 18. Top 20 changed metabolites in fetal thymus between the LOW and CON group 108

Table 19. Metabolic pathways demonstrating the most significant differences in the thymuses of the LOW and CON fetuses 110

List of Figures

Figures **Page No.**

Figure 1. A functional scheme of the immune system 9

Figure 2. Time span of experimental and gestation periods 21

Figure 3. Proportional change in body weight during nutritional treatment in late pregnancy and postpartum (PP) period 27

Figure 4. Effects of nutritional treatment on concentrations of hormones 29

Figure 5. Average values of the areas under the secretory curve (AUC) for hormones 30

Figure 6. Effects of nutritional treatment on the concentrations of metabolites 32

Figure 7. Average values of the areas under the secretory curve (AUC) for metabolites 33

Figure 8. Body growth of calves born to cows given one of two diets during late pregnancy until parturition 45

Figure 9. Overall secretion of somatotropic hormones in calves born to cows given one of two diets during late pregnancy until parturition 47

Figure 10. H&E staining provides an overview of the representative histological structure for the CON and LOW groups 63

Figure 11. H&E staining depicts the representative thymic medullary histology for the CON and LOW groups 64

Figure 12. Representative images of immunofluorescent staining for $CD4^+$ T cells and thymic nuclei 66

Figure 13. Representative images of immunofluorescent staining for $CD8^+$ T cells and thymic nuclei 67

Figure 14. Comparison of $CD4^+$ and $CD8^+$ T cells in the bovine fetal thymus between the CON and LOW groups 69
Figure 15. The pattern of DNA methylation in the Wagyu fetal thymus 81
Figure 16. Scatter plot of KEGG pathway enrichment, depicting the top 20 significant pathways associated with DMRs 83
Figure 17. Gene expression profile of the Wagyu fetal thymus 100
Figure 18. Expression of six target immune-related genes 102
Figure 19. Results of the functional enrichment analysis on the protein-protein interaction (PPI) networks for six target genes 103
Figure 20. Diagram illustrating the KEGG pathway terms related to primary immuno-deficiency associated with the six target genes 104
Figure 21. Sankey plot, illustrating the connections of overlapping genes identified using RNA-seq and DNA methylation analysis with the leading KEGG pathways 106
Figure 22. Heatmap of the hierarchical clustering of the top 50 metabolites 109
Figure 23. Theoretical framework comprising the pathways associated with the DMGs and DEGs associated with molecular function networks and metabolism in the thymuses of LOW fetuses 126

Chapter 1

General introduction

1.1. Global issues in livestock agriculture

Livestock production has been essential throughout history, providing meat, milk, and eggs valued for their nutrition. It also contributes to society by supplying fertilizer, labor, and materials, such as hides and bones, and by playing roles in education, entertainment, and spirituality (Hollmann et al., 2008). With increasing economic development, escalating incomes, and burgeoning urbanization across numerous countries, populations are empowered to broaden their dietary horizons, incorporating a greater proportion of meat and dairy products (Cockx et al., 2018). Recently, the livestock sector has faced challenges in feed, water, breeding, sustainability, and meeting global demand. Addressing these issues requires a multifaceted, evidence-based strategy, including genetic improvements and advanced technologies, such as genome sequencing, breeding, and precision nutrition to enhance productivity (Thornton, 2010). Moreover, environmental concerns regarding the sustainability of livestock husbandry persist, as livestock activities contribute significantly to global greenhouse gas emissions and land utilization (Mitra et al., 2019). In recent decades, various production techniques have emerged to increase productivity and economic benefits for livestock farmers, such as grazing ruminants, silvopastoral systems, and using food by-products for ruminants. Nevertheless, these approaches appear insufficient to meet the demand for high-quality beef among contemporary consumers (Akbar and Jahiruddin, 2010).

1.2. Metabolic programming in postnatal growth and beef production concept

The environmental conditions to which organisms are exposed, especially nutritional changes during critical developmental periods, can significantly alter organogenesis and physiology, affecting lifelong health. This phenomenon was first identified by Dr. David Barker in the late 1980s, which is referred to as the Developmental Origins of Health and Disease (DOHaD) paradigm (Fall and Osmond, 2013). The biological processes by which the organism is affected in this way are commonly referred to as "metabolic imprinting/programming" (de Almeida Brasiel and Luquetti, 2020). The fetal stage is recognized as a pivotal period for organ and tissue development in mammals, with disruptions during this time potentially leading to enduring anatomical, physiological, and metabolic changes. Research indicates that maternal undernutrition followed by high nutrient intake during the neonatal period is correlated with postnatal growth catch-up in sheep (Ford et al., 2007), and Hereford cattle (Tudor and O'rourke, 1980). Similarly, neonatal programming, which involves early weaning and high-nutrition diets, has been demonstrated to enhance feed efficiency, promote postnatal growth, and improve beef quality in comparison to conventional feeding practices in beef cattle (Scheffler et al., 2014; Reddy et al., 2017). In Japanese Black Wagyu, neonatal metabolic programming has been shown to be associated with improved beef quality and alterations in metabolic hormone secretion (Khounsaknalath et al., 2021).

Wagyu cattle are esteemed for their unique capacity to produce highly marbled beef within conventional production systems. However, the Japanese Wagyu industry faces a significant challenge owing to its reliance on imported feed (Gotoh et al., 2018). A novel investigative paradigm, predicated on the concept of "metabolic programming," has been developed to enhance feed conversion efficiency and mitigate reliance on intensive

agricultural practices in the production of high-quality beef from Japanese Black cattle. This approach offers promising avenues for advancing beef production (Gotoh, 2014). Nonetheless, changes in maternal nutrition during pregnancy can have profound implications for fetal development, particularly affecting immune-related processes. Maternal nutrient restriction (MNR) triggers a cascade of biological responses, collectively known as fetal programming, which can induce long-lasting changes in the offspring's physiology and immune system (Duttaroy, 2023). This phenomenon often leads to anomalies in immune function, as the developing fetal thymus undergoes significant alterations in epigenetic modifications, including DNA methylation, gene expression, and cellular metabolism (Heppolette et al., 2016). These changes compromise the immune system's ability to respond effectively to infections, such as diarrhea and pneumonia, which account for the majority of neonatal calf mortality (Abuelo, 2020). Understanding the cellular and molecular mechanisms underlying the epigenetic regulation of growth trajectories, metabolic homeostasis, and immunological function at an early stage is crucial for the effective application of metabolic programming strategies in animal husbandry, particularly in beef cattle production.

1.3. Fetal development

The development of organs, metabolic physiology, endocrine and immune systems, and thermoregulatory mechanisms in bovine pregnancy depends on the generative processes that take place during the intrauterine period. This period can be divided into three stages: zygote formation, trophectodermal adhesion to the endometrium, and fetal phase (Valadão et al., 2018). The duration of gestation varies across cattle breeds, although it averages approximately 283 days (Casas et al., 2012).

The period of oocyte fertilization encompasses a complex series of events beginning with spermatozoon–oocyte interaction and culminating in the amalgamation of maternal and paternal chromosomes during the metaphase of the embryo's first mitotic division (Østrup et al., 2011). After fertilization in the oviduct, the zygote within the zona pellucida divides into blastomeres. Early development relies on proteins and RNAs from the oocyte and sperm. Once the genome is activated, the zygote becomes a morula. During compaction, outer morula cells form the trophectoderm, and inner cells form the inner cell mass, resulting in a blastocyst. In bovines, blastocyst initiation usually occurs shortly after uterine entry, around 4 days post-ovulation. Subsequently, the blastocyst hatches from the zona pellucida on days 8 to 9, exposing the trophectoderm's outer surface directly to the uterine milieu (Imakawa et al., 2016). The critical phase of maternal recognition of pregnancy spans days 15–18 post-ovulation, followed by early placentation. Placental attachment occurs at caruncles on the uterine wall, which are nodular glandular proliferations. Placental membranes attach to these sites via chorionic villi, forming cotyledons (Vonnahme et al., 2018). The development of a functional fetal/placental vascular system is crucial early in gestation. Caruncular vascularization begins around day 90, with day 120 being vital for increasing nutrient transfer to support the growing fetus (Ford, 1995). Establishing the vascular network in the second trimester is critical for supporting the rapid growth, as over 75% of fetal weight gain occurs in the last trimester, highlighting the importance of maternal nutrition during this period in bovines (Fandiño et al., 2019).

Fetal organogenesis

In bovine fetuses, organogenesis and placental development occur together. Cardiac activity is detectable by days 21–22 post-ovulation. Limb formation starts around day 25, followed by the development of organs such as the pancreas, liver, adrenals, lungs, thyroid,

spleen, brain, thymus, and kidneys. Testicular differentiation in male calves begins around day 45, while ovarian development follows shortly thereafter, typically around days 50–60 of gestation (Vonnahme et al., 2007).

The thymus, essential for the lymphoid and immune systems, facilitates T-lymphocyte differentiation and selection through its intricate architecture. Situated above the heart and posterior to the sternum, the bilobed thymus originates from the endoderm of the pharyngeal pouch within a mesenchymal milieu, in conjunction with the development of the parathyroid glands. During embryonic and early fetal stages, stem cells from the para-aortic splanchnopleura, yolk sac, and liver generate lymphomyeloid precursors (Figueiredo et al., 2020). The liver is the primary site of fetal hematopoiesis, while after the fifth gestational week, precursors migrate to the bone marrow to establish lymphomyeloid activity. The thymus begins to emerge from the third pharyngeal pouch endoderm around the same time (Tortora and Derrickson, 2018). Thymic epithelial cells (TECs) start secreting hormones at 5–6 weeks, followed by colonization by T-cell precursors from 7 to 14 weeks, a crucial phase for thymic growth. Mid-pregnancy, when the thymus peaks in size relative to body weight, is pivotal for thymic education. In the thymic education, $CD4^+$ and $CD8^+$ thymocytes undergo selection, making this phase both critically important and vulnerable to disruption (Tabilas et al., 2023).

Fetal physiology and metabolism

The physiology of the fetus is different from that of the neonate in terms of its structure and function. In many animal species, the umbilical circulation is essential for providing necessary substances from the placenta and maternal environment to the fetal body. This circulation serves two main purposes: 1) supporting fetal oxidative metabolism and 2) supplying materials for tissue development (Battaglia and Meschia, 1978). Throughout

intrauterine development, the placenta acts as an interface for the exchange of nutrients, gases, and waste products, while also synthesizing and releasing hormones, growth factors, cytokines, and other essential bioactive molecules (Morton and Brodsky, 2016). The shift from intrauterine to extrauterine life triggers significant metabolic changes, regulated by the mature endocrine system at birth but continuing to evolve postnatally. During the peripartum period, key biomarkers such as stress hormones, glucoregulatory factors, thermogenic agents, and growth-regulatory hormones undergo significant changes, facilitating the neonate's adaptation to extrauterine life (Danijela, 2015). Fetal development depends heavily on nutrient supply through the placenta, affected by maternal nutrition and metabolism. Inadequate energy intake during pregnancy can alter fetal growth. Growth hormone (GH) directs nutrient distribution through various physiological means. In dams, GH can enhance fetal growth by directing nutrients towards it. Studies on polytocous pigs revealed that early-pregnancy treatment with porcine somatotropin (pST) enhances maternal insulin-like growth factor 1 (IGF-1) secretion and boosts placental and fetal weights (Rehfeldt et al., 2001). Similarly, administration of bovine GH to pregnant ewes from day 35 to 80 of gestation has been shown to enhance maternal GH, IGF-1, and insulin secretion, elevating fetal growth (Wallace et al., 2004).

1.4. Somatotropic axis

The somatotropic axis comprises the hypothalamus, anterior pituitary gland, liver, and peripheral tissues such as adipose, muscle, and bone. Its hormones and binding proteins interact with growth-regulating hormones such as thyroid hormones, glucocorticoids, leptin, testosterone, estrogen, insulin, and locally produced growth factors under normal conditions (Breier, 1999). The pituitary gland releases GH, controlled by two hypothalamic hormones:

growth hormone-releasing hormone (GHRH), which stimulates GH secretion; and somatostatin (SS), which inhibits it. GH primarily exerts its effects through IGF-1 (Mogi et al., 2004). IGF-1, a polypeptide hormone mainly synthesized in the liver and peripheral tissues, functions via endocrine, autocrine, or paracrine pathways. It provides negative feedback to the hypothalamus and pituitary, inhibiting GH synthesis. The interactions between insulin and the GH/IGF-1 axis play complex roles in regulating glucose levels, metabolism, and growth dynamics (Mohammed et al., 2022). GH raises blood glucose, while IGF-1 supports insulin secretion and sensitivity. GH prompts IGF-1 production, which in turn can lower GH levels through negative feedback. Balancing insulin and GH is crucial owing to their opposing effects on glucose homeostasis; GH increases blood glucose, whereas insulin aids glucose uptake and storage (Nijenhuis-Noort et al., 2024). Primarily, GH and IGF-1 stimulate skeletal and tissue growth, while also exerting complex metabolic effects and playing essential roles in the immune system (Mejia-Naranjo et al., 2003). Basically, the somatotropic axis exhibits substantial modifications during bovine gestation, characterized by elevated GH secretion and concomitant reductions in IGF-I levels. These endocrine adaptations, in conjunction with heightened nutritional demands, function synergistically to facilitate fetal development and maintain maternal homeostasis. Perturbations in maternal nutrition can induce dysregulation of the somatotropic axis and alter insulin function. Such metabolic disruptions may contribute to adipose tissue dysfunction and immunomodulation, with potential insulin resistance and obesity later in the life of the offspring (Muscogiuri et al., 2019).

1.5. Immune system

The immune system is a complex cellular network that protects the body from infections and other harmful factors. It consists of three layers of defense: physical barriers (skin, linings of gastrointestinal and respiratory tracts), biochemical mechanisms (secretions, mucus, gastric acid), and immune responses (activation of immune cells like granulocytes, T cells, and B cells) (Abul Abbas et al., 2021). Simplistically, the immune system consists of two interdependent lines of defense: innate immunity and adaptive immunity. Innate immunity is the first line of defense against pathogens and is activated quickly by the body. However, it does not have immunologic memory (Turvey and Broide, 2010). In contrast, adaptive immunity is specific to antigens and has a time delay before the maximum immune response is reached. One key feature of adaptive immunity is its ability to remember antigens, which allows a more rapid and effective response upon subsequent encounters (Figure 1). Innate and adaptive immunities work together and deficiencies in either system can lead to increased susceptibility or inappropriate responses (Murphy and Weaver, 2016).

Innate immunity

The primary mechanism of innate immunity involves the recruitment of immune cells to infected sites and the initiation of inflammation through the secretion of cytokines and chemokines. Cytokine production during innate immunity coordinates defense mechanisms and activates local cellular responses to infection or injury. Several cell types participate in the innate immune response, including macrophages, neutrophils, dendritic cells (DCs), mast cells, basophils, eosinophils, natural killer (NK) cells, and innate lymphoid cells (Marshall et al., 2018).

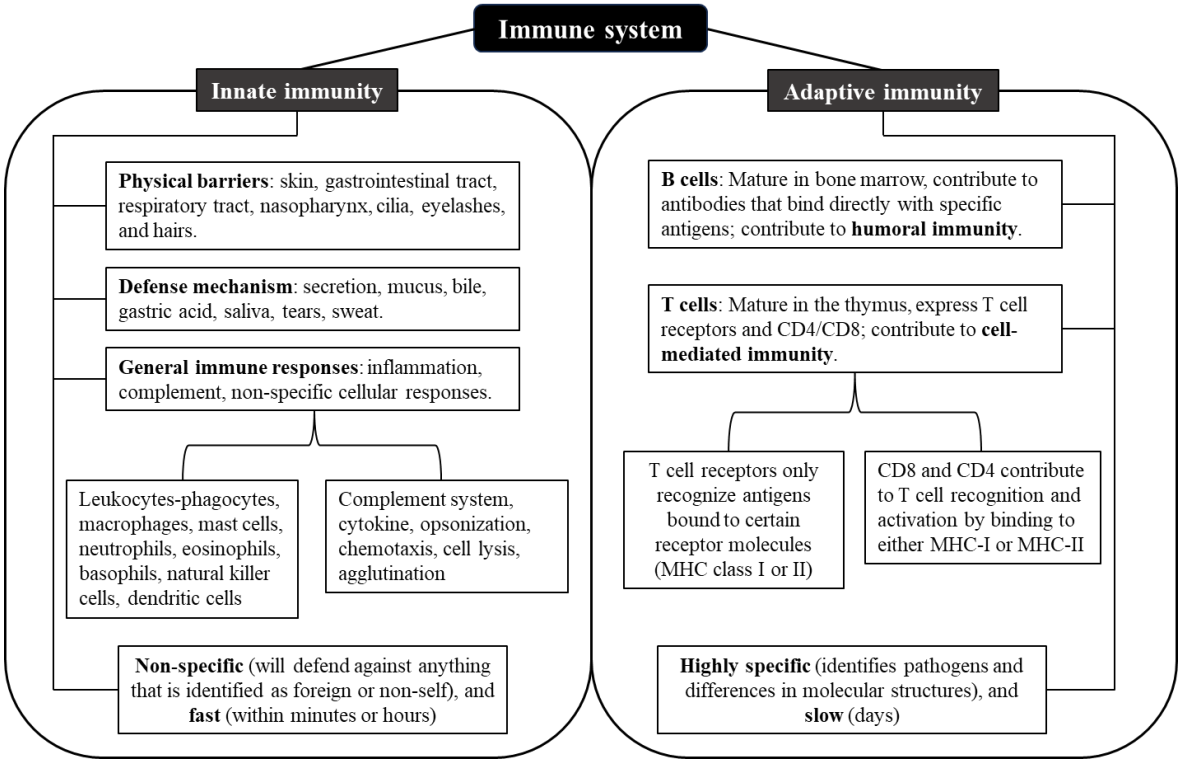

Figure 1. A functional scheme of the immune system. The immune system includes innate and adaptive immunity. Innate immunity acts as the primary defense against infections by promptly engaging physical barriers and other fundamental mechanisms upon detecting foreign agents. Subsequently, adaptive immunity is mobilized, involving the orchestrated actions of B and T cells through humoral and cell-mediated immune responses, although with a delayed onset. Humoral immunity and cell-mediated immunity are two complementary branches of the adaptive immune system, each playing distinct roles in defending the body against pathogens. Humoral immunity deals with pathogens in the body's fluids ("humor" means fluid), mainly through antibodies, while cell-mediated immunity deals with infected cells or cells that have become abnormal. Humoral immunity is most effective against extracellular pathogens, while cell-mediated immunity is crucial for defense against intracellular pathogens.

Myeloid cells form the core of innate immunity, including resident macrophages and dendritic cells, as well as circulating monocytes and granulocytes (neutrophils, basophils, and eosinophils), which can swiftly migrate to infection sites (Medina, 2016). The primary functional mechanism of myeloid cells is phagocytosis, which results in pathogen destruction and is crucial for activating adaptive immunity. Functionally, after pathogen uptake, phagocytic cells can process pathogen antigens, migrate to lymphoid organs, and present antigenic peptides to lymphocytes, thus serving as antigen-presenting cells (Manna et al., 2022). Myeloid cells can release chemokines to draw other cells to infection sites, produce cytokines to boost the functions of immune cells locally, and generate reactive oxygen species (ROS) and antimicrobial peptides (Valdivia-Silva et al., 2015). The NK cells, a major lymphocyte subset, derive from lymphoid progenitors and resemble T cells in gene expression but lack antigen-specific receptors; they are thus classified as innate lymphoid cells (ILCs). Key early inflammatory cytokines in bacterial infection include tumor necrosis factor (TNF), interleukin 1 (IL-1), and interleukin 6 (IL-6), which are crucial for initiating cell recruitment and local inflammation to clear pathogens (Janeway Jr, 1997).

Adaptive immunity

Adaptive immunity encompasses two primary branches: T and B lymphocytes. B lymphocytes express the B-cell receptor (BCR), an immunoglobulin receptor capable of binding soluble antigens, and their principal function is antibody production (Cano and Lopera, 2013). Meanwhile, T lymphocytes express the T-cell receptor (TCR), recognizing antigens presented by other cells via the major histocompatibility complex (MHC). They have two effector functions: CD8 T cells (T cytotoxic cells) directly eliminate infected or aberrant cells, whereas CD4 T cells (T helper cells) activate other cells through cytokine production or direct interactions (Shah et al., 2021). The Th cells are categorized by their

function and cytokine secretion. Th1 cells produce interferon γ, activating macrophages and cytotoxic T cells; Th2 cells secrete IL-4, IL-5, or IL-10, promoting the generation of eosinophils and B cells; and Th17 cells produce IL-17, mainly playing pro-inflammatory roles (Hirahara and Nakayama, 2016). Another important subtype of CD4 T cells is the regulatory T (Treg) cells. The FOXN1 transcription factor is essential for the development of thymic regulatory T cells (tTregs). Its expression in thymic epithelial cells (TECs) creates a microenvironment conducive to Treg differentiation and is critical for the proper selection of $CD4^+$ and $CD8^+$ T cells in the thymus (Romano et al., 2013).

Both T and B cells rely on receptor checkpoints that regulate subsequent cell development, and they share similar signaling molecules for proliferation and survival. B- and T-cell precursors originate from hematopoietic stem cells (HSCs) in the bone marrow. HSCs possess self-renewal capacity and give rise to all hematopoietic lineages. To commit to the lymphocyte lineage, HSCs initially differentiate into multipotent progenitors (MPPs) with limited self-renewal ability. MPPs subsequently differentiate into common lymphoid progenitors (CLPs), from which both B and T cells originate. B cells undergo their development, termed B lymphopoiesis, in the bone marrow, whereas T cells undergo it in the thymus, via a process known as thymopoiesis (Rolink et al., 2006).

Thymopoiesis within the thymus

The thymus serves as a unique organ capable of facilitating the dynamics of T-cell differentiation and fostering the predominant repertoire of the immune system. Within the thymus, two types of T lymphocytes are generated: those bearing αβ and γδ TCR. However, γδ cells constitute only a minor fraction of the cells developed within the thymus (Mirzaei et al., 2016). Progenitor cells originating from bone marrow migrate into the thymic cortex, where they are termed early thymic progenitors (ETPs). Within the cortical region, distinct

differentiation stages of thymocytes can be discerned on the basis of the expression of the surface markers CD4 and CD8 (Ciofani and Zúñiga-Pflücker, 2007). The earliest subpopulation, comprising approximately 5% of total thymocytes, is referred to as double-negative (DN) cells owing to their lack of CD4 and CD8 expression. DN1 thymocytes progress to the DN2 stage (referred to as pro-T cells) upon the acquisition of regulatory CD4 expression, marked by significant proliferation (Oh et al., 2023). DN2 precursors retain NK cell and dendritic cell (DC) potential. The transition to the first strictly T-lineage-committed stage occurs at the DN3 (early pre-T cells) stage, marked by the loss of CD44 expression. Subsequently, DN4 cells, termed pre-mature T cells, emerge following the downregulation of CD25 (Rothenberg et al., 2008). TCR gene rearrangement is initiated at the DN2 and DN3 stages, leading to the expression of a pre-TCR consisting of a CD3 complex associated with a rearranged β chain and a pre-α chain. The presence of a pre-TCR is a prerequisite signal for survival and progression to the double-positive (DP) stage. DP cells express both CD4 and CD8 molecules on their surface and represent the major subset of thymic T cells, accounting for approximately 80% of the total (Ellmeier et al., 2013). Upon interaction with stromal cells expressing MHC class II or class I, signaling through the mature TCR induces lineage restriction, generating $CD4^+$ or $CD8^+$ single-positive (SP) cells, respectively (Dervović et al., 2013). Thymocytes that fail to receive survival signals and encounter peptide-loaded self-MHC molecules through their TCR undergo a default death pathway termed “death by neglect,” which is a fate suffered by approximately 90% of thymic cells (Szondy et al., 2012). Within the SP population, comprising approximately 15% of total thymocytes, $CD8^+$ cytotoxic and $CD4^+$ helper T cells are found (Lutes et al., 2021). Finally, the most mature subset of thymocytes subsequently migrates to the medulla, where they undergo a brief maturation period before being released into the peripheral lymphoid pool (Ciofani and Zúñiga-Pflücker, 2007). Thymopoiesis in the bovine fetal thymus begins after

thymus formation at approximately 4 weeks of gestation, with lymphoid progenitors beginning to colonize the thymus by days 35–40. T-cell precursors migrate to the fetal thymus, and by around day 60 of gestation, mature naïve and memory αβ T cells are detectable in the fetal spleen and lymph nodes (Knapek et al., 2020).

Fetal immune system

The placenta serves two key evolutionary functions across animal species. First, it facilitates nutrient exchange through the chorioallantoic placenta, consisting of an epithelial barrier and fetal blood vessels. Second, trophoblast cells interact closely with the uterus, which produces histotroph containing vital growth factors, nutrients, and immune cell regulators to support blood flow and nutrient delivery to the fetus (Cross et al., 2003). During intrauterine development, the placenta transports oxygen, nutrients, and waste and synthesizes hormones, growth factors, cytokines, and other bioactive molecules. Syncytiotrophoblast cells contain the Brambell receptor or FcRn, which binds to IgG subclasses with different affinities (Leach et al., 1996). Maternal IgG binds to FcRn in the syncytiotrophoblast, then transfers to the cytotrophoblast. This layer degrades over the course of the pregnancy, enhancing antibody transfer and increasing fetal IgG levels with gestational age. An endothelial organelle with FcgRIIb2 aids IgG transport across the placental endothelium to the fetus (Takizawa et al., 2005).

Early fetal immune development occurs without antigen exposure, while later stages depend on it. As the fetus develops, both non-immune and immune defense mechanisms mature. Adaptive immunity relies on antigen recognition by antibodies or lymphocytes, whereas innate immunity does not. Both mechanisms can function independently but often work together for better protection (Barrington and Parish, 2001). Bovine fetal serum shows bactericidal activity by 75 days gestation and hemolytic complement activity by around 90

days (Osburn et al., 1982). Non-immune defenses include enzymatic activities, gastric acid, epithelial fatty acids, and post-birth colonization by normal flora. The complement system and phagocytic cells (neutrophils and macrophages) also derive from these stem cells. However, they may offer limited protection in early fetal life as they remain in their original sites until around 130 days gestation when they enter the bloodstream (Banks and McGuire, 1989).

During the first trimester of gestation, T and B lymphocytes transition from primary lymphoid organs to populate lymph nodes, spleen, and mucosal lymphoid tissues, independently of antigen exposure (Barrington and Parish, 2001). Fetal exposure to foreign antigens determines whether an immune reaction occurs, based on fetal development and antigen type. For example, a bovine fetus at 120 days gestation can produce antibodies against parainfluenza 3 virus, but not against any other viruses or bacteria (Banks and McGuire, 1989). By 190 days gestation, the fetus can produce antibodies against bovine viral diarrhea virus, and at birth, against *Brucella abortus*. As gestation progresses, exposure to more antigens triggers immune responses. At birth, calves can respond to various antigens, although not as many as in adulthood (Barrington and Parish, 2001). Neonates can acquire immune elements such as immunoglobulins, immune cells, and various cytokines from the dam through colostrum consumption via the mammary gland (Wells and Osborne, 1921). Maternal antibody concentrations in infants markedly decline by 3 months of age, primarily owing to hemodilution, with antibodies being fully catabolized by approximately 6 months of age (Palmer, 2011).

1.6. Interaction of the somatotropic axis and immune system

The somatotropic axis, particularly GH and IGF-1, plays a pivotal role in thymus development and physiology, which are crucial for T-cell maturation (Puche and Castilla-Cortázar, 2012). Moreover, GH, IGF-1, and their lineages have been found to confer protective effects against infections, boosting immune responses such as macrophage bactericidal activity and dampening inflammation (Reis et al., 2023). The initial observation of a direct correlation between the endocrine gland and lymphoid organ was demonstrated through hypophysectomy in rats, which induced thymus involution (Smith, 1930). Subsequent studies revealed that GH treatment in Snell–Bagg mice could prevent thymo-dependent immunodeficiency (Baroni et al., 1971). Hormones and neuropeptides modulate interactions within the thymic microenvironment, influencing cytokine production and thymic endocrine activity, thereby regulating intra-thymic T-cell proliferation, apoptosis, and differentiation (Borghetti et al., 2009). Various hormones such as cortisol, GH, prolactin, thyroid hormones, and neuropeptides can modulate thymic hormone secretion via TEC, potentially acting on TEC-specific receptors. While both TEC and thymocytes can secrete various neuroendocrine hormones (Mocchegiani et al., 2006), thymic hormones also regulate the production of hypothalamus/pituitary hormones and neuropeptides. Thymic nude mice exhibit low levels of GH and lineage hormones demonstrate an in vitro stimulatory effect on perfused rat pituitaries, enhancing GH (Savino and Dardenne, 2000). During antigen-mediated activation, $CD4^+$ and $CD8^+$ lymphocytes can also produce hormones such as GH (Mocchegiani et al., 2006). GH or IGF-1 treatment has also been reported to enhance the thymic output of naïve T cells in mice (Smaniotto et al., 2005).

1.7. Epigenetic modification

Epigenetic modifications, particularly DNA methylation, play a crucial role in the regulation of gene expression and tissue metabolism. DNA methylation, the addition of a methyl group to the cytosine residues of DNA, is a key epigenetic mechanism that can alter gene activity without changing the underlying DNA sequence (Moen et al., 2015). The patterns of DNA methylation are dynamic and responsive to environmental cues, allowing the adaptation of gene expression profiles in response to environmental stress factors, including nutritional intake status (Moore et al., 2013). This process is pivotal in modulating the expression of genes, thereby influencing cellular differentiation, development, and metabolic functions of tissues. The interplay between epigenetic modifications and metabolic pathways is intricate and bidirectional. Metabolic states can influence the epigenetic landscape, while epigenetic modifications can, in turn, affect metabolic processes. For instance, the availability of metabolic intermediates such as S-adenosylmethionine (SAM), a key methyl donor for DNA methylation, can modulate the degree of DNA methylation. Furthermore, alterations in mitochondrial function and energy production can impact the epigenetic regulation of genes involved in metabolism, thereby influencing overall tissue homeostasis (Sibuh et al., 2023). Research has demonstrated that dietary change in pregnant ewes affects DNA methylation in fetal tissues, including the thymus (Lan et al., 2013). Additionally, nutrient restriction in pregnant Wagyu cattle impacts metabolic functions in fetal muscle and liver (Muroya et al., 2021; Muroya et al., 2023). Tissue metabolism adaptations are associated with mitochondrial oxidative phosphorylation, which is critical for maintaining precise metabolic homeostasis, ensuring cellular function and survival (Wilson, 2017). These biological mechanisms may be associated with the alteration of immune system regulation.

1.8. General objectives

Research has revealed the influence of the intrauterine environment on various organs and systems, particularly the metabolic and immune systems, suggesting that epigenetic mechanisms such as DNA methylation and gene expression modification play a crucial role in this (Deodati et al., 2019). However, the impact of early-life nutrition on immune function in high-marbling beef producers, such as Wagyu, remains incompletely understood. A study demonstrated that nutritional restriction during late gestation can influence metabolic physiology, leading to alterations in colostrum quality in Simmental-Angus crossbred cows (Redifer et al., 2023). Maternal nutritional modulation can also impact physiological processes and bioactive constituents in colostrum, with potential downstream effects on offspring immune functionality. This study was established to investigate the influence of MNR during gestation on fetal development, specifically targeting growth of fetal thymus—an organ intimately linked to immune system function—and its subsequent impact on neonatal growth performance. To achieve these objectives, I first assessed the effects of late-gestation MNR on alterations in somatotropic hormone concentrations in pregnant cows and the resultant physiological and growth outcomes in neonatal calves. Second, I evaluated fetal thymus growth, histological structure, and immunohistochemical attributes influenced by MNR. Third, I investigated the impacts of MNR on DNA methylation patterns, gene expression, and metabolite profiles in the fetal thymus. Finally, I elucidated the biological functions of differentially methylated genes (DMGs) and differentially expressed genes (DEGs) affected by MNR using KEGG pathway analysis and metabolomic profiling.

Chapter 2

Effects of nutrient restriction during late gestation on the physiology of cows and their offspring, and subsequent growth in neonatal calves

2.1. Effects of nutritional status on hormone concentrations of the somatotropin axis and metabolites in plasma and colostrum of Japanese Black cows

2.1.1. Introduction

Colostrum is fundamental for the growth of neonates (Blum and Baumrucker, 2008), thus extending the maternal influence on offspring beyond birth. As proposed by the lactocrine hypothesis (Bartol et al., 2008), bioactive factors in maternal colostrum have long-lasting effects on the development and physiological function of offspring (Chen et al., 2011; Soberon et al., 2012). Previous studies have concluded that maternal nutritional status is the main factor affecting the quality of colostrum in dairy cows (Christiansen et al., 2010) and sheep (Banchero et al., 2006). However, few studies have considered the role of growth hormone (GH), insulin-like growth factor 1 (IGF-1) and insulin, or other bioactive components in colostrum. Pregnant animals require more feed in order to support the growth of the fetus, and they must accumulate considerable energy for lactogenesis (Roche et al., 2009). To regulate these changes, concentrations of the key hormones, including GH, IGF-1 and insulin, are tightly controlled in order to maintain homeostasis (Bell, 1995; Kim, 2014). Therefore, the metabolic endocrine status is an important indicator of nutritional and

reproductive status (Johnston et al., 2002). Although these changes can alter the composition of colostrum, thereby affecting offspring development and physiology, it remains unclear how nutritional status during late gestation affects the secretory activity of the somatotropic axis, which in turn, influences the concentrations of hormones and metabolites in plasma and colostrum in Japanese Black cows. The objectives of this study were to determine the effects of the nutritional status of Japanese Black cows late in gestation on the secretion of hormones in the somatotropic axis (GH and IGF-1), and insulin as well as its effect on the secretion of metabolites; and to examine the concentrations of these factors in plasma and colostrum during the early postpartum period.

2.1.2. Materials and Methods

All procedures conducted in this experiment were approved by the Animal Care and Use Committee, Scientific Research Promotion Division, Scientific Research Promotion Department, Kyushu University, according to the Guide for the Care and Use of Agricultural Animals in Research and Teaching.

Experimental treatments

This experiment was conducted at the Kuju Agricultural Research Center, Kyushu University, Oita Prefecture, Japan. Eight multiparous cows (3–7 years old), with the range of parity from one to four, were assigned at random to either the control group (CON) or to the restricted group (LOW) on day 181 of gestation. The control group comprised four cows, 5.1 ± 0.7 years old, with an average parity of 3.0 ± 0.8 and a body weight of 484.75 ± 26.2 kg, whereas the four cows from the LOW group were 5.1 ± 0.8 years old, had an average parity of 3.0 ± 0.7, and weighted 488.00 ± 40.3 kg. Animals were secured individually with

self-locking stanchions for feeding, which occurred twice daily at 09.00 and 15.00 hours. Control (CON) cows were fed Italian rye grass and a concentrate (Yamato, JA Nishinihon Kumiai Shiryo Corp, Hyogo, Japan) that provided 100% of their nutritional requirements (NARO, 2008) until parturition. The LOW group was provided with the same diet as the CON cows at 100% of their nutritional requirements at -14 days (181 days gestation). Subsequently, feed was decreased by 5% per day from -14 days to 0 day (195 days gestation), until the LOW group attained the experimental level of 60% of their nutritional requirements until parturition, as in Figure 2. After day 0 of the postpartum interval, the cows had free access to Italian ryegrass hay and were provided a concentrate (Yamato, JA Nishinihon Kumiai shiryo Corp, Hyogo, Japan) at 1% of their body weight once daily at the morning meal. Details of these diets are provided in Table 1.

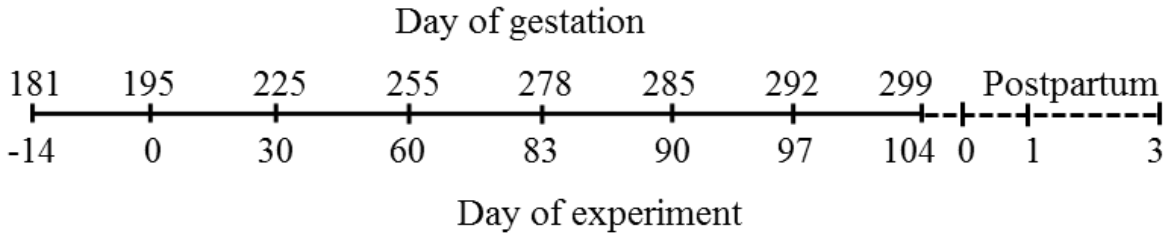

Figure 2. Time span of experimental and gestation periods. Numbers above the axis represent days of gestation. Numbers below the axis represent days of the experiment and the number of days postpartum.

Table 1. Dietary components (% on a fresh matter basis) and nutrient composition (% on a dry matter basis) of feeds. The additional components were molasses, calcium carbonate, alfalfa meal, alfalfa, salt, kelp meal, clay silicate, fodder yeast, tofu dregs, soft brown sugar, tofu dregs fermentation product and lactose

Diet ingredient	Concentrate	Rye hay
Dietary components		
Grains	44.0	-
Rice and wheat bran	41.0	-
Soybean and rape cake	9.0	-
Additional components	6.0	-
Nutrient composition		
Dry matter	88.0	83.8
Crude protein	12.5	6.1
Ethereal extract	2.0	1.5
Crude fiber	10.0	24.3
Crude ash	10.0	6.3
Calcium	0.5	0.3
Phosphorus	0.4	0.27
Total digestible nutrients	68.0	62.9

Sample collection and processing

The secretion of GH in cattle is pulsatile (Gluckman et al., 1987) and therefore, a single blood sample may not reflect average concentrations. However, secretion of GH is synchronized around the anticipated time of feeding with a secretory burst immediately before feeding and no secretion during or for at least 1 h after feeding (McMahon et al., 2001). Therefore, I collected blood samples to coincide with the secretory episode just before morning feeding (08.30 hours) in order to reduce variability in the concentrations of GH and other substances. Blood samples were collected by jugular venipuncture into 10mL heparinized vacuum tubes on days -14, 0, 30, 60, 83 and once per week after day 83 until parturition (day 83 was 1 week before expected calving). The relationship between gestation and experimental periods is shown in Figure 2. After delivery, blood and colostrum samples were collected on days 0 (within 24 h of calving), 1 and 3 at 08.30 hours, before morning feedings. We were able to confirm that calves drank colostrum within 2 h of delivery. Blood samples were centrifuged at 2000 × g for 20 min at 4°C with 100 kallikrein inactivation units aprotinin per mL of blood. Harvested plasma and whole colostrum were frozen at -40°C until assayed for hormones and metabolites.

Hormone and metabolite assay

Concentrations of GH in plasma and colostrum were measured using time-resolved fluoroimmunoassay (TR-FIA) following a method (Sugino et al., 2004). Coefficients of variation of the intra- and inter-assay were 4.1 and 9.3%, respectively.

Concentrations of IGF-1 in plasma and colostrum were assayed with TR-FIA following a protocol (Laarman et al., 2012). IGF-1 was extracted from plasma by adding 1mL of 1 N acetic acid (pH 2.0) to 1mL of plasma, and plasma protein was precipitated by addition of 2mL acetone. The mean recovery of IGF-1 from bovine plasma was 98.2%, as confirmed by

dose-response displacement of the IGF-1 tracer after the addition of bovine plasma. The intra- and inter-assay coefficients of variability (CVs) were 6.9 and 5.5%, respectively.

Concentrations of insulin were measured using a sandwich-type immunoassay commercial kit (Mercodia Ultrasensitive Bovine Insulin ELISA; Mercodia AB, Uppsala, Sweden). The intra- and inter-assay CVs were 2.3% and 6.7%, respectively.

Concentrations of metabolites in bovine plasma and colostrum were measured using commercial kits via the mutarotase-glucose oxidase test (glucose B-test) for glucose and the acyl-coenzyme A (CoA) synthetase-acyl CoA oxidase test (NEFA 50 C-test) for nonesterified fatty acids (NEFA) (Wako Pure Chemical, Osaka, Japan). The abundance of total plasma protein was evaluated using a hand-held refractometer with automatic temperature compensation (Master-Sur/Jα-2751-J05; Atago, Co., Ltd., Tokyo, Japan).

In addition, the areas under the curves (AUC) for hormone and metabolite concentrations were calculated as indicators of their concentrations before and during treatment periods. The average values of the AUC were calculated as follows: AUC-PT: from -14 to 0 day; T30: from 0 to 30 days; T60: from 30 to 60 days; and PC: from 90 days to pre-calving; and AUC-PP and AUC-CS from 0 to 3 days postpartum, respectively.

Statistical analyses

Results are presented as mean ± SEM. All statistical analyses were performed using SAS version 9.0 (SAS Institute Inc., Cary, NC, USA). For analyses involving repeated measures over time, PROC MIXED incorporated in SAS was used to estimate main effects of time and treatment as well as time-by-treatment interactions following a method (Littell et al., 1998). For each of the plasma and colostrum components analyzed, antepartum and postpartum samples were analyzed separately. Significant differences among the means were evaluated with Tukey's multiple range tests at the $p \leq 0.05$ level; differences at the $p <$

0.10 level were considered tendencies. The statistical model for the two-way analysis of variance (ANOVA) was as follows:

$$Y_{ijk} = \mu + B_i + T_j + e_{ijk}$$

Where Yijk is the observation, μ is the overall mean, Bi is the effect of i treatment (i= 1 (CON), 2 (LOW)), Tj is the effects at j time during antepartum and postpartum, j is the time of sampling, BTij is the effect of treatment by time interaction and eijk is the residual error.

2.1.3. Results

Changes in body weight

Body weight at the initiation of nutritional treatment was similar for both groups (484.75 ± 26.2 and 488.00 ± 40.3 kg for CON and LOW, respectively; $p = 0.95$). The CON group gained proportionately more weight than the LOW group between days 0 and 30 ($p < 0.05$), 30 and 60 ($p < 0.01$) and 60 and 83 ($p < 0.01$) (Figure 3).

The composition of feed and nutrient intake is summarized in Table 2. Parturition occurred on day 93 (n= 1), day 99 (n= 2), and day 105 (n= 1) for each group; therefore, there was no difference in the length of gestation between the two groups.

Somatotropic axis

Due to the limited amount of colostrum produced by each individual on day 0 after calving, colostrum samples on that day were only sufficient to determine the concentrations of IGF-1. Hormone concentrations in plasma and colostrum are shown in Figure 4. Plasma GH at day −14 was significantly higher in the individuals subsequently assigned to the LOW group than in those subsequently assigned to the CON group ($p < 0.05$). The concentrations of GH during the nutritional treatment period were significantly higher in the LOW group

than in the CON group ($p < 0.05$). Thus, the concentrations of GH in the LOW group were significantly higher than those in the CON group on days 60, 83 and 97 ($p < 0.05$), with a marked peak in the LOW group on day 97. The concentrations of GH in the plasma and colostrum of LOW cows were also significantly higher on days 0 and 1 of the postpartum period, respectively, compared to those of the CON cows ($p < 0.05$) (Figure 4A).

The concentrations of IGF-1 in plasma on day −14 did not differ between the animals subsequently assigned to different treatment groups ($p = 0.18$). Differences in the concentrations of IGF-1 in the plasma between the two groups were not significant in either the antepartum or postpartum periods ($p = 0.49$ and $p = 0.76$, respectively). The concentrations of IGF-1 in colostrum decreased significantly with the number of days postpartum ($p < 0.001$) but were not significantly different between the groups ($p = 0.59$) (Figure 4B).

Concentrations of insulin

The concentrations of insulin in plasma and colostrum were not significantly different between the two groups (Figure 4C), although changed significantly over time ($p < 0.05$), where cows in the LOW group tended to have lower concentrations of insulin ($p = 0.07$). The concentrations of insulin in colostrum were three-fold higher compared to those in the plasma in both groups, decreasing significantly with increasing postpartum time ($p < 0.05$).

AUC of GH, IGF-1 and insulin

The AUC for GH, IGF-1 and insulin increased prior to calving and were not different after calving in both groups (Figure 5). For LOW cows, the AUC-GH was significantly higher than that for CON cows at both pre-calving (PC) ($p < 0.01$) and post-calving (PP and CS) ($p < 0.05$) periods.

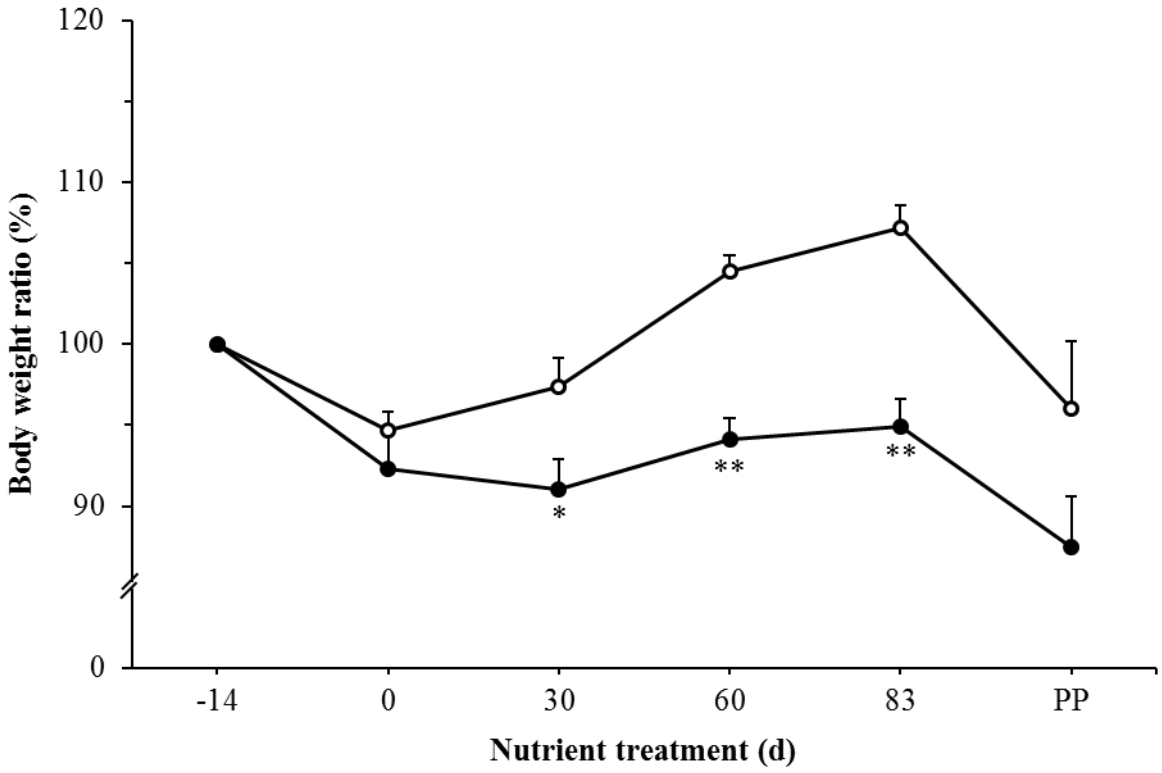

Figure 3. Proportional change in body weight during nutritional treatment in late pregnancy and postpartum (PP) period. Data are presented as mean ± SEM. Control (CON) groups are indicated by open circles (○) and restricted (LOW) groups by closed circles (●). *: $p < 0.05$; **: $p < 0.01$, between LOW and CON groups (n = 4).

Table 2. Total nutrient intake of late antepartum cows during nutritional treatments after 195-day gestation to calving. CON is control groups and LOW is restricted groups. Data are presented as mean (kg) ± SEM

Item	Groups	
	CON	**LOW**
Dry matter	694.0 ± 29.36	447.34 ± 34.07
Crude protein	30.69 ± 0.91	28.84 ± 1.86
Ethereal extract	11.75 ± 0.53	7.37 ± 0.52
Crude fiber	130.26 ± 4.90	89.94 ± 7.97
Crude ash	53.66 ± 2.51	33.04 ± 2.23
Calcium	2.62.95 ± 0.12	1.60 ± 0.11
Phosphor	2.22 ± 0.10	1.38 ± 0.10
Total digestible nutrients	450.23 ± 19.35	288.07 ± 21.54

SEM: standard error of the mean.

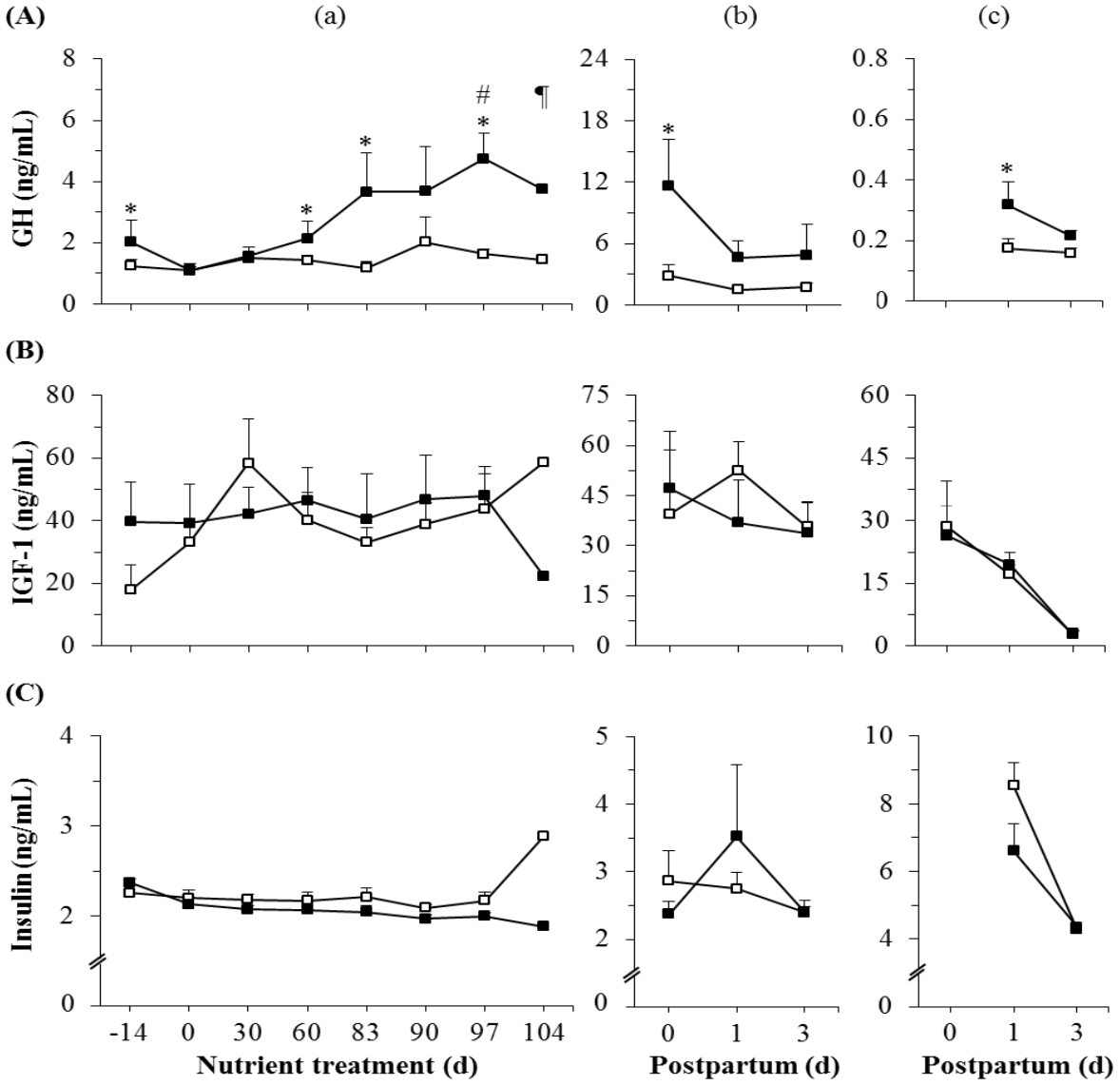

Figure 4. Effects of nutritional treatment on concentrations of hormones: (**A**) growth hormone (GH), (**B**) insulin-like growth factor 1 (IGF-1) and (**C**) insulin. Panels (a), (b) and (c) correspond to antepartum plasma levels, postpartum plasma levels, and colostrum levels, respectively. Data are presented as mean ± SEM. Control (CON) groups are indicated by open squares (□) and restricted (LOW) groups by closed squares (■). *: $p < 0.05$, between LOW and CON groups (n = 4). At day 97, there were n = 3 in each group (#) and at day 104, there was n = 1 in each group (¶).

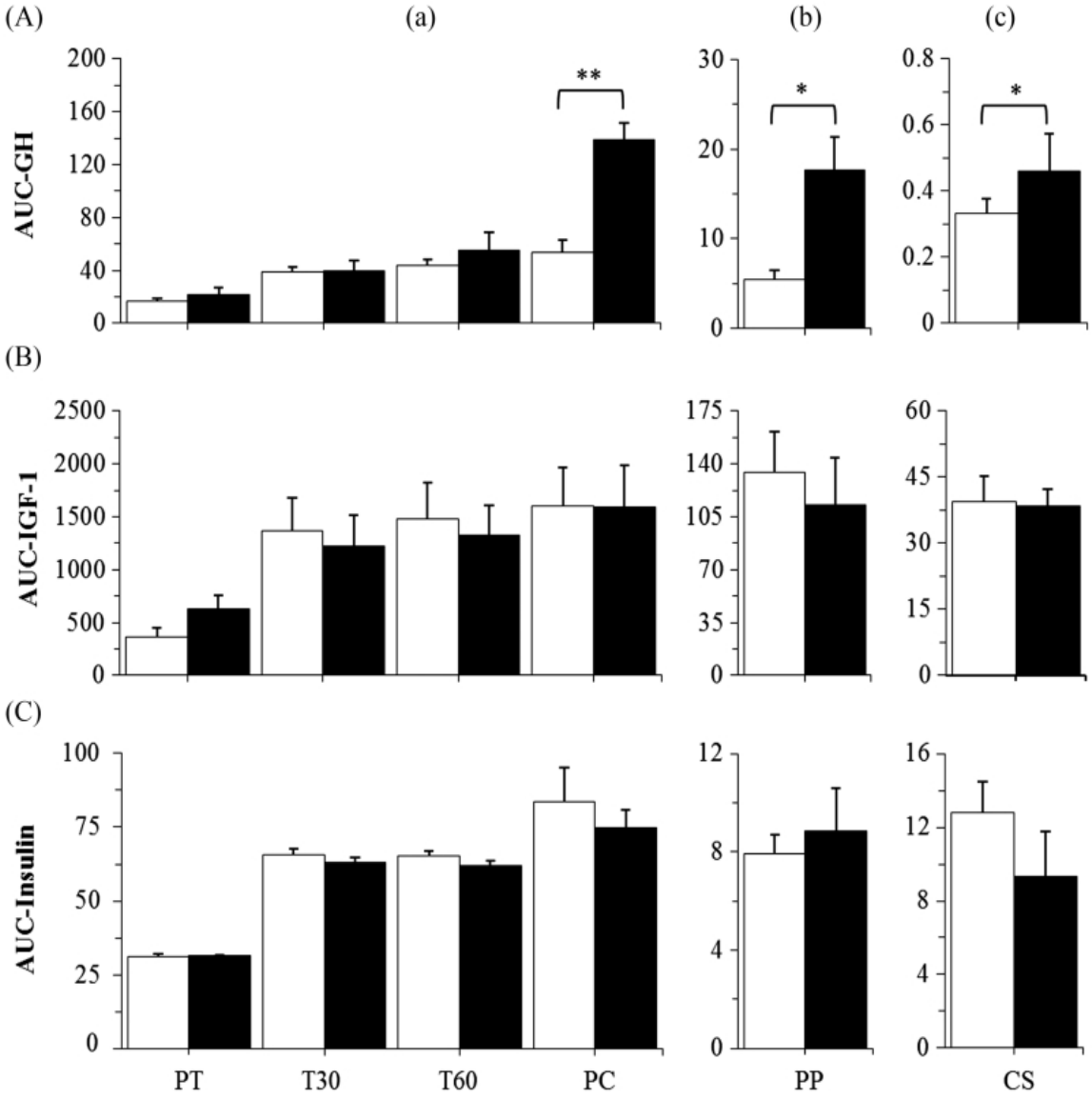

Figure 5. Average values of the areas under the secretory curve (AUC) for hormones: growth hormone (GH) (**A**), insulin-like growth factor 1 (IGF-1) (**B**) and insulin (**C**). PT: pre-nutritional treatment, T30: from 0 to 30 days of nutritional treatment, T60: from 30 to 60 days of nutritional treatment, PC: pre-calving (a); PP: postpartum day 0 to day 3 (b); COL: colostrum day 1 to day 3 (c). Data are presented as mean ± SEM. Control (CON) (□) and restricted (LOW) (■) groups. *: $p < 0.05$; **: $p < 0.01$, between LOW and CON groups (n = 4).

Concentration of metabolites

The LOW group had significantly lower concentrations of glucose in plasma compared with the CON group during the nutritional treatment period ($p < 0.001$). In contrast, the concentrations of glucose in colostrum were initially twice as high as those in plasma, but decreased significantly with time during the postpartum period ($p < 0.01$) (Figure 6A). The AUC for glucose was significantly higher in the CON cows after T30 (0–30 days) and T60 (30–60 days) of nutritional treatment compared to that of LOW cows ($p < 0.05$) (Figure 7A).

The concentrations of total protein in plasma changed significantly over time ($p < 0.001$); however, they were not different between the two groups. In contrast, the concentrations of total protein in colostrum were significantly higher in the CON group than in the LOW group ($p < 0.01$) (Figure 6B).

On average, the LOW group had higher concentrations of NEFA in plasma throughout the experimental period ($p < 0.001$). This difference was especially distinct on days 0, 30, 60 and 83 ($p < 0.01$ on days 0 and 60, $p < 0.05$ on days 30 and 83). There was a marked peak in concentrations of NEFA in the LOW group on day 30. After calving, the concentrations of NEFA in plasma decreased significantly with increasing time postpartum ($p < 0.05$). Concentrations of NEFA in colostrum were more than 13- and 14-fold higher than those measured in plasma of CON and LOW cows, respectively (Figure 6C).

The AUC of NEFA was greater in the LOW group than in the CON group from PT to PC after beginning the nutritional treatment ($p < 0.01$ on T30 and T60, $p < 0.05$ on PT and PC).

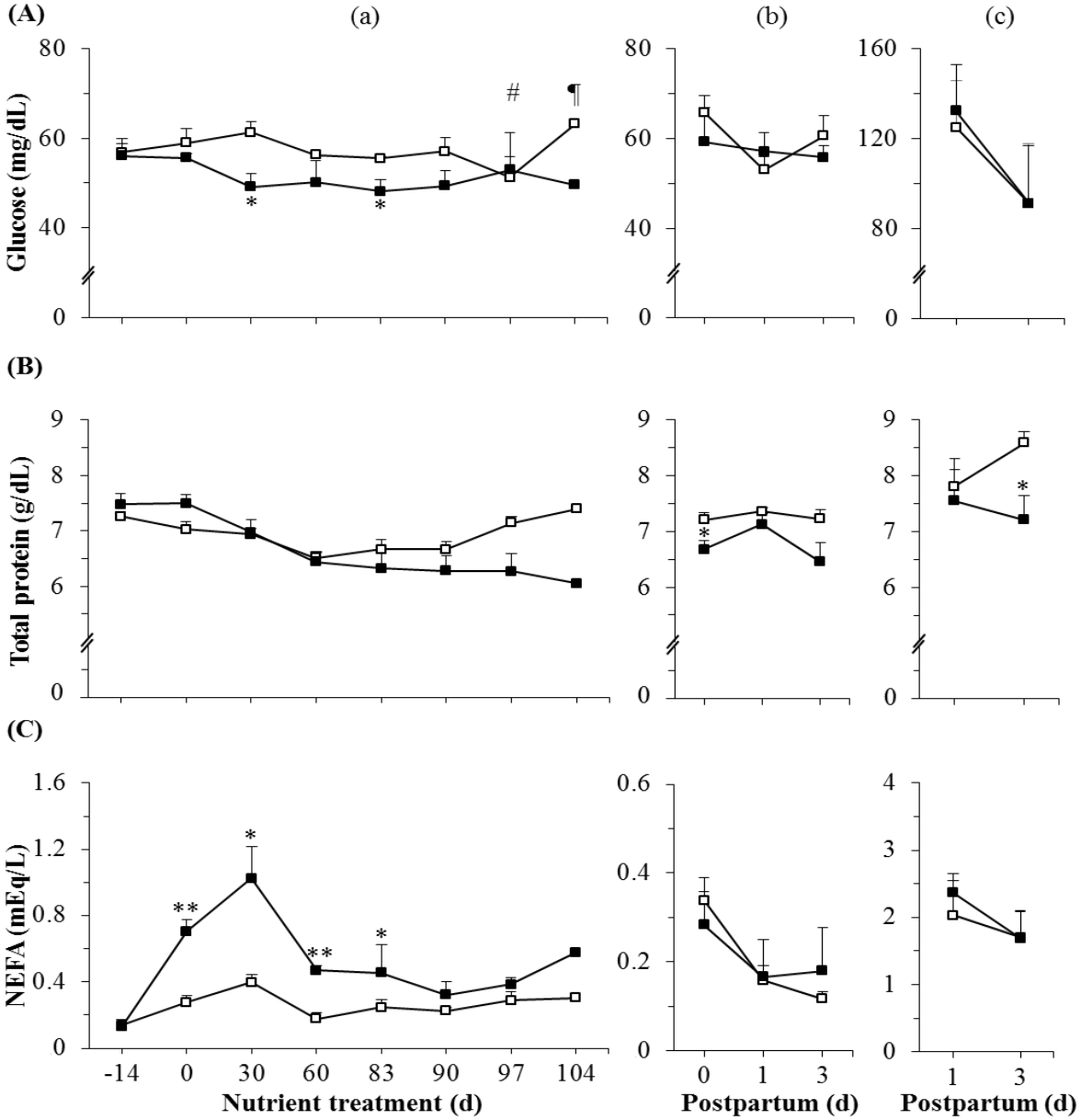

Figure 6. Effects of nutritional treatment on the concentrations of metabolites: glucose (**A**), total protein (**B**), and nonesterified fatty acids (NEFA) (**C**). Panels (a), (b) and (c) correspond to antepartum plasma levels, postpartum plasma levels and colostrum levels, respectively. Data are presented as mean ± SEM. Control (CON) (□) and restricted (LOW) (■) groups. *: $p < 0.05$; **: $p < 0.01$, between LOW and CON groups (n = 4). At day 97, there were n = 3 in each group (#) and at day 104, there was n = 1 in each group (¶).

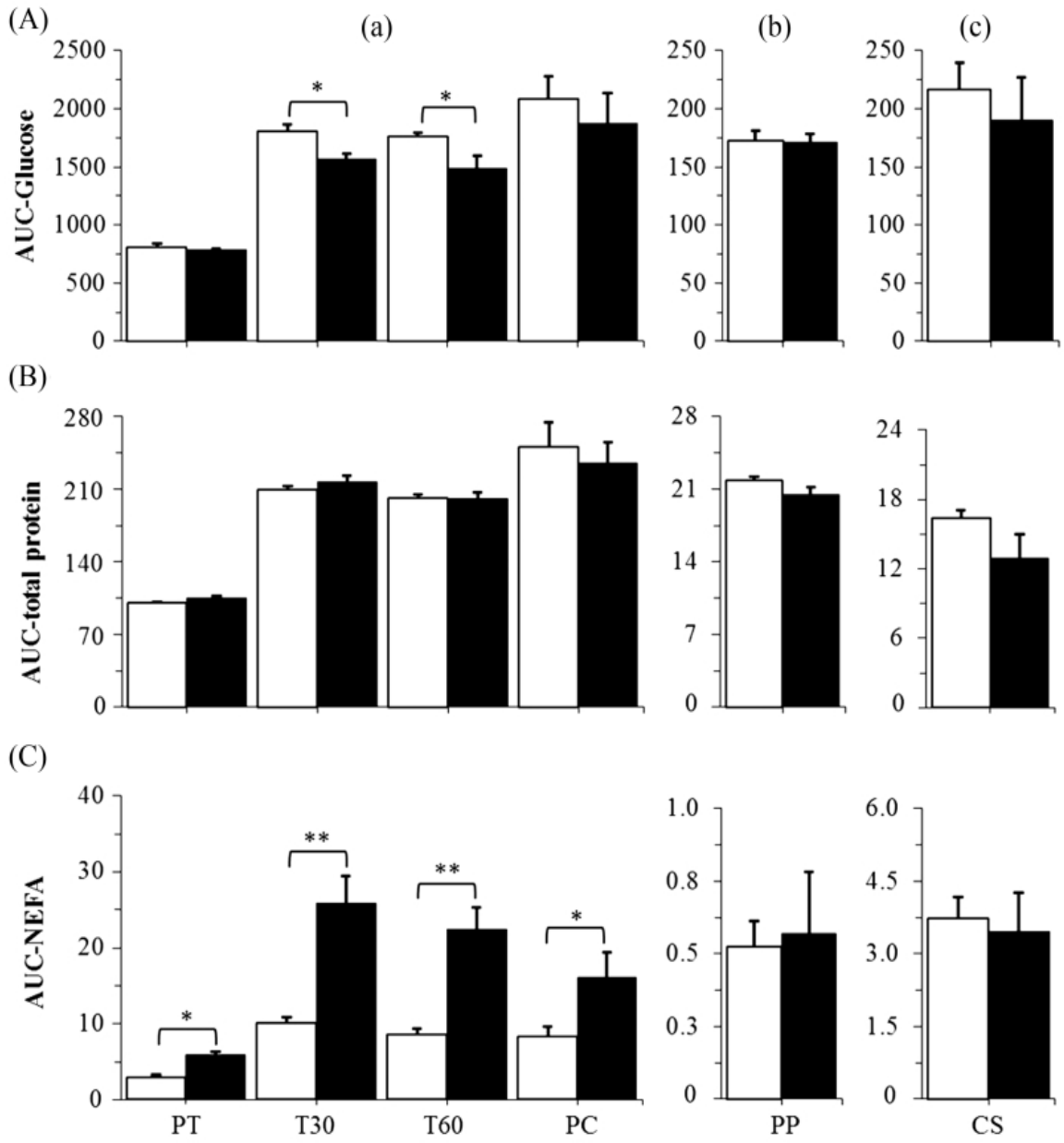

Figure 7. Average values of the areas under the secretory curve (AUC) for metabolites: (**A**) glucose, (**B**) total protein and (**C**) nonesterified fatty acids (NEFA). PT: pre-nutrient treatment, T30: from 0 to 30 days of nutritional treatment, T60: from 30 to 60 days of nutritional treatment; PC: (a) pre-calving; PP: (b) postpartum day 0 to day 3; CS: (c) colostrum day 1 to day 3. Data are presented as mean ± SEM. Control (CON) (□) and restricted (LOW) (■) groups. *: $p < 0.05$; **: $p < 0.01$, between LOW and CON groups (n = 4).

2.1.4. Discussion

The present study demonstrates that concentrations of GH in plasma and colostrum can be increased by nutritional restriction during the last trimester of pregnancy in Japanese Black cows. Furthermore, I find that these effects are maintained after calving. I have thus demonstrated for the first time that it is possible to increase the concentration of GH in colostrum by maternal nutritional restriction in Japanese Black cows.

Concentrations of GH in plasma correlate with long-term nutritional status (Scacchi et al., 2003). Numerous studies of dairy cows have demonstrated markedly elevated concentrations of GH during negative energy balance (Zulu et al., 2002; Roche et al., 2006). This is in agreement with the finding that dairy cows have significantly higher concentrations of GH in the plasma during nutritional restriction in the antepartum period (Burke and Roche, 2007), which is sustained into the early postpartum period (Butler et al., 2003). Therefore, it is reasonable to conclude that the antepartum nutritional treatment in LOW cows is responsible for the elevated concentrations of GH in plasma during late pregnancy.

The richest colostrum is produced during the first 3 days postpartum and is crucial for newborn calves (Hammon and Blum, 1999). The components of colostrum are known to be influenced by maternal endocrine status (Oda et al., 1989; Wallace et al., 1997). In the present study, postpartum concentrations of GH in plasma on day 0 and in the colostrum on day 1 were significantly higher for LOW cows than for CON cows. This suggests that restricted feeding in late pregnancy increases the secretion of GH into blood, which is then transferred into the alveolar lumen of the mammary glands, and hence, accumulates in colostrum.

Concentrations of IGF-1 in plasma increase with an increase in crude protein in the diet (Gotoh et al., 2014). In contrast, concentrations of IGF-1 decline in conjunction with a

decrease in the dietary energy consumed (Busato et al., 2002; Meikle et al., 2004). However, our study found that concentrations of IGF-1 remained unchanged throughout the period of nutritional restriction, despite differences in the concentrations of GH between the two groups. This phenomenon can be explained by a reduction in the hepatic binding of GH in undernourished animals (Breier et al., 1988). Biologically, the action of GH is initiated when GH binds to its receptor (GHR) on target cells. The GHR-1A receptor is abundant in the liver and functions by enhancing the synthesis and secretion of IGF-1 in nutritional partitioning (Etherton, 2004; Roche et al., 2009). In dairy cows, during the transition from late gestation to lactation, concentrations of GHR-1A transcripts and IGF-1 in plasma are reduced, whereas concentrations of GH in plasma are elevated (Radcliff et al., 2003; Lucy et al., 2009). This phenomenon is referred to as the uncoupling of the somatotropic axis. The reduced binding rate of GH to GHR-1A in late antepartum Japanese Black cows may be responsible for the pattern observed in our study. The present results are consistent with previous findings, wherein the concentrations of IGF-1 in colostrum were not affected by maternal nutritional treatment (Hough et al., 1990).

Insulin is an important hormone controlling nutrient metabolism, and concentrations of plasma insulin respond to changes in concentrations of plasma glucose (Sartin et al., 1988). In accordance with previous findings, the concentration of plasma glucose depends on nutritional status (Schoenberg et al., 2012). However, the concentrations of plasma insulin did not differ significantly between the LOW and CON cows in the present study, despite a significant difference in the concentration of glucose in plasma of the antepartum cows. A reduction in insulin sensitivity is a metabolic adaptation to the nutrient accumulation necessary for fetal growth and lactogenesis in late antepartum cows with negative energy status (Sano et al., 1993). This physiological alteration is associated with a decrease in the

insulin-dependent uptake of glucose (Sadri et al., 2010). Taken together, insulin seems to be less affected by nutritional treatment than GH in Japanese Black cows.

There are few data on the relationship between maternal nutritional status and concentrations of insulin in the colostrum of cows. The present study did not find any influence of nutritional treatment on concentrations of IGF-1 and insulin in plasma or colostrum. This suggests that calves receive similar concentrations of insulin and IGF-1 through colostrum, regardless of a restriction in maternal nutrition of up to 60% in late pregnancy.

Colostrum provides essential nutrients and immunoglobulins to newborn animals (Yvon et al., 1993). I show in this study that the concentration of protein was reduced in colostrum in LOW cows, which is consistent with Nowak and colleagues, who reported that the concentration of protein in colostrum was affected by maternal nutritional treatment of Polish Holstein-Friesian cows (Nowak et al., 2012).

Despite a reduced plane of nutrition in LOW cows, the timing of the peak in concentrations of GH and NEFA were different. Increased concentrations of NEFA in blood are an indication that animals are in a negative energy balance (Takahashi et al., 2009). In this study, both groups of cows were fed at a plane of nutrition that adhered to the Japanese feeding standard for beef cattle (NARO, 2008). Thus, the amount of feed was increased from day 30 to parturition to maintain the level at 60% of the cows' nutritional requirements for the LOW group. Therefore, the impact of increasing the feed may have led to a decrease in concentrations of NEFA from day 30 until parturition. In contrast, concentrations of GH are increased in plasma during late pregnancy, with a peak occurring at parturition (Bell, 1995). Burke and colleague observed that the elevation in GH before calving was greater in cows fed at lower planes of nutrition prepartum (Burke and Roche, 2007). Additionally, NEFA inhibits the synthesis and secretion of GH (Luque et al., 2006). Therefore, I speculate that

concentrations of GH were increased in the LOW group due to a reduced plane of nutrition and the proximity of parturition. García-Aragón and colleagues suggested that pituitary GH has a regulatory role in organ development, which may affect the growth of the fetus through GH receptors (Garcia-Aragón et al., 1992). Therefore, the increase in GH concentrations as a result of maternal nutrient restriction (MNR) might be essential in order to encourage efficient growth of the fetus.

In conclusion, maternal restriction of nutrition leads to increased concentrations of GH in plasma and colostrum. The concentrations of glucose in plasma were strongly affected by the level of nutrition, which also influenced the concentration of total protein in colostrum. These findings suggest that the level of nutrition and the secretion of GH are important contributors to the composition of colostrum in Japanese Black cows. Further studies are required to determine whether or not GH in colostrum affects growth or influences the metabolites in blood of calves.

2.1.5. Summary

This chapter investigated the effect of late-gestational nutrient restriction on the physiological changes in blood plasma and colostrum. The LOW exhibited elevated concentrations of GH and NEFA, while reduced plasma levels of glucose and insulin compared to the CON group. Postpartum, plasma GH concentrations were significantly higher in the LOW group, while total plasma protein levels were significantly lower compared to the CON group. In colostrum, the LOW group showed significantly higher GH levels, yet significantly decreased total protein concentrations relative to the CON group. The finding indicates that MNR during late gestation affects GH secretion and total protein concentrations in the blood and colostrum of Japanese Black cows.

2.2. Effects of fetal and neonatal programming on physiological parameters and growth performance of Japanese Black calves

2.2.1. Introduction

Maternal nutrition significantly influences both fetal development and postnatal performance. Research has identified factors that are crucial for accurately predicting animal growth and carcass composition, closely linked to various physiological and metabolic traits (Oka et al., 2007). The growth of animals is intricately regulated by nutrients and growth factors through hormonal actions and signaling pathways. The GH/IGF axis has been reported to serve as a pivotal regulator of both prenatal and postnatal growth in vertebrates (Domené and Domene, 2018). Studies have indicated that fetal programming and early high-energy intake can impact metabolic disorders and obesity later in life owing to the dysregulation of GH/IGF-1 secretion in both humans and animals (Reynolds et al., 2017; Tuersunjiang et al., 2017). GH, a polypeptide hormone secreted by the anterior pituitary, regulates somatic growth, metabolism, and body composition. Studies have demonstrated that GH promotes muscle growth and reduces adipose tissue accumulation (Kopchick et al., 2014). GH deficiency has been shown to increase body fat accumulation, an effect that can be reversed by exogenous GH replacement therapy (Tamboli et al., 2017). IGF-1 plays a critical role in adipogenesis, as demonstrated by studies where IGF-1 stimulation promoted adipogenesis across various preadipocyte models. Clinical research also indicates that maternal metabolic conditions, such as insulin resistance, gestational diabetes, and preeclampsia, which influence maternal IGF-1 and insulin levels, are associated with alterations in fetal and postnatal physiology, impacting growth patterns (Mohsen et al., 2016). Evidence further suggests that fetal programming associated with low birth weight is linked

to modifications in somatotropic axis secretion and subsequent catch-up growth later in life. In a Wistar rat model, dams fed 30% of their standard intake during pregnancy produced smaller pups. Postnatally, all pups were fed ad libitum; however, GH and IGF-1 secretion was reduced in the offspring of restricted-fed dams compared with that from well-fed dams during early life (Woodall et al., 1996a). By 210 days of age, the body weight of offspring from restricted-fed dams surpassed that of their well-fed counterparts in both males and females, when analyzed separately (Woodall et al., 1996b).

In the subsequent section, I explore the effects of nutrient restriction in late-pregnant cows and its impact on the somatotropic hormone axis and essential metabolites in plasma and colostrum. The effects of these changes in maternal physiology on offspring development in Wagyu cattle are not yet fully understood. The objective of this section was to investigate the effects of metabolic programming on early growth performance and the secretion patterns of GH, IGF-1, insulin, and metabolic biomarkers in Japanese Black calves.

2.2.2. Materials and Methods

Experimental treatments

All experimental procedures were performed as previously described in the initial section of this chapter. Upon delivery, at 3 days of age, all calves were separated from their mothers and allocated to receive high-nutrient milk replacer via an automated feeder. The milk replacer concentration began at 125 g/l (w/v) and was incrementally increased by 25 g/l until reaching 200 g/l to accommodate individual consumption rates of up to 2 kg/d or 10 l/d. Additionally, calves had ad libitum access to high-nutrient calf starter, hay, minerals, and clean water. Weaning of all calves occurred at 90 days of age. Body weight and body

frame size were recorded on days 0 (within 24 hours after calving), 3, 10, and subsequently once a month. Details of the milk replacer and calf starter are provided in Table 3.

Blood sample processing and assay

Blood samples were collected on day 0 (within 24 hours post-calving), day 3, day 10, and monthly thereafter until the age of 150 days. The laboratory procedures for blood collection, processing, as well as statistical analyses followed the protocols outlined in the preceding section.

Table 3. Ingredient and nutrient composition of calves' diets (% DM basis)

Diet Ingredient	**Milk replacer**	**Calf starter**
Milk powder	67.0	2.0
Soybean meal	5.0	27.0
Non-fiber vegetable powder	28.0	12.0
Grain	-	55.0
Rice and wheat bran	-	4.0
Nutrient composition		
Crude protein	26.0	18.0
Ether extract	25.5	2.0
Crude fiber	1.0	12.0
Crude ash	8.0	10.0
Calcium	0.6	0.5
Phosphor	0.4	0.3
Total digestive nutrients	116.0	74.0

DM: dry matter.

2.2.3. Results

Growth performance and milk consumption

The body weight (BW) and body frame size data at each time point are presented in Table 7. Offspring from cows in the study were classified by different genders, with male and female calves for CON and LOW groups, respectively. The average BW from birth to 150 days of age was significantly lower in calves born to LOW cows compared to those born to CON cows ($p < 0.001$). At birth, LOW offspring had a lower birth weight (BWT) compared to CON offspring (29.0 ± 2.63 vs. 40.25 ± 1.70 kg; $p < 0.05$), and this difference in BW persisted until weaning at 90 days of age (130.3 ± 3.5 and 90.6 ± 5.0 kg for CON and LOW offspring, respectively; $p < 0.01$). Even after weaning at 150 days of age, LOW offspring remained lighter compared to CON offspring (141.25 ± 8.38 vs. 197.63 ± 5.83 kg; $p < 0.01$), Table 5. Although CON offspring were heavier in actual body weight compared to LOW offspring, there were no discernible differences in body growth ratio from birth to 150 days of age (Figure 8A and 8B). Total milk consumption tended to be lower in LOW offspring compared to CON offspring (68.27 vs. 96.10 kg, SEM = 6.19; $p = 0.07$). The average daily gain (ADG) calculated for each group of calves throughout the suckling period was significantly lower in LOW offspring than in CON offspring (0.69 vs. 1.00 kg/d; SEM = 0.03; $p < 0.05$). However, there was no significant difference in the feed conversion ratio (FCR) between the two groups of calves (1.06 and 1.11 for CON and LOW offspring, respectively), Table 4.

Profile of somatotropic hormone secretion

The statistical analyses for the hormone assay results are summarized in Table 6. GH secretion was significantly higher in LOW offspring compared to CON offspring ($p < 0.05$)

on calving day (day 0). There was a considerable decrease in GH secretion in both offspring groups; the comparison between levels just after birth and weaning showed a decrease of 93.59% and 34.10% for LOW and CON offspring, respectively (Figure 9A). Additionally, LOW offspring exhibited significantly higher GH secretion at 30 days of age compared to the CON group ($p < 0.05$). Subsequently, GH concentrations in LOW offspring declined to lower levels than in CON offspring at 60 and 90 days of age ($p < 0.05$). However, differences in GH secretion were not observed during the post-weaning (POW) period (Figure 9A).

On average, the LOW group had lower IGF-1 secretion throughout the sampling period ($p < 0.001$). Nonetheless, plasma IGF-1 concentration was significantly higher in LOW offspring compared to CON offspring ($p < 0.05$) on calving day. Fluctuations in IGF-1 secretion were more pronounced in CON offspring, with secretion increasing after 30 days of age, reaching peak levels at 60 days, and remaining elevated at 90 days of age ($p < 0.01$). At POW, concentrations of IGF-1 remained significantly greater in CON offspring compared to LOW offspring ($p < 0.01$) at 120 and 150 days of age (Figure 9B).

Table 4. Body weight, total milk consumption, and growth rate of Japanese Black calves

Items	Calf groups		SEM	*p-value*
	CON	LOW		
Birth weight, kg	40.25	29.00	2.57	0.02
Weaning weight (90 d of age), kg	130.25	90.63	8.00	0.003
Body weight at 150 d of age, kg	197.63	141.25	11.66	< 0.001
Total milk consumption, kg	96.10	68.27	6.19	0.07
ADG, kg/d	1.00	0.69	0.03	0.04
FCR	1.06	1.11	0.05	0.50

ADG: average daily gain.
FCR: feed conversion ratio.

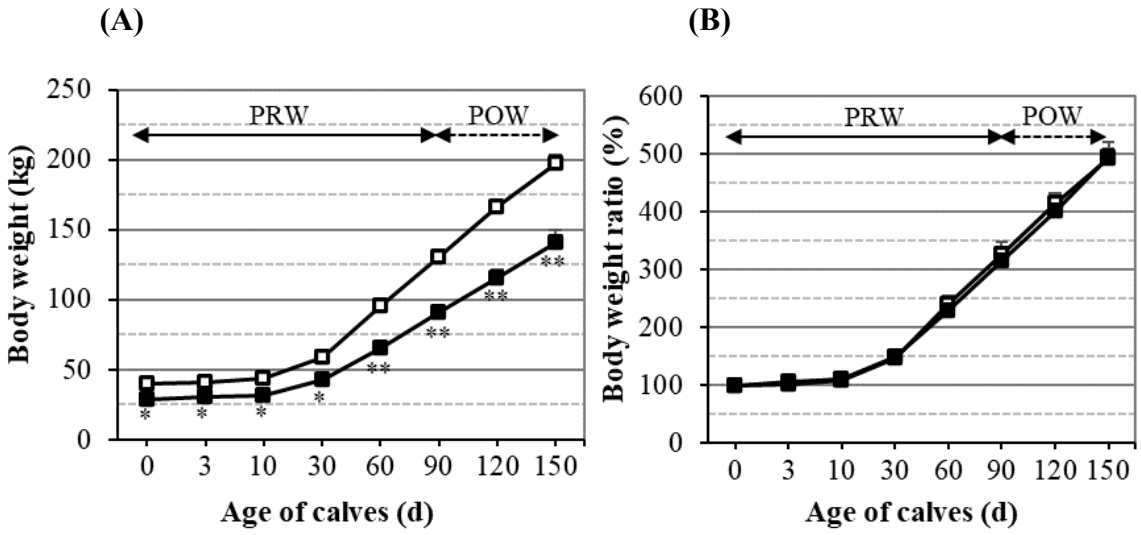

Figure 8. Body growth of calves born to cows given one of two diets during late pregnancy until parturition. (**A**) actual body weight. (**B**) body weight ratio. Control group (CON offspring, □) and Low-nutrition group (LOW offspring, ■). All calves were projcted 2 kg/d of high nutrient milk replacer feeding, weaned at 90 d of age. *: $p < 0.05$; **: $p < 0.01$, between LOW and CON groups (n = 4). PRW : pre-weaning; POW : post-weaning. Data are presented in mean ± SEM.

Table 5. Changes in body weight and body frame size of calves. Data are presented in mean ± SEM

Body composition	Age of calves (d)							
	0	**3**	**10**	**30**	**60**	**90**	**120**	**150**
Body weight, kg								
CON	40.25 ± 1.70	40.50 ±1.40	43.63 ± 1.48	59.13 ± 1.55	95.50 ± 3.35	130.25 ± 3.52	166.50 ± 2.35	197.63 ± 5.83
LOW	29.00 ± 2.63*	30.88 ± 3.02*	31.75 ± 3.07*	43.13 ± 3.14**	65.63 ± 4.71**	90.63 ± 4.99**	115.13 ± 6.59**	141.25 ± 8.39**
Wither height, cm								
CON	-	75.95 ± 1.55	77.62 ± 0.96	82.00 ± 0.48	90.45 ±1.26	95.93 ± 0.84	-	-
LOW	-	70.40 ± 1.78*	71.35 ± 1.13*	75.15 ± 1.03*	81.75 ± 1.18*	88.35 ± 1.71*	-	-
Hip height, cm								
CON	-	80.85 ± 1.17	82.63 ± 1.24	85.53 ± 0.43	92.25 ± 1.45	100.13 ± 0.53	-	-
LOW	-	72.98 ± 1.20*	74.53 ± 1.52*	78.75 ± 1.68*	84.70 ± 1.40*	90.50 ± 1.24**	-	-
Body length, cm								
CON	-	64.33 ± 0.43	66.28 ± 0.99	75.05 ± 0.46	86.40 ± 1.27	95.95 ± 1.18	-	-
LOW	-	58.00 ± 1.48*	62.45 ± 1.52*	67.60 ± 0.91*	75.88 ± 1.27*	87.13 ± 1.78*	-	-
Heart girth, cm								
CON	-	78.75 ± 1.44	81.25 ± 1.38	89.23 ± 0.80	104.25 ± 1.44	114.75 ± 1.31	-	-
LOW	-	72.50 ± 2.10*	73.00 ± 1.78*	81.50 ± 2.25*	92.63 ± 2.56*	104.25 ± 2.87*	-	-
Waist girth, cm								
CON	-	76.63 ± 1.21	80.50 ± 1.85	94.25 ± 0.48	114.63 ± 1.14	129.00 ± 0.41	-	-
LOW	-	73.25 ± 1.89*	70.75 ± 3.68**	84.13 ± 1.51**	99.25 ± 2.50*	114.50 ± 3.10**	-	-

SEM: standard error of the mean. *: $p < 0.05$; **: $p < 0.01$, between LOW and CON groups (n = 4).

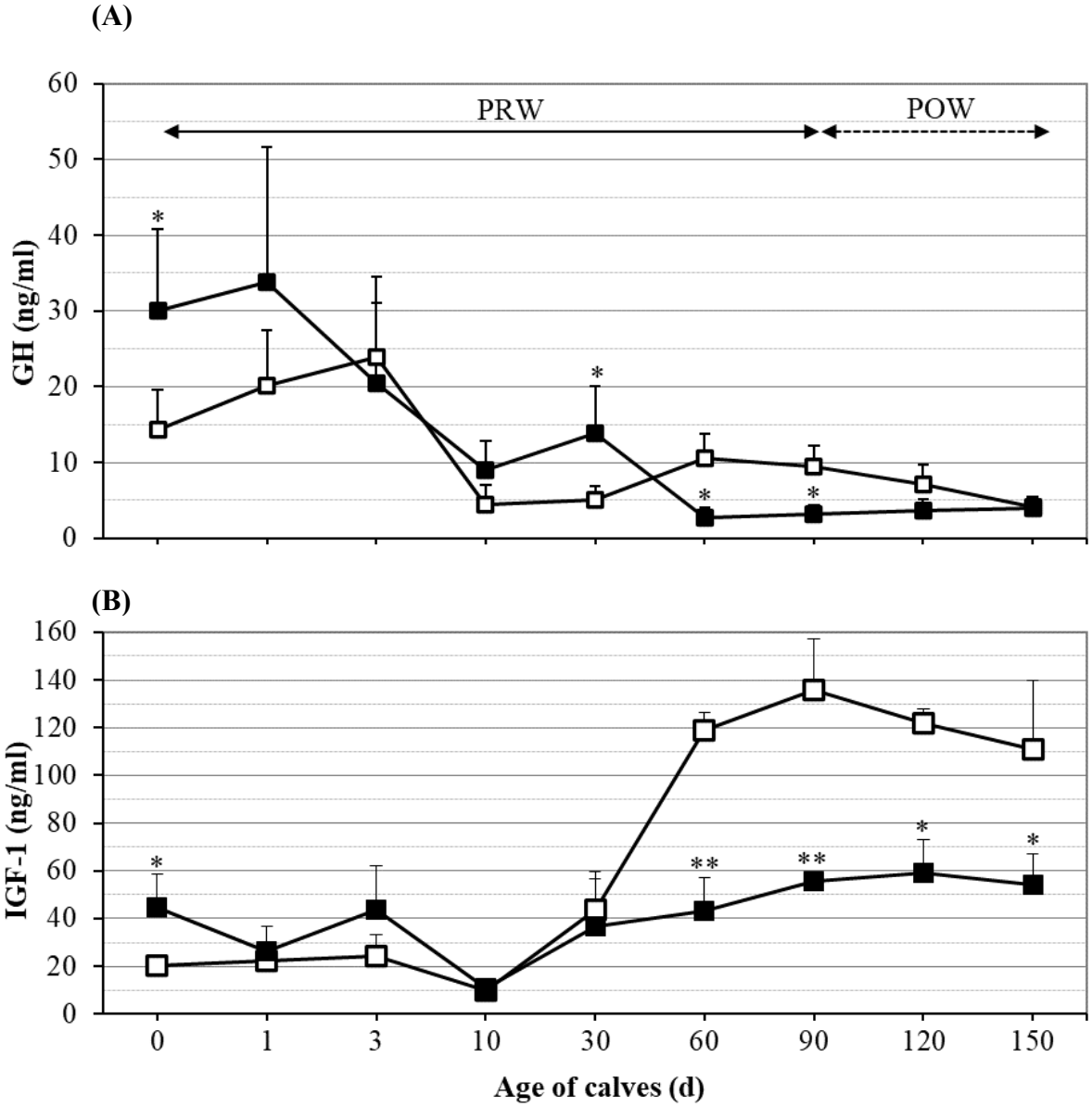

Figure 9. Overall secretion of somatotropic hormones in calves born to cows given one of two diets during late pregnancy until parturition. (**A**) Growth hormone (GH) and (**B**) insulin-like growth factor 1 (IGF-1). The control group (CON offspring, □) and low-nutrition group (LOW offspring, ■). All calved were projected 2 kg/d of high nutrient milk replacer feeding, weaned at 90 days of age. *: $p < 0.05$; **: $p < 0.01$, between LOW and CON groups (n = 4). PRW: pre-weaning; POW: post weaning. Data are presented in mean ± SEM.

Table 6. Comparison of overall hormone secretion and metabolite concentrations in Japanese Black calves from birth to five months of age

Items	Calf groups		SEM	ANOVA *p-value*		
	CON	LOW		group	time	group*time
GH, ng/ml	11.02	13.41	1.79	0.46	0.003	0.60
IGF-1, ng/ml	65.22	41.59	5.11	< 0.001	< 0.001	< 0.001
Insulin, ng/ml	2.69	2.52	0.10	0.33	0.001	0.45
Glucose, mg/dl	110.00	109.94	2.53	0.99	< 0.001	0.58
Total protein, g/dl	5.75	5.98	0.10	0.21	0.04	0.40
NEFA, mEq/l	0.30	0.37	0.03	0.10	< 0.001	0.39
Total cholesterol, mg/dl	95.88	94.77	8.23	0.88	< 0.001	1.00
Triglyceride, mg/dl	65.94	69.22	3.21	0.55	< 0.001	0.59

SEM: standard error of the mean. GH: growth hormone; IGF-1: insulin-like growth factor 1.

Concentrations of metabolites in offspring

On average, there were no significant differences in plasma glucose concentrations between the two groups of calves ($p > 0.05$). However, both groups showed unstable fluctuations in plasma glucose concentrations over time ($p < 0.001$). Plasma NEFA concentrations decreased as the calves aged ($p < 0.001$), with fluctuations observed particularly in the LOW offspring on day 10, where concentrations were significantly higher compared to the CON offspring ($p < 0.05$). The average concentrations of plasma NEFA tended to be higher in LOW offspring compared to CON offspring ($p = 0.10$) (Table 6).

2.2.4. Discussion

The growth and development of fetal tissue predominantly occur during the third trimester of gestation, constituting approximately 75% of fetal growth, underscoring the considerable maternal nutrition demand during this critical period (Fandiño et al., 2019). The present study found that offspring born to the LOW cows exhibited lighter birth weight (BWT) compared to the CON group. This finding is consistent with prior observations in sheep (Trotta et al., 2020), in Angus cattle (Valiente et al., 2021), and in Hereford × Simmental-Angus (Wichman et al., 2023), which restricted maternal nutrition during pregnancy limits nutrient access to the fetus, adversely affecting cell growth and leading to low birth weight. Moreover, studies have shown that the difference in BWT between male and female calves persists regardless of maternal feeding conditions. Typically, this disparity in birth weight between male and female calves in dairy and other beef cattle does not exceed 10% (Kertz and Chester-Jones, 2004; Dhakal et al., 2013). In addition, a study reported that inadequate maternal nutrition during early gestation could diminish BWT in both male and female calves (Long et al., 2012). In the present study, it was observed that the disparity in

BWT between LOW and CON offspring amounts to approximately 28%. This suggests that the impact of maternal nutrient restriction (MNR) is more pronounced than any variation attributed to the sex factor of the calves. Furthermore, earlier studies have suggested that growth rates are higher in heavier calves compared to lighter ones (Beam et al., 2015), with male calves exhibiting faster growth rates than females (Bayou et al., 2015; Gemuh, 2020). Even though notable differences in growth rates between calves in the two experimental cohorts were not evident in the present study. Additionally, there were no discernible distinctions in feed efficiency. These findings imply that maternal undernutrition strongly impacts BWT but does not significantly influence milk replacer intake or the early growth performance of the Wagyu offspring.

The GH/IGF-1 axis plays a critical role in regulating growth and metabolism, with plasma GH and IGF-1 secretion being influenced by factors such as levels of nutrient intake, age, and sex of animals (Jia et al., 2018). In the present study, on the day of calving, LOW offspring exhibited significantly higher plasma GH concentrations compared to CON offspring. This finding may be attributed to maternal hormone transfer via colostrum intake, as colostrum composition is influenced by maternal endocrine status, as discussed in the previous section of this chapter. This biological phenomenon has also been observed in other studies (Gauthier et al., 2006; Ghorbani et al., 2012). Additionally, a significant reduction in GH secretion with advancing age was observed in both groups of calves. Subsequently, the LOW offspring demonstrated lower GH secretion at 60 and 90 days of age compared to the CON offspring; however, GH secretion levels in both groups converged by 150 days of age. Previous studies in rat models have indicated that male pups exhibit higher GH secretion compared to female pups (Robinson et al., 1998). The early decline and differences in GH secretion observed in the LOW offspring in the present study are consistent with these observations. IGF-1 is crucial for neonatal survival and development. Research has

demonstrated that fetal IGF-1 production is directly influenced by maternal nutrient intake (Hellström et al., 2016), and early infancy, before transitioning to GH-regulated synthesis in the postnatal period (Yumani et al., 2020). Interestingly, our study found that IGF-1 secretion on the day of calving was consistent with GH secretion levels, which were significantly higher in LOW calves compared to CON calves. This suggests a significant interplay between GH and IGF-1 at peripartum, indicating that IGF-1 secretion is regulated by GH levels but not dependent on maternal nutrient intake in Wagyu fetuses. Additionally, GH-dependent hepatic IGF-1 synthesis has been demonstrated in neonatal calves (Sauter et al., 2003), and the transition from a monogastric or pre-ruminant to a ruminant state progresses with postnatal age (Blum, 2006). In the current study, IGF-1 secretion levels in LOW offspring fluctuated before stabilizing after one month of age, while CON offspring exhibited a significant increase in IGF-1 secretion after one month onward. The increase in IGF-1 secretion positively correlated with body size, consistent with previous findings (Mullen et al., 2011). The anabolic effects of IGF-1 contribute to increased body size and live weight.

Despite the consistent plasma insulin and glucose concentrations observed throughout the study period, the early differences in GH and IGF-1 secretion between the two groups of calves may not be solely attributed to nutrient intake and sex. These differences may also be related to intrinsic cellular development, potentially influenced by prenatal nutrient status. Limited comparative research exists on the association between poor maternal nutrition, subsequent reduction in the GH/IGF-1 axis, and their effects on body mass index (BMI) in cattle. However, alterations in the secretion of the GH/IGF-1 axis have been reported to be associated with elevated BMI in obese individuals, leading to reduced protein synthesis in muscle cells and increased adipose deposition (Gluckman and Pinal, 2003). Thus, the early reduction in GH and IGF-1 secretion observed in the LOW offspring in our study is likely

attributable to fetal and neonatal programming, which is influenced by nutrient stimuli during the fetal and neonatal periods.

2.2.5. Summary

This section investigated body growth, secretion of GH, IGF-1 and insulin, and concentrations of glucose, NEFA, total protein, total cholesterol, and triglycerides involved in calf growth and nutrient metabolism. Both groups of calves exhibited a decline in GH secretion, with LOW offspring showing earlier reduction in GH levels than CON offspring. Consequently, LOW offspring had lower IGF-1 secretion compared to CON offspring began at 60 days of age until post-weaning period. However, differences in concentrations of plasma glucose, total protein, and NEFA were not observed throughout the experimental period. Although differences in body weight, there were no differences in FCR. These findings suggest that MNR in late gestation cows leads to a decline in GH and IGF-1 secretion in Japanese Black cattle.

Chapter 3

Effects of maternal nutrient restriction on histological structure and immunochemical properties of the Wagyu fetal thymus

3.1. Introduction

The thymus is a primary lymphoid organ essential for the development and maturation of T lymphocytes (T cells), a vital subset of white blood cells crucial for the immune repertoire (Thapa and Farber, 2019). In humans, the thymus reaches its largest size relative to overall body size and highest activity before birth and during childhood, peaking at puberty. Following puberty, it undergoes involution, gradually shrinking and being replaced by adipose tissue, although it continues to produce necessary T cells throughout an individual's lifespan (Kato et al., 2018). In cattle fetuses, the thymus is identifiable by the fourth week of gestation, with T-cell selection starting between weeks 7 and 14 (Tabilas et al., 2023). Hassall's corpuscles (HCs) begin developing at week 14, increasing in number, size, and maturity as gestation progresses (Prabavathy, 2014). Histologically, the thymus is encapsulated by connective tissue that extends septa into the parenchyma, forming incomplete lobules. Each lobule consists of a dark-stained cortex and a lighter-stained medulla. The cortex is densely populated with thymocytes (immature T cells) and epithelial reticular cells, which facilitate early T-cell development (Curtis et al., 1979). Maternal nutrition is critical for both prenatal and postnatal thymus development. A low-protein diet during pregnancy results in a reduced thymic index and altered medullary areas in murine

offspring (Armengaud et al., 2020). Similarly, inadequate maternal energy intake affects the cellular compartment and T-cell subsets in the fetal thymus of lambs (Liu et al., 2015).

As described in Chapter 2, I investigated the impact of maternal nutrition on the secretion of somatotropic hormones and metabolite concentrations in pregnant cows and their offspring. Maternal nutrition influences growth regulatory hormones and colostral compounds, which are vital for immune function. Understanding the histological structure and T-cell development during the fetal period is crucial for elucidating how immunopoietic mechanisms are affected by maternal nutrition. This study aimed to determine the effects of maternal nutrient restriction (MNR) on the histology and T-cell subset expression in the Wagyu fetal thymus.

3.2. Materials and Methods

Experimental animals and diets

The experiment involved 11 multiparous Japanese Black cows with similar body masses at the Iriki farm of Kagoshima University and the Western Region Agricultural Research Center, National Agriculture and Food Research Organization (NARO). They were treated in accordance with the Guide for the Care and Use of Experimental Animals, and the experimental design was approved by the Animal Care and Use Committee of Kagoshima University (approval number A18007). The cows were synchronized using a controlled internal drug release (CIDR) device (Easybreed; InterAg Co. Ltd., Hamilton, New Zealand) and inseminated with frozen male-sorted semen from the same sire (Yurikatsuyasu, Kedaka line). Upon the confirmation of pregnancy, the pregnant cows were randomly assigned to a low-nutrition (LOW) group (n = 5), which was fed 60% of the nutritional requirement, or a high-nutrition group (n = 6), which was fed 120% of the nutritional requirement. The nutrient

calculations, including the energy requirements, were based on the standard diet per unit body mass, as per the JFSBC guidelines (NARO, 2008). During pregnancy, Wagyu cattle have increased nutritional demands compared to non-pregnant cows; therefore, the high-nutrition group was designated as the control (CON) group in this study. The experimental diet included formula feed, total mixed ration (TMR), and rice straw (Table 7). The experimental animals were individually fed in the morning (09:00) and in the afternoon (16:00). Throughout the experimental period, pregnant cows had free access to clean tap water and mineral blocks.

Thymus sample collection

After confirming pregnancy and allocating the cows to the experimental groups, the pregnancies were allowed to proceed until 8.5 months, when the fetuses were euthanized by exsanguination, following lidocaine injection into a jugular vein. Subsequently, samples were collected for the anatomic and physiologic analysis of the carcass and internal organs. Cesarean sections were conducted at the Veterinary Teaching Hospital of Kagoshima University. Thymus samples were collected, promptly frozen in liquid nitrogen, and stored at −80°C until subsequent analysis.

Sample sectioning

The frozen thymus samples were sectioned at a thickness of 7 μm using a Leica CM1850 cryostat (Leica Biosystems, Wetzlar, Germany). This precision instrument ensures that the tissue is uniformly sliced at the desired thickness while maintaining the integrity of cellular and tissue structures, which is critical for accurate histological analysis. Once sectioned, the tissue slices were carefully mounted onto adhesive glass slides (MAS-01-15; Matsunami

Glass Ind., Ltd., Osaka, Japan). These specialized slides are designed to firmly adhere to the tissue sections, preventing detachment during subsequent staining procedures.

Thymic histological structure analysis

Hematoxylin and eosin (H&E) staining was performed by initially fixing the sections in 10% formalin solution at 4°C for 5 min. Subsequently, the sections were stained with hematoxylin (Meyer's Hematoxylin; Sigma-Aldrich, Hannover, Germany) for 2 min. The sections were then rinsed with tap water for 30 min and stained with eosin (Soluzioni Di Eosina Y; Sigma-Aldrich) for 8 min. After staining, the sections were sequentially dehydrated in 70%, 80%, 90%, 99%, and absolute ethanol, followed by xylene. Slide samples were rinsed with distilled water between each step prior to dehydration. Following dehydration, the sample slides were mounted using Mounting-Quick (Daido Sangyo Co., Ltd., Osaka, Japan) and covered with micro-cover glass of thickness No. 1 (Matsunami Glass Ind., Ltd.).

Immunohistochemistry analysis

Immunohistochemistry was conducted using specific antibodies for CD4 and CD8 T-cell staining. Tissue sections were initially fixed in 2% paraformaldehyde, diluted in a 1:9 (v/v) ratio with 10× phosphate-buffered saline (10× PBS) and distilled water, at pH 7.4 and 4°C for 30 min. The samples were subsequently washed with 0.2% Triton X-100 solution for 20 min, followed by incubation in a blocking buffer containing normal goat serum (Jackson ImmunoResearch Laboratories, Inc., West Grove, PA, USA) at a 1:500 dilution. The sections were then incubated overnight with a primary antibody, specifically, a rat monoclonal antibody against mouse CD4 (Santa Cruz Biotechnology, Inc., Oregon, CA, USA) at a 1:200 dilution. Following this, the sections were stained with a secondary antibody,

goat anti-mouse IgG conjugated with FITC (Tokyo Chemical Industry Co., Ltd., Tokyo, Japan) at a 1:300 dilution, and counterstained with DAPI at a 1:1000 dilution for 60 min. Throughout the procedure, the samples were washed with normal phosphate-buffered saline (1× PBS) solution four times for 5 min each, except after the application of the blocking buffer before primary antibody incubation.

For CD8 T-cell subset staining, a rabbit anti-mouse CD8a/Lyt2 primary antibody (Nihon Shinobiological Co., Ltd., Tokyo, Japan) was used at a 1:60 dilution. The secondary antibody was goat anti-rabbit IgG conjugated with FITC (Tokyo Chemical Industry Co., Ltd.) at a 1:500 dilution. All other steps were conducted as described for CD4 staining. All chemical reagents were diluted in 1× PBS. After washing with PBS, the sample slides were mounted using Mounting Medium (Funakoshi Co., Ltd., Tokyo, Japan) and covered with micro-cover glass of thickness No. 1 (Matsunami Glass Ind., Ltd.).

Table 7. Dietary compositions fed to the pregnant Wagyu cows during nutrient treatment period

Item	Amount
Ingredient, % of diet (fresh matter basis)	
Formula feed	7.30
Rice straw	31.61
Rice whole crop silage	21.02
Dried timothy grass	7.88
Rye straw	7.55
Brown rice	3.94
Beer lees	3.28
Sugar cane pellets	3.28
Tofu lees	2.63
Soy sauce cake	2.30
Sugar cane bagasse	1.97
Rice bran	1.31
Corn steep liquor	0.99
Condensed potato distilled soluble	0.66
Rice trienol	0.66
Calcium	0.33
Moisture	3.28
Nutrient composition, % Dry matter (DM) basis	
Dry matter (DM)	68.00
Neutral detergent fiber	56.10
Acid detergent fiber	36.00
Crude ash	11.10
Crude protein	8.00
Calcium	0.60
Phosphorus	0.30
Metabolizable energy, MJ/kg DM	8.56

Data analyses

Following staining, images of samples for histological and immunohistochemical analyses were acquired using a Keyence BZ-9000 Fluorescence Microscope (Keyence Corporation, Osaka, Japan). The areas of the medulla and HCs were measured. Nuclei and T-cell subsets ($CD4^+$ and $CD8^+$) were quantified from four representative images at the peak detection medullary area for each sample at 40× magnification, encompassing an area of 98,849.053 square micrometers (μm^2) per image. Measurements of medullary area, HC size, and the counts of nuclei and T-cell subsets were performed using Keyence BZ-II analyzer software (Keyence Corporation). The numbers of nuclei and T-cell subsets per image were normalized to cell density per square millimeter ($cell/mm^2$) using the following mathematical equation:

$$Cell\ density\ (cells/mm^2) = \left(\frac{N_{cells}}{A_{\mu m^2}}\right) \times 1{,}000{,}000$$

Here, N_{cells} represents the average number of nuclei or T cells counted per image of each sample, $A_{\mu m}{}^2$ represents the area of the image used for cell counting (98,849.053 μm^2), and 1,000,000 is the conversion factor from mm^2 to μm^2.

A statistical comparison of thymus components between the two groups was performed using Student's t-test. Results were considered statistically significant at $p \leq 0.05$ and indicative of a trend at $p \leq 0.10$.

3.3. Results

Effect of MNR on thymus phenotype

To investigate the effects of maternal nutrient restriction (MNR) on the physiological adaptation of the fetal thymus, I initially measured the body and thymus masses of the calves and found substantially lower fetal body and thymus masses in the low-nutrient (LOW) group than in the high-nutrient (CON) group ($p < 0.01$; Table 8). Furthermore, the ratios of the fetal thymus and total fetal masses were significantly lower in the LOW group ($p < 0.05$; 0.65 and 0.45 in the CON and LOW groups, respectively). Thus, fetal growth and thymic growth were impaired in the MNR group.

Histological structure

Hematoxylin and eosin (H&E) staining revealed the overall structure of the bovine thymus. The LOW group exhibited a richer capsule and intralobular septum, with a clearer intralobular compartment compared with the CON group (Figure 10A and 10B). By contrast, the CON group displayed adipose cells in the intralobular septa junction and capsule (Figure 10A, 10C, and 10E). The smallest medulla areas were 743.39 and 677.03 μm^2, whereas the largest were 3,558.43 and 3,422.61 μm^2 for the CON and LOW groups, respectively. Statistical analysis revealed that the medulla area was significantly smaller in the LOW group than in the CON group ($p < 0.01$). Both groups showed variability in the size and number of medullary areas within the intralobular regions (Figure 11A–F). The size of HC cells varied, with the smallest sizes being 62.93 and 56.94 μm^2, and the largest being 890.71 and 684.69 μm^2 for the CON and LOW groups, respectively. There was no significant difference in the size of HC cells between the two groups (Table 9).

Both groups exhibited key histological components, including mature thymocyte (MT), immature thymocyte (IMT), dead cell (D), venule (Ve), epithelioreticular cell (EpR), and keratin ring, within the HCs (Figure 11C and 11D).

Immunohistochemistry

Immunohistochemistry staining revealed a high density of $CD4^+$ and $CD8^+$ T cells within the medulla, an area characterized by low thymic nucleus density (Figures 12 and 13). Comparison of thymic nuclei between the two groups indicated that the LOW thymus exhibited a trend towards a smaller number of nuclei than that in the CON group ($p < 0.10$, Table 10). Analysis of T-cell subsets showed that the LOW group had a significantly greater number of $CD4^+$ T cells and a higher $CD4^+$ T-cell-to-nucleus ratio than the CON group ($p < 0.001$). However, the number of $CD8^+$ cells and the $CD8^+$ T-cell-to-nucleus ratio did not differ significantly between the two groups ($p > 0.10$). Additionally, the $CD4^+$ to $CD8^+$ ratio in the LOW group was significantly higher ($p < 0.05$) than that in the CON group (Figure 14).

Table 8. Effect of low maternal on the phenotype of the fetal thymus

Component	CON (n = 6)		LOW (n = 5)		Ratio	
	Mean	**SEM**	**Mean**	**SEM**	**LOW/CON**	***p*-value**
Fetal age, d	261.2	1.3	261.6	1.6	1.0	0.835
Fetal weight, g	32,653.3	448.5	23,976.0	2,540.9	0.7	0.005
Thymus, g	212.0	21.2	110.5	22.2	0.5	0.009
Ratio, %	0.65	0.001	0.45	0.001	0.7	0.046

SEM: standard error of the mean.

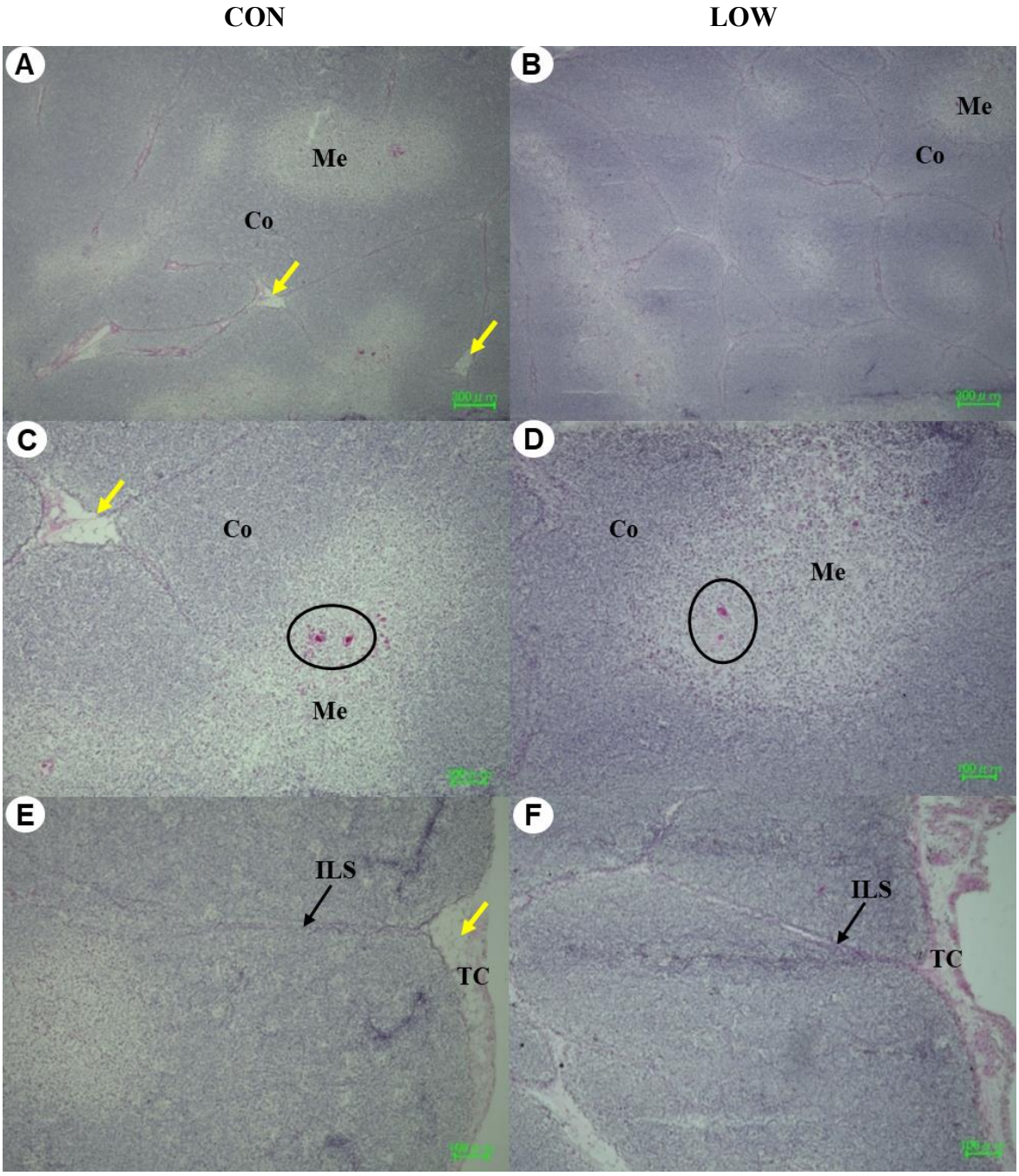

Figure 10. H&E staining provides an overview of the representative histological structure for the CON and LOW groups. The CON group is shown in images **A**, **C**, and **E**, while the LOW group is shown in images **B**, **D**, and **F**. Me: medullary region; Co: cortical region. Yellow arrows highlight adipose cells within the thymic capsule and intralobular septa. ILS: intralobular septum; TC: thymic capsule. The circles in **C** and **D** indicate Hassall's corpuscles (HCs) located within the medullary region. Images were captured at magnifications of 4× (**A** and **B**) and 10× (**C**–**F**).

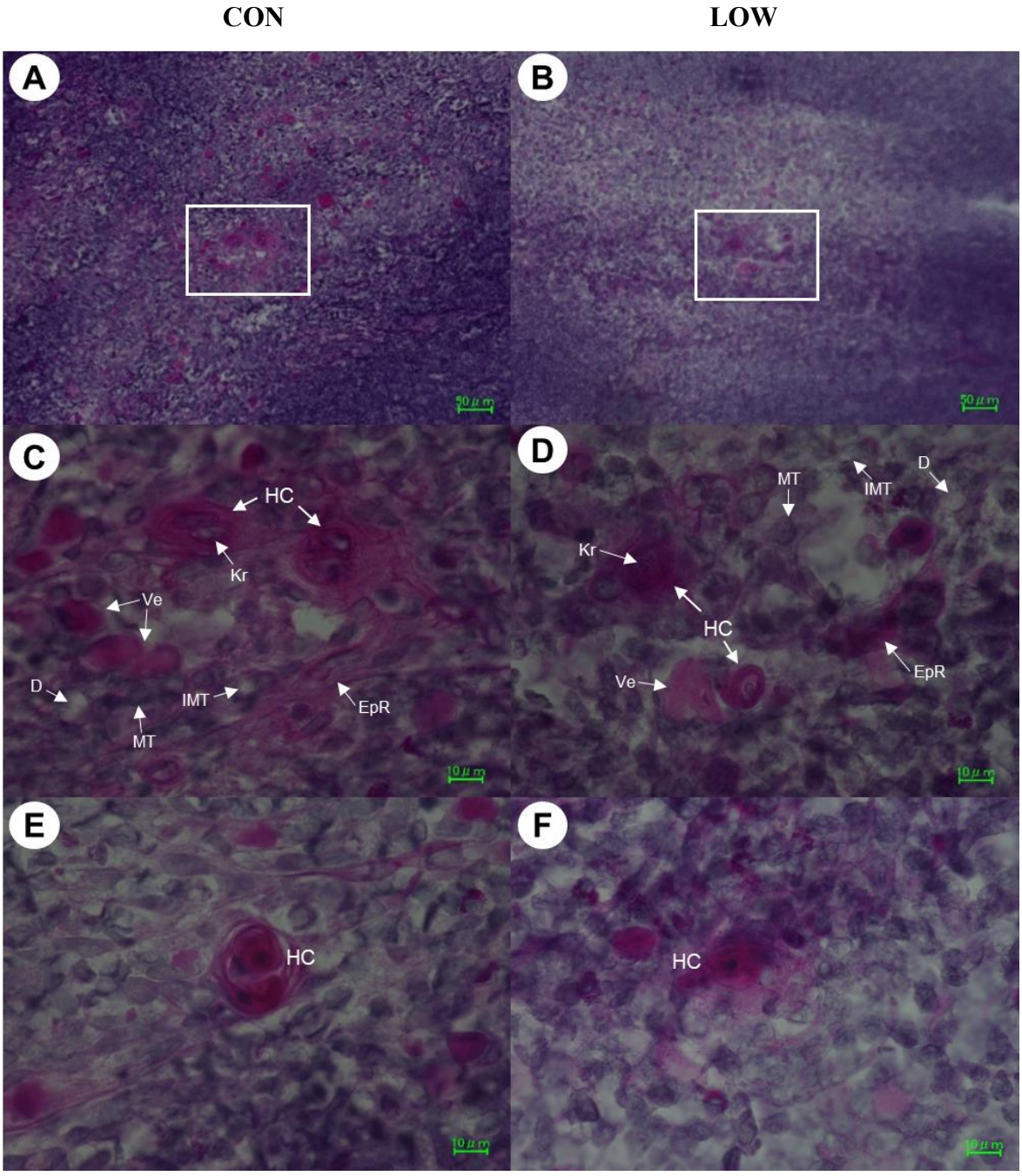

Figure 11. H&E staining depicts the representative thymic medullary histology for the CON and LOW groups. The CON group is shown in images **A**, **C**, and **E**, while the LOW group is shown in images **B**, **D**, and **F**. **A** and **B** highlight multiple HC cells, indicated by square frames. **C** and **D** illustrate the histological structure, showing multiple HC cells in the medullary area at a broader perspective than **A** and **B**. **E** and **F** depict a representative single HC cell for each group. D: dead cell; EpR: epithelioreticular cell; IMT: immature thymocyte; Kr: keratin ring; MT: mature thymocyte; Ve: venule. E and F show a single HC cell. Images were captured at magnifications of 40× (**A** and **B**) and 100× (**C**–**F**).

Table 9. A comparative analysis of the areas of Hassall's corpuscles and the medulla in the fetal thymus between the CON and LOW groups

Item	CON (n = 6)		LOW (n = 5)		CON/LOW	*p-value*
	Mean	**SEM**	**Mean**	**SEM**		
Hassall's corpuscle (μm^2)						
No.	90		70			
Min	62.93		56.94		1.11	
Max	890.71		684.69		1.30	
Mean	*232.91*	*18.97*	*205.05*	*17.70*	*1.14*	*0.295*
Medulla (μm^2)						
No.	35		35			
Min	743.39		677.03		1.10	
Max	3,558.43		3,422.61		1.04	
Mean	*2,033.40*	*114.12*	*1,469.02*	*96.59*	*1.38*	*0.0003*

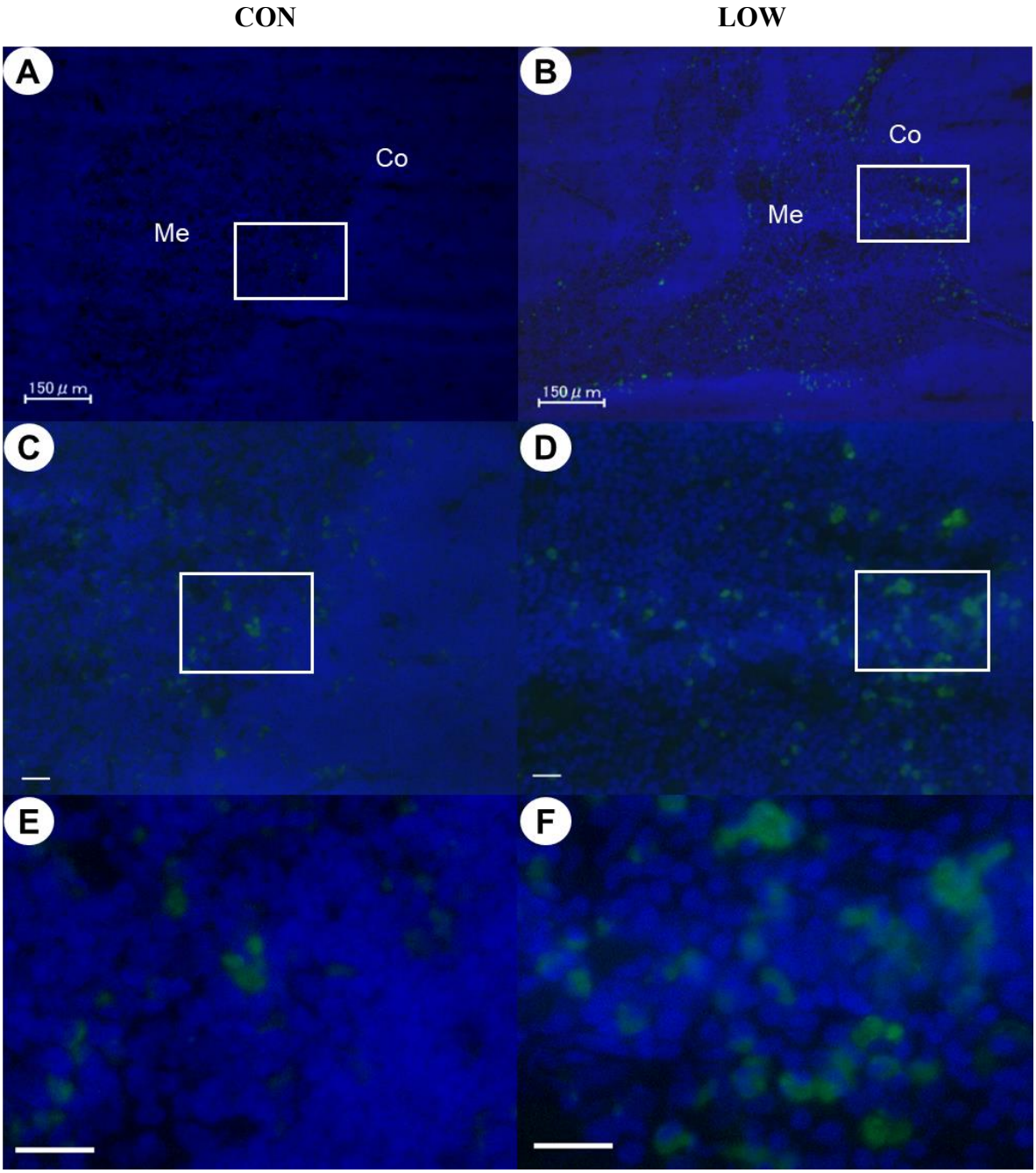

Figure 12. Representative images of immunofluorescent staining for $CD4^+$ T cells and thymic nuclei. $CD4^+$ T cells (green) and thymic nuclei stained with DAPI (blue) are shown for both CON and LOW groups. **A** and **B** depict the lower density of thymic nuclei with $CD4^+$ in the medullary region (Me) and the higher density of thymic nuclei without $CD4^+$ in the cortical region (Co). **C** and **D** show the medullary region, including $CD4^+$ T cells, at a higher magnification than **A** and **B**. Images E and F provide a further zoomed-out view of the medullary region displayed in **C** and **D**. Images were captured at 10× magnification (**A** and **B**) and 40× magnification (**C** and **D**), with additional regions displayed at 1.5× zoom-out (**E** and **F**). Scale bars: 20 μm (**C**–**F**).

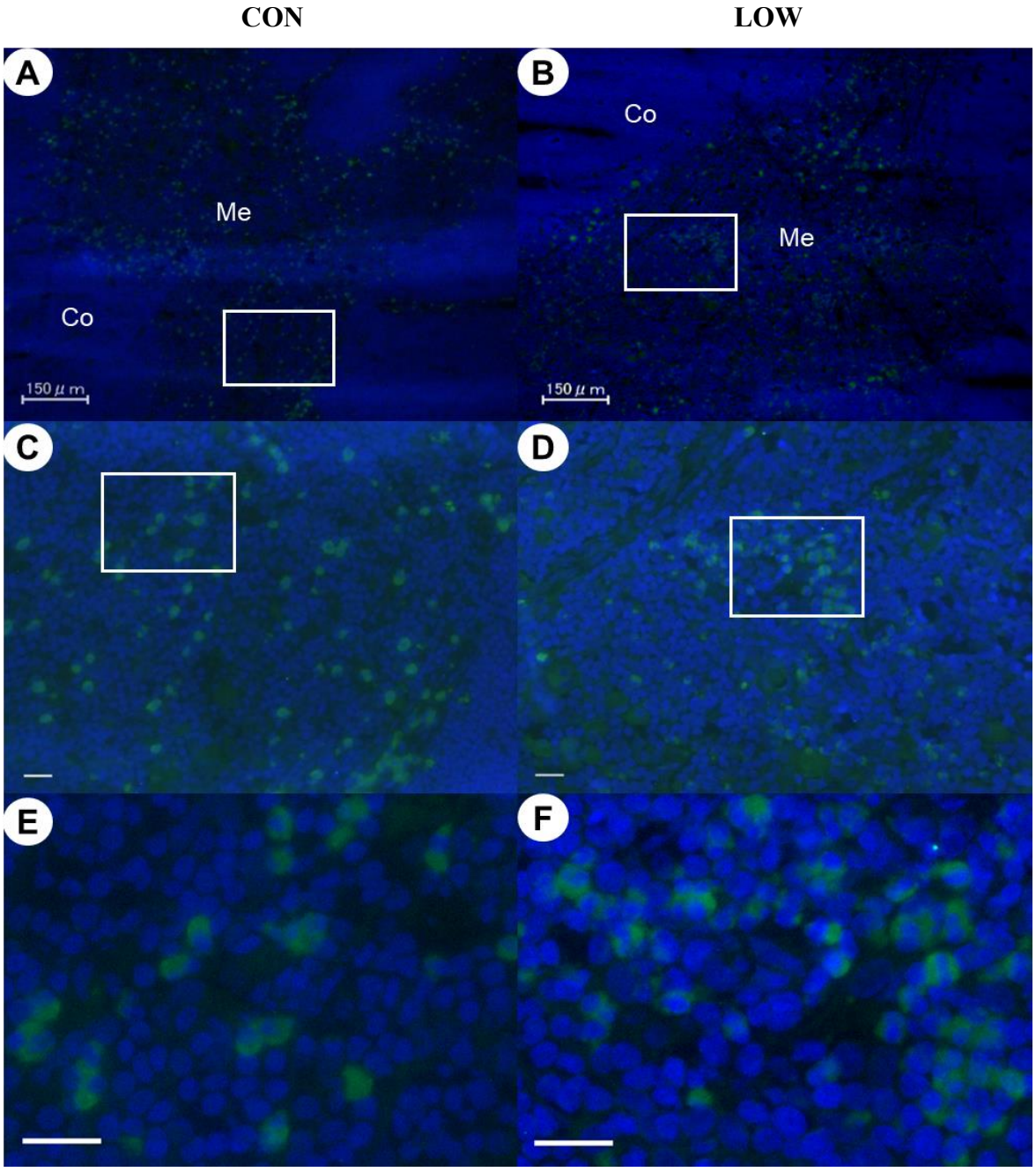

Figure 13. Representative images of immunofluorescent staining for $CD8^+$ T cells and thymic nuclei. $CD8^+$ T cells (green) and thymic nuclei stained with DAPI (blue) are shown for both CON and LOW groups. **A** and **B** depict the lower density of thymic nuclei with $CD8^+$ in the medullary region (Me) and the higher density of thymic nuclei without $CD8^+$ in the cortical region (Co). **C** and **D** show the medullary region, including $CD8^+$ T cells, at a higher magnification than **A** and **B**. Images **E** and **F** provide a further zoomed-out view of the medullary region displayed in **C** and **D**. Images were captured at 10× magnification (**A** and **B**) and 40× magnification (**C** and **D**), with additional regions displayed at 1.5× zoom-out (**E** and **F**). Scale bars: 20 μm (**C**–**F**).

Table 10. Comparative analysis of the nucleus, and $CD4^+$ and $CD8^+$ T cells in the bovine fetal thymus between the CON and LOW groups

Item	CON		LOW		Ratio LOW/CON	*p-value*
	Mean	**SEM**	**Mean**	**SEM**		
Sample no.	6		5			
Nucleus, cell/mm^2	20,313.8	755.8	18,470.1	341.8	-1.10	0.068
$CD4^+$, cell/mm^2	319.9	26.7	757.7	83.3	2.37	0.0004
Ratio[a], %	1.58	0.14	4.08	0.39	2.58	0.0001
Nucleus, cell/mm^2	20,188.6	801.7	18,404.3	291.6	-1.10	0.086
$CD8^+$, cell/mm^2	486.0	61.2	526.5	107.1	1.08	0.470
Ratio[b], %	2.47	0.37	3.12	0.56	1.26	0.343
CD4/CD8	0.74	0.14	1.06	0.28	1.44	0.038

[a,b] Ratio of T cell subsets to nucleus number in the selected areas for $CD4^+$ and $CD8^+$ counts, respectively.

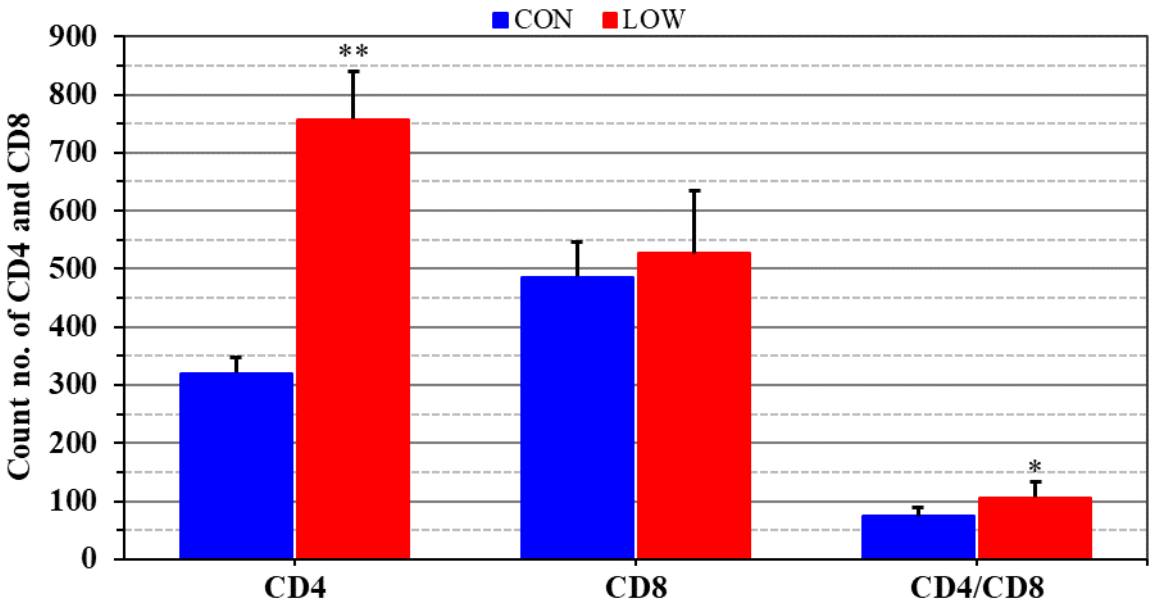

Figure 14. Comparison of $CD4^+$ and $CD8^+$ T cells in the bovine fetal thymus between the CON and LOW groups (cell/mm^2). CD4/CD8 represents the ratio of $CD4^+$ to $CD8^+$ T cells within each group (ratio value × 100). *: $p < 0.05$; **: $p < 0.01$. Error bars indicate standard error of the mean (SEM).

3.4. Discussion

There is a growing debate in the livestock industry regarding stress and its negative effects on animal welfare, as well as regarding the psychologic and physiologic responses of animals to conventional agricultural practices and advanced production technologies. Stress has various causes in animals that are both internal and external and affect their immune function, feed intake, fertility, and overall well-being (Grandin, 2018). Adequate nutrition during gestation is crucial for maternal health and fetal development, optimal growth, the prevention of congenital anomalies, and the long-term health of the offspring. In contrast, maternal nutrient restriction (MNR) can cause significant congenital anomalies by reducing the supply of vital nutrients, which reduces cellular proliferation and differentiation, and, therefore, fetal organ development (Wu et al., 2004).

In humans, placental insufficiency, leading to fetal growth restrictions, is linked to a lower birth weight and smaller visceral organs, including the thymus gland (Takeno and Nomura, 2023). Research in Wistar rats has shown that nutrient restriction during the latter two-thirds of pregnancy results in smaller fetuses and a low fetal thymic mass, compared to fetuses from adequately nourished mothers (Gotardo et al., 2017). Likewise, pregnant guinea pigs that experience nutrient restriction during pregnancy exhibit changes in fetal body composition and thymus mass (Sohlstrom et al., 1998). In addition, nutrient-restricted pregnant ewes have been shown to produce offspring of small sizes, organ dimensions, and thymic mass (Osgerby et al., 2002). The present findings are consistent with these previous observations made in various animal models, suggesting that MNR alters fetal composition and organ development (Zhang et al., 2021). In particular, I have identified the thymus as an organ that is particularly susceptible to the detrimental effects of nutritional deficiency.

The thymus exhibits bilateral symmetry with two lobes connected by an isthmus. Each lobe contains multiple lobules, defined by intralobular septa extending from the capsule. These lobules consist of distinct regions: the outer cortex, densely packed with immature T thymocytes and exhibiting intense staining; and the inner medulla, which has lighter staining and lower cellular density, contains HCs, and is the site at which mature T cells localize (Wang et al., 2019). In a study of lamb fetal thymus, low maternal energy intake during late pregnancy resulted in an enlarged medullary region (Liu et al., 2015). By contrast, the present study indicates that the LOW group exhibited a reduced medullary region in the Wagyu fetal thymus compared with the CON group. This discrepancy suggests that the medullary structure is influenced by overall organ size in the bovine fetal thymus, implying a species-specific response to maternal nutritional status. Thus, maternal nutritional restriction appears to differentially affect thymic development in lambs and bovines, potentially reflecting variations in developmental and adaptive mechanisms across species.

The development of T cells within the thymus is essential for establishing a functional and self-tolerant adaptive immune system. The population of $CD4^+CD8^+$ DP thymocytes peaks early in fetal thymic development and progressively declines as gestation advances. Concurrently, there is an accumulation of mature $CD4^+$ and $CD8^+$ SP thymocytes, particularly in late gestation, when the thymus favors the positive selection of the $CD4^+$ lineage (Fairchild and Austyn, 1995). In this study, the expression of $CD4^+$ and $CD8^+$ single-positive (SP) T cells was observed within the thymic medullary region. This observation strongly supports the notion that $CD4^+$ and $CD8^+$ T cells, subsequent to positive selection, migrate to and populate the thymic medulla. Within this medullary microenvironment, selected SP thymocytes undergo additional differentiation and functional maturation processes before egressing as mature naive T cells into circulation and peripheral lymphoid tissues, thereby contributing to immune system functionality (Xu and Ge, 2014). This

process is essential for the fetal thymus in preparing intrauterine immunity for the external environment postnatally. This study revealed a notable increase in the $CD4^+$ thymocyte population and the $CD4^+/CD8^+$ ratio in the Wagyu fetal thymus under conditions of low maternal nutrition (LOW) compared with those in the high-nutrition (CON) group. However, this nutritional restriction did not affect the $CD8^+$ thymocyte expression. This observation is consistent with findings in fetal lambs, where low maternal energy intake during late gestation increased $CD4^+$ expression, while $CD8^+$ expression remained unchanged (Liu et al., 2015). Similarly, an increased proportion of $CD4^+/CD8^+$ single-positive T cells was observed in the thymus of adult rats subjected to low-protein maternal diets compared with that in control animals (Armengaud et al., 2020). The increase in $CD4^+$ T cells in this study may indicate a compensatory mechanism in response to maternal nutritional stress, prioritizing the development of helper T cells ($CD4^+$). Helper T cells are crucial for orchestrating immune responses by facilitating the activation of other immune cells, such as B cells and cytotoxic T cells (Alberts et al., 2002). This skewing towards $CD4^+$ cell proliferation could be an adaptive response to ensure robust immune capability under adverse conditions. The lack of change in the $CD8^+$ T-cell population under MNR suggests that cytotoxic T-cell development is less sensitive to nutritional variations during the fetal period. This stability might indicate a more resilient developmental pathway for $CD8^+$ T cells, ensuring the preservation of cytotoxic immune functions even when maternal nutrition is compromised.

Similarly, the size of HCs remained unaffected by low maternal nutrition. HCs play a role in the maturation and regulation of T cells, including the induction of regulatory T cells and the facilitation of negative selection, which might be regulated by different mechanisms that are less dependent on nutritional status. The size of HCs showed a wide range (100–900 μm) in the human fetal thymus (Asghar et al., 2012). It is reported that the growth of

thymic HCs rapidly increased around 28 weeks of gestation. In advanced stages of gestation, the increase in size of some HCs reduced the spaces between them, and some patterns suggested the fusion of multiple corpuscles into larger single structures (Asghar et al., 2012). Our present study found that the area of HCs ranged from approximately 57 to 685 and 63 to 891 μm^2 for the LOW and CON groups, respectively (Table 9). The stability in HC size suggests that the structural integrity and function of these components are maintained, ensuring the continued ability of the thymus to support T-cell maturation and selection processes. These findings suggest a compensatory mechanism prioritizing helper T-cell development to maintain robust immune function under nutritional stress.

3.5. Summary

The objective of this investigation was to elucidate the impact of MNR on the histological features and expression of T-cell subsets within the fetal thymus of Wagyu cattle. The findings demonstrate that MNR during gestation results in reduction of the medullary compartment, and an augmentation in the $CD4^+$ thymocyte population and an elevated $CD4^+/CD8^+$ ratio, while exerting no discernible effect on the $CD8^+$ population or the size of HC cells in the Wagyu fetal thymus. These results provide significant insights into the crucial role of maternal nutrition in shaping the developmental trajectory of the immune system in Wagyu cattle.

Chapter 4

Maternal nutrient restriction affects DNA methylation and gene expression associated with metabolism and immunopoiesis in the Wagyu fetal thymus

4.1. Maternal nutrient restriction influences DNA methylation linked to cellular function stability in the Wagyu fetal thymus

4.1.1. Introduction

Maternal undernutrition, characterized by inadequate intake of essential nutrients during pregnancy, has profound implications for the developing fetus, particularly impacting the immune system through epigenetic modifications such as DNA methylation. The thymus, an essential organ for immune system development, is especially susceptible to these changes (Morimoto et al., 2021). DNA methylation, a key epigenetic mechanism, involves the addition of methyl groups to DNA, typically at CpG sites, regulating gene expression without altering the DNA sequence. Maternal nutrition is crucial in providing necessary methyl donors required for these methylation processes. Inadequate maternal nutrition can disrupt these processes, leading to aberrant methylation patterns that affect tissue development and function (Randunu and Bertolo, 2020). Research on human populations experiencing high rates of maternal and child undernutrition has shown that seasonal variations in maternal nutrition influence methylation status at various loci, affecting genes associated with immune responses and disease susceptibility in offspring (Quilter et al.,

2021). Studies in animal models have also demonstrated that maternal nutrient restriction (MNR) impairs fetal thymus development and immune system function (Liu et al., 2015; Armengaud et al., 2020). However, the understanding of immune system development during the fetal period in large ruminants, including Wagyu cattle, remains limited. As described in Chapter 3, I investigated the fetal thymus and found that MNR affected fetal thymus mass, medullary compartment, and $CD4^+$ T-cell expression. I hypothesized that differences in fetal thymus size, histology, and T-cell subsets may be related to changes in cellular function due to epigenetic regulation, such as DNA methylation. This study was intended to investigate the effect of MNR on DNA methylation and its association with cellular function stability in the Wagyu fetal thymus.

4.1.2. Materials and Methods

Experimental treatments

The experimental design, animal management, and sample collection were carried out as previously detailed in Chapter 3.

Whole genome bisulfite sequencing (WGBS) and library preparation

Genomic DNA was extracted from the thymuses of three fetuses from each of the LOW and CON groups. The DNA methylation analysis was conducted by Rhelixa Co. Ltd., Tokyo, Japan. Genomic DNA was extracted from 30 mg frozen bovine fetal thymus tissue per sample using a Monarch Genomic DNA Purification Kit (New England Biolabs, Ipswich, MA, USA). The purity, concentration of nucleic acids, and degree of degradation of the isolated DNA were assessed using the NanoDrop One system (Thermo Fisher Scientific, Waltham, MA, USA). The DNA was quantified using Genomic DNA ScreenTape

and Genomic DNA ScreenTape Sample Buffer, according to the protocol outlined in the Agilent Genomic DNA ScreenTape System Quick Guide (Agilent Technologies, publication number G2964-90040 rev.C, 2014). Libraries were generated according to the manual for the DNA Swift Biosciences™ Accel-NGS® Methyl-Seq DNA Library Kit (Swift Biosciences, Inc., Ann Arbor, MI, USA). To ensure robust protection against DNA denaturation during WGBS analysis, I applied the EZ DNA Methylation-Gold Kit (Zymo Research, Irvine, CA, USA), which combines DNA denaturation and bisulfite conversion in a single step, enhancing conversion efficiency and reducing the processing time for high-throughput sequencing.

Whole-genome bisulfite sequencing data processing

A quality assessment of the raw paired-end sequence reads was conducted using FastQC v0.11.7. The trimming of low-quality bases (Phred score <20) or the first 10 bases from the 5′ end, as well as the removal of adapter sequences, was performed using TrimGalore (Version 0.5.0) and the options "-q 20 --phred33 --clip_R1 10 --clip_R2 10 –paired" (Asselman, 2019). The reads were aligned to the bovine reference genome (ARS-UCD1.2/bos, available online at https://www.ncbi.nlm.nih.gov/datasets/genome/GCF_002263795.1/), accessed on 15 October 2023; and processed using methylpy v1.4.6 and the options "--remove-clonal True --trim-reads FALSE" (Schultz et al., 2015).

Analyses of DMRs and DMGs

The tileMethylCounts function in the methylKit (Version 1.10.0) package was employed to estimate the number of methylated cytosines in 1,000-base non-overlapping windows across the entire genome. Normalization was conducted using the normalizeCoverage function in methylKit. Bases with <10 read coverage and bases with

coverage exceeding the 99.9th percentile in each sample were filtered out using the filterByCoverage function of methylKit. Subsequently, all the samples were merged using the unite function in the methylKit with the destrand = FALSE option (Akalin et al., 2012). DMRs were identified with $q < 0.01$, and regions showing a difference in methylation of >25% between groups were considered to be significantly differentially methylated. In instances where there was an overlap between a DMR and a specific gene functional element, the associated gene was classified as a DMG.

Hierarchical clustering analysis

To depict the patterns of methylation, an online data visualization and graphing platform (http://www.bioinformatics.com.cn/en; accessed on 18 January 2024) (Tang et al., 2023) was employed Hierarchical clustering analysis (HCA). The HCA was executed using a matrix with Euclidean distance as the distance metric and complete linkage as the method, facilitating the graphical classification of DNA methylation patterns, and sample relationships.

Gene functional enrichment analysis

To characterize the biologic functions of DMGs, a KEGG pathway enrichment analysis using the ShinyGO Bioinformatics database v.0.80 (http://bioinformatics.sdstate.edu/go/ (Ge et al., 2020); accessed on 14 February 2024) was performed.

4.1.3. Results

Mapping Landscape of DNA Methylation

For the WGBS analysis, I selected six bovine fetal thymuses: the three from the LOW group that had the lowest body mass, and the three from the CON group that had the highest body mass, thereby aiming to exaggerate the potential differences between the groups. WGBS generated a total of 610 million and 623 million raw reads, respectively. After filtering the raw read data, 609 million and 622 million clean reads were obtained. Approximately 331 million and 351 million of these clean reads were successfully mapped to the reference genomes, with unique matches for the LOW and CON groups, respectively. The mapping efficiency for the LOW group ranged from 53.4% to 55%, and for the CON group, it ranged from 53.6% to 58.3% of the bovine genome, respectively (Table 11). The overall methylation patterns of the two groups were visualized using a heatmap of the results of hierarchical clustering analysis (Figure 15A).

Pattern of methylation (DMR and DMG)

A total of 13,796 DMRs were identified for the fetal thymuses of the two groups ($q < 0.01$), encompassing 8,869 DMGs. Of these, 4,566 genes exhibited hypomethylation, and 4,303 genes showed hypermethylation in the LOW group compared to the CON group. The DMRs were predominantly situated in intergenic regions, comprising more than half of the total methylation percentage, followed by introns, intron-exon boundaries, and 1-5 kb regions around the genes, promoters, and exons, respectively (Table 12).

The chromosomal distribution of DMRs was characterized by higher abundance on chromosomes 3, 2, 1, and 4. Conversely, chromosomes 25, 24, 27, and X had the fewest DMRs, with respect to both hypo- and hypermethylation (Figure 15B).

Table 11. DNA methylation mapping efficiency of the fetal thymus of two groups

Sample	Total reads	Trimmed Reads	Mapped reads	Mapping rate (%)
LOW187	601,244,050	600,376,764	327,934,280	54.6
LOW663	621,172,290	620,552,580	340,998,054	55.0
LOW795	609,158,064	608,472,000	325,000,478	53.4
CON4615	604,944,926	604,323,810	323,766,500	53.6
CON678	660,953,290	660,117,480	379,730,304	57.5
CON796	603,299,248	602,351,394	351,257,702	58.3
LOW	**610,524,801.3**	**609,800,448.0**	**331,310,937.3**	**54.3**
CON	**623,065,821.3**	**622,264,228.0**	**351,584,835.3**	**56.5**

Table 12. Number of differentially methylated regions for each genomic region in LOW fetal thymus[1]

Genomic Regions	Hypo-DMR		Hyper-DMR		Ratio (Hypo/Hyper)
	Count	%	Count	%	
Promoter	63	0.9	111	1.7	0.6
1-5 kb	278	3.8	253	3.9	1.1
Exon	55	0.8	76	1.2	0.7
Intergenic	3,876	52.9	3,317	51.2	1.2
Intron	2,220	30.3	1,891	29.2	1.2
Intron-exon boundary	764	10.4	765	11.8	1.0
None	65	0.9	62	1.0	1.0
Total	**7,321**	**100.0**	**6,475**	**100.0**	

[1] Number of differentially methylated counts in the thymuses of LOW and CON fetuses, separately indicated as hypermethylation or hypomethylation.

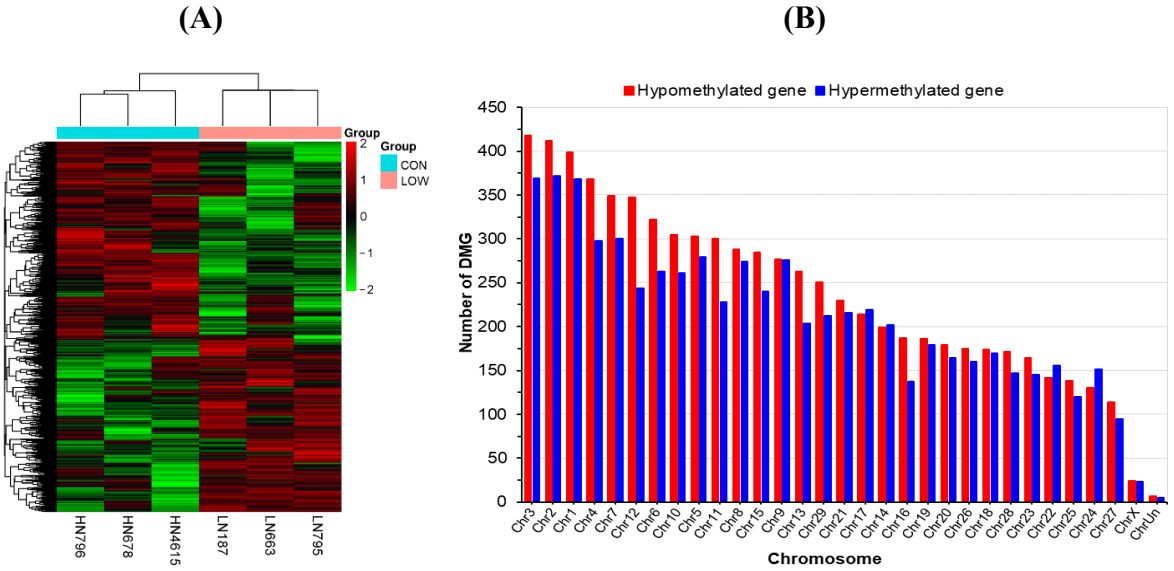

Figure 15. The pattern of DNA methylation in the Wagyu fetal thymus. (**A**) Heatmap showing the hierarchical clustering of differential methylation in the genomic regions for LOW (salmon pink) and CON (green blue) fetal thymuses, comparing DNA methylation levels between LOW and CON ($q < 0.01$). There were 4,566 hypoDMGs and 4,303 hyperDMGs in the LOW group and the CON group. The row represents the gene, and the column denotes the sample. Red: hypermethylated genes; green: hypomethylated genes. The darkness of each color corresponds to the magnitude of the difference vs. the mean value. (**B**) Chromosomal distribution of DMRs in the LOW and CON thymuses. ChrUn: unplaced chromosome. Hypermethylation and hypomethylation DMGs in LOW fetal thymuses are indicated in blue and red, respectively.

Functional enrichment analysis of DMG

To investigate the potential biological roles of DMGs, I used the Kyoto Encyclopedia of Genes and Genomes (KEGG) to identify relevant pathways. The top 20 pathways that differed ($q < 0.0001$) included the cAMP signaling pathway, the Rap1 signaling pathway, and the inflammatory mediator regulation of the TRP channels, all of which were represented by both hypomethylated and hypermethylated DMGs. Notably, Hippo signaling and the parathyroid hormone pathway were predominantly associated with the hypermethylated genes, whereas the hypomethylated genes were significantly associated with the cGMP-PKG signaling pathway, GABAergic synapses, and insulin secretion (Figure 16).

For the remaining pathways which significantly differed ($q < 0.001$), I excluded common pathway terms. Among the pathways associated with hypoDMGs were the Ras signaling pathway and insulin, GnRH, cortisol, oxytocin, and aldosterone secretion. In addition, hyperDMG was associated with Fc gamma R-mediated phagocytosis and the Wnt signaling pathway (Tables 13). Several DMGs are important regulators of metabolic processes, growth dynamics, and the responses to various stressors. These genes, which include *CREB1*, *ADCY1*, *SLC25A4*, *FGF10*, *IGF1R*, *CACNA1D*, *MAPK3*, *SOS1*, *PAK1*, and *STAT3*, are associated with diverse signaling pathways (Table 14).

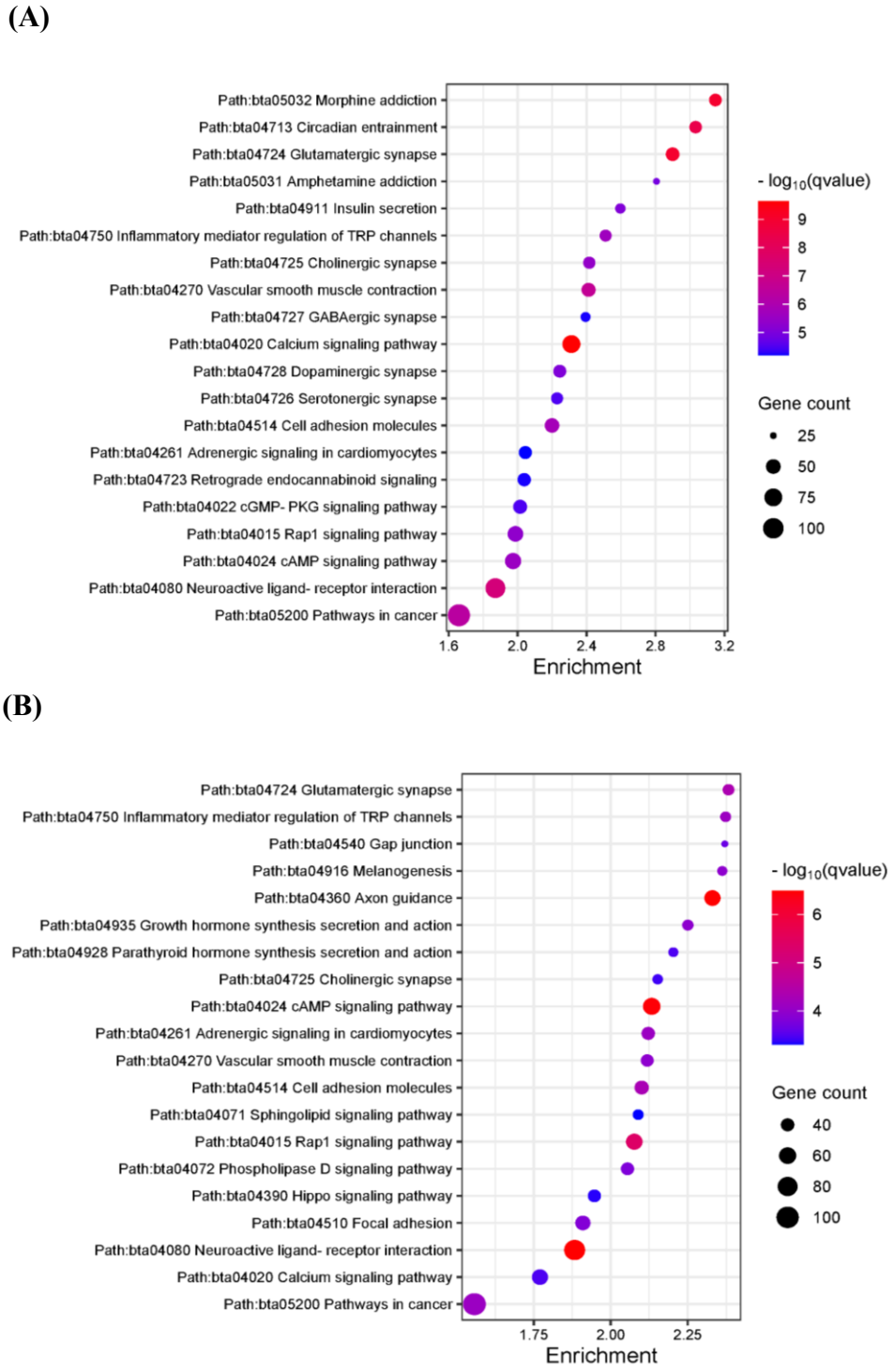

Figure 16. Scatter plot of KEGG pathway enrichment, depicting the top 20 significant pathways associated with DMRs. (**A**) Genes associated with all hypoDMRs. (**B**) Genes associated with all hyperDMRs. The y-axis represents the pathway terms, and the x-axis represents fold enrichment (the proportion of differentially methylated genes (DMGs) vs. all genes annotated with a specific pathway term). The size of the dots indicates the number of genes, and the color reflects the −log10(*q*-value).

Table 13. Top significant pathways out of the top 20 KEGG pathways, extracted from hypo- and hypermethylated genes in the promoter, gene body, and/or UTRs[1]

Methylated Genes	KEGG Pathway	nGene[2]	*q*-value
Hypo			
	Path:bta04720 Long-term potentiation	23	0.00007
	Path:bta04360 Axon guidance	47	0.00010
	Path:bta04924 Renin secretion	24	0.00015
	Path:bta04072 Phospholipase D signaling pathway	40	0.00015
	Path:bta04927 Cortisol synthesis and secretion	23	0.00015
	Path:bta04921 Oxytocin signaling pathway	40	0.00018
	Path:bta04925 Aldosterone synthesis and secretion	29	0.00018
	Path:bta04971 Gastric acid secretion	24	0.00027
	Path:bta04540 Gap junction	27	0.00035
	Path:bta04912 GnRH signaling pathway	27	0.00035
	Path:bta04916 Melanogenesis	29	0.00038
	Path:bta04935 GH synthesis secretion and action	32	0.00039
	Path:bta04970 Salivary secretion	27	0.00039
	Path:bta05207 Chemical carcinogenesis-receptor activation	48	0.00039
	Path:bta05033 Nicotine addiction	15	0.00039
	Path:bta05414 Dilated cardiomyopathy	28	0.00039
	Path:bta04810 Regulation of actin cytoskeleton	51	0.00040
	Path:bta04730 Long-term depression	20	0.00041
	Path:bta04014 Ras signaling pathway	55	0.00050
	Path:bta04926 Relaxin signaling pathway	34	0.00081
Hyper			
	Path:bta04666 Fc gamma R-mediated phagocytosis	27	0.00070
	Path:bta05032 Morphine addiction	26	0.00070
	Path:bta05231 Choline metabolism in cancer	27	0.00070
	Path:bta04310 Wnt signaling pathway	40	0.00096

[1] KEGG pathways obtained from DM genes in the LOW fetal thymuses, separately indicated as related to hypermethylation or hypomethylation.
[2] number of genes are enriched to each pathway term.

Table 14. Hypo- and hypermethylated genes associated with thymus growth, immunity, and protein, cholesterol, and mitochondrial metabolism

Gene Name	Entrez	Chr	Position	Genomic region	Methylation
CREB1	281713	2	95.846071	Intergenic, Intron	Hypo, Hyper
ADCY1	281601	4	76.174089	Intergenic	Hypo
SOS1	537682	11	21.308259	Intergenic/Intron	Hypo
STAT3	508541	19	42.417949	Intron	Hypo
FGF10	326285	20	30.504441	Intron	Hypo
IGF1R	281848	21	7.780293	Intronexonboundary	Hypo
CACNA1D	408013	22	47.162857	Intronexonboundary/Intron	Hypo
MAPK3	531391	25	26.178468	Intronexonboundary, Promoter	Hypo, Hyper
SLC25A4	282478	27	15.48947	Intronexonboundary	Hyper
PAK1	533729	29	18.521064	Intergenic/Intron	Hypo

4.1.4. Discussion

The finding in the chapter 3 revealed significant alterations in the phenotype of fetal thymuses in the LOW group, indicating potential disruptions to genomic features crucial for thymic molecular and cellular functions due to inadequate maternal nutrition. This chapter aimed to investigate the effects of substantial MNR during pregnancy on the DNA methylation patterns within the fetal thymus. I identified significant alterations to the phenotype of the thymuses of the fetuses in the LOW group, implying MNR-induced disruptions to genomic features which are crucial for thymic molecular and cellular functions. The analysis of DNA methylation patterns revealed diverse profiles, with the intergenic regions exhibiting the highest methylation levels, followed by the intronic regions, and lower methylation levels in the promoter regions, showing both hypo- and hypermethylation. These findings are consistent with the results of previous investigations conducted in bovine embryos (Duan et al., 2019). Gene promoter methylation is conventionally thought to cause transcriptional suppression and the inhibition of gene expression (de Mendoza et al., 2022). While hypomethylation predominated in shared genomic regions, a different pattern was observed for the LOW group's promoters, in which the hypermethylated genes outnumbered the hypomethylated genes by nearly twofold (Table 13). Previous studies have shown that DNA methylation within the gene body may alter the chromatin structure and thereby influence transcriptional elongation (Lorincz et al., 2004). In addition, DMRs were found to be more abundant in the intergenic and intronic regions, with higher frequencies of methylation being present on chromosomes 1, 2, 3, and 4 and lower frequencies being present on chromosomes 24, 25, 27, and X (Figure 15B). The factors that influence these DNA methylation responses to environmental stimuli include gene density, developmental programming, nutrient-responsive genes, and chromatin

accessibility (Tekola-Ayele et al., 2020). The present findings suggest that chromosomes with a substantial number of DMGs exhibit high sensitivity to MNR in the thymuses of fetal Wagyu cattle.

The KEGG pathway analysis of the DMGs revealed several important upstream pathways among the top 20 significant pathway terms, including cAMP signaling, calcium signaling, and the growth hormone. The downstream pathways included Rap1 signaling, phospholipase D, and the glutamatergic synapse (Figure 16A and B). These pathways play crucial roles in growth, metabolism, gene expression, synaptic plasticity, and neuronal function (Shahoha et al., 2022). These upstream pathways may have significant effects on the metabolism, particularly under conditions of MNR. After excluding the top 20 terms and filtering out the shared pathways, the analysis revealed a 5.0-fold greater proportion of pathways that were associated with hypoDMG compared to hyperDMG (Table 14). This finding implies that MNR influences DNA methylation in the fetal thymus throughout gestation and is consistent with the findings of prior studies that maternal undernutrition modifies the DNA methylation profile of the bovine fetal liver (Muroya et al., 2023).

The hypoDMG-associated pathways were involved in the regulation of cell proliferation, survival, differentiation, and apoptosis, including thymocyte development, such as Ras signaling. In murine studies, the Ras signaling pathway has been shown to be crucial for thymocyte development and T cell selection. This role is mediated via Ras guanine exchange factors, which influence the T cell repertoire at the second T cell receptor checkpoint (Jun et al., 2013). In Ras-deficient mice, *CD4* function is compromised, resulting in a reduction in the production of IFN-γ, a cytokine which is crucial for Th1 cell differentiation (Iborra et al., 2011). The cGMP–PKG signaling pathway is an important regulator of vascular tone, platelet function, and neuronal signaling, and it is also recognized for its involvement in the regulation of the actin cytoskeleton, which can be affected by

nutrient stress (Roy et al., 2022). Cortisol, the primary stress hormone, significantly affects the immune system. Chronic stress increases cortisol concentrations, which reduces the production of inflammatory mediators and cytokines, thereby affecting T cell activity (Padgett and Glaser, 2003). In addition, the GABAergic synapse has been associated with hypoDMG, meaning that, therefore, inhibitory neurotransmitters and synaptic plasticity may also be affected by hypoDMG. The results further imply that the activation of GABAergic synapses is associated with the stress response, and the disruption of these pathways results in cellular dysfunction and an abnormal immune response (Swaney and Li, 2016). HyperDMG was identified in association with the Hippo and Wnt signaling pathways, which are essential for the regulation of organ size, tissue regeneration, and cell proliferation during embryonic development (Li et al., 2019). The present findings suggest that MNR influences DNA methylation, thereby activating these pathways, in a process which would have affected the phenotypic outcomes of the fetus and thymus in the LOW group. Furthermore, the parathyroid hormone (PTH) is important for calcium and phosphate homeostasis. The secretion of PTH during pregnancy is important to prevent vitamin D and calcium deficiency and to promote optimal fetal development (Ali et al., 2021). In addition, the Fc gamma R (FcγR)-mediated phagocytosis of pathogens is crucial for the innate immune response. The activation of FcγRs is required for effector responses, endosomal maturation, and antigen processing (Bournazos et al., 2017), and the results of the present study imply that MNR may inhibit these pathways.

Several DMGs play crucial roles in the regulation of metabolic processes, growth dynamics, and stress responses. These regions are frequently located at the intron-exon boundaries and in introns and intergenic regions. Genes such as *SOS1* demonstrated hypomethylation in both introns and intergenic regions, *STAT3* and *FGF10* exhibited hypomethylation in the intronic regions, whereas *IGF1R* displayed hypomethylation at the

intron-exon boundaries. *ADCY1* was characterized by hypomethylation in the intergenic regions, and *CREB1* displayed hypomethylation in the intergenic regions but hypermethylation in the introns. Similarly, *MAPK3* showed hypomethylation at the intron-exon boundaries and hypermethylation in the promoter region. These findings indicate that MNR affects the gene body, rather than the promoter region, in the thymuses of fetal Wagyu cattle. Conventionally, promoter methylation is thought to have larger effects on gene expression than the methylation of other genomic regions (de Mendoza et al., 2022). However, its effects may not be consistently linear because of complex interactions between the promoter and other genomic regions. For instance, the promoter hypermethylation of *MAPK3* was found to be linked to the FcγR pathway, and it may, therefore, impair immune responses associated with phagocytosis. Conversely, the *MAPK3* hypomethylation at the intron-exon boundary may affect cellular coordination via upstream pathways, such as the glutamatergic synapse, Ras signaling, and GnRH pathways. These findings suggest that MNR modifies DNA methylation patterns. Despite these methylation changes, no significant differences in the gene expression levels were detected, suggesting that these genes might remain transcriptionally inactive under MNR. This may represent a significant mechanism whereby fetuses adapt to survive under conditions of nutrient stress. However, such adaptations may also have consequences for the immunity of the calves.

4.1.5. Summary

This chapter analyzed DNA methylation profiles correlated with cellular changes in the fetal thymus due to MNR. The findings indicated that intergenic regions had the highest levels of methylation, followed by intronic regions, with promoter regions exhibiting relatively low methylation levels, characterized by both hypo- and hypermethylation. KEGG

pathway analysis showed a 5-fold greater prevalence of pathways associated with hypoDMGs compared with hyperDMGs. Hypomethylated genes were linked to the Ras signaling pathway, cGMP–PKG signaling, cortisol synthesis and secretion, and the GABAergic synapse. By contrast, hypermethylated genes were connected to the Hippo and Wnt signaling pathways, and Fc gamma R-mediated phagocytosis. These findings suggest that MNR alters DNA methylation patterns, which in turn affect cellular functionality, and that this may contribute to anomalies in immune-related processes.

4.2. Maternal nutrient restriction alters gene expression in thymic metabolism, stress response, and cellular defense linked to immune function

4.2.1. Introduction

As described above, I investigated alterations in DNA methylation patterns induced by maternal nutrient restriction (MNR), subsequently impacting fetal thymus functionality as evidenced by KEGG pathway analysis. Notably, maternal undernutrition had discernible effects on thymus development, indicated by the differential methylation of genes linked to growth and immune-related processes. Research has highlighted the role of epigenetic mechanisms, encompassing DNA methylation, histone modifications, and regulation by non-coding RNA, in mediating the enduring impact of early-life exposures on gene expression and function (Bure et al., 2022). Environmental factors such as maternal nutrition can influence these epigenetic modifications. Initial investigations have shown that MNR influences DNA methylation and the expression of genes that participate in glucose and lipid metabolism in the fetal liver (Muroya et al., 2022; Muroya et al., 2023). The thymus, which is crucial for immune system development through thymopoietic processes, is required to maintain homeostasis within its microenvironment to ensure optimal T-cell maturation and enhancement of the immune repertoire, particularly in conditions of nutrient deficiency. Several studies have underlined the importance of mitochondrial activity in regulating immune responses and viability under various environment stresses in laboratory animals (Elhage et al., 2024). However, an understanding of the intricate immune orchestration during the fetal period under MNR in large ruminants, including Wagyu cattle, remains

elusive. The work described in this section was intended to investigate the effect of MNR on the expression of genes involved in metabolism in the fetal thymus.

4.2.2. Materials and Methods

4.2.2.1. RNA sequencing analysis

Sample preparation for RNA-seq analysis

RNA was extracted from 30 mg of tissue per sample from the LOW (n = 5) and CON (n = 6) groups using a TruSeq Stranded mRNA LT Sample Prep Kit. The extracted RNA underwent DNase I treatment to degrade double-stranded and single-stranded DNA, and the ribosomal RNA (rRNA) was sequenced using a NovaSeq 6000 S4 Reagent Kit, according to the manufacturer's instructions (Illumina, Inc., San Diego, CA, USA). The RNA-seq analysis was performed by Macrogen Co. Ltd. (Tokyo, Japan).

Quantification of gene expression and differential expression analysis

Quality control of the data was performed using FastQC v0.11.7 (Schaarschmidt et al., 2020), and raw sequences were subjected to quality trimming by Trimmomatic v.0.38 (Bolger et al., 2014) prior to analysis to ensure data integrity. After quality control and raw data filtering, the clean reads were aligned to the bovine reference genome (ARS-UCD1.3/bos, accessible online at https://ftp.ncbi.nlm.nih.gov/genomes/all/GCF/002/263/795/GCF_002263795.2_ARS-UCD1.3/), accessed on 18 August 2023; using the fast spliced aligner in HISAT2 v.2.1.0 (Pertea et al., 2016). Bowtie2 v.2.3.4.1 was used to count the read numbers mapped to each gene (Li et al., 2009). Following read mapping, Stringtie v.2.1.7 was employed for transcript assembly, and the expression profile was determined for each sample and transcript/gene on the basis of the read counts.

Differential gene expression analysis of the LOW and CON groups was performed using the DESeq2 package in R v.4.3.2 (Love et al., 2014). The *p*-values were adjusted using the Benjamini-Hochberg method (Li and Barber, 2019), with a false discovery rate (*q*-value) threshold of <0.05 and a log2-fold difference of >1 required to accept significant differential expression. A hierarchical clustering analysis was conducted on the matrix using Euclidean distance as the distance metric and the complete linkage method to depict the expression patterns of genes and samples.

Quantitative PCR (qPCR) Analysis

qPCR was conducted to compare gene expression using a CFX96 thermal cycler (Bio-Rad, Hercules, CA, USA) and a Thunder Bird SYBR qPCR kit (Toyobo Co., Ltd., Osaka, Japan), with the mRNA encoding ribosomal protein S18 (*RPS18*) as the reference gene. The evaluation of candidate gene expression was performed using the $2^{-\Delta\Delta CT}$ method (Livak and Schmittgen, 2001) and the one-sided Student's *t*-test, with statistical significance being accepted when $p \leq 0.05$ and a trend when $p \leq 0.10$. The primers used in this study are listed in Table 15.

Gene overlap analysis

To characterize the relationships between the DEGs identified using the RNA-seq analysis and the DMGs identified using the DNA methylation analysis, shared genes were filtered using the dplyr package in R v.4.3.2.

Table 15. Primer pairs used for quantitative PCR analysis

Gene	GeneBank accession #	Primer sequences
IFI16	CK952947	For: GGAGTGATGGAAGTCGTGGT Rev: CCCACTTTCTCCCAATTCAA
CD4	NM_001103225.1	For: GGGCAGAACGGATGTCTCAA Rev: ATAGGTCTTCTGGAGCCGGT
CD8a	NM_174015.1	For: TACATCTGGGCTCCCTTGGT Rev: CCACAGGCCTGGGACATTTG
CD8b	NM_001105344.2	For: AGCTGAGTGTGTTGATGTTCT Rev: TTCTGAGTCACCTGGGTTGG
CD205	NM_001001158.1	For: GAGTTGTCTGCAAAGTTCCCTTG Rev: AACTGAAGAGAAGCCCAACCAG
FOXN1	NM_001192452.1	For: TCTCACCGACTTTGACTTCCAG Rev: CGATGAGGTCACCAGTACCAAG
RPS18	NM_001033614.1	For: CTTAAACAGACAGAAGGACGTGAA Rev: CCACACATTATTTCTTCTTGGACA

Gene functional enrichment analysis

To characterize the cellular functions of differentially expressed genes (DEG), and overlapping genes, I performed KEGG pathway enrichment analysis as described in previous section of this chapter. In addition, to elucidate the roles of specific proteins in the biologic functions of target gene products, PPI networks using the online database STRING v.12.0 (https://string-db.org/ (Volzhenin et al., 2023); accessed on 14 February 2024) was employed.

4.2.2.2. Metabolomic analysis

Sample preparation for CE-FTMS analysis

Frozen thymus samples weighing 31–43 mg were suspended in 750 μL of a 50% acetonitrile solution (*v*/*v*) and a 2 μM internal standard solution from Human Metabolome Technologies (HMT), Tsuruoka, Japan. The mixture was then homogenized at 3,500 rpm for 60 s, a step which was repeated 13 times at 0°C to inhibit enzymatic activity. Subsequently, an equal volume of the 50% acetonitrile solution was added, before centrifugation at 2,300 × *g* and 4°C for 5 min. The resulting supernatant was filtered through a Millipore 5 kDa cutoff filter using an ultrafiltration tube (Ultrafree MC PLHCC, HMT Inc., Tsuruoka, Japan). To eliminate macromolecules, the samples underwent further centrifugation at 9,100 × *g* and 4°C for 120 min. The solvent was then allowed to evaporate and reconstitute in Milli-Q water for a subsequent metabolomic analysis at HMT.

CE-FTMS analysis

The CE–FTMS analysis was performed using MasterHands ver.2.19.0.2, an automatic integration software (Keio University, Tokyo, Japan), to identify peaks based on the signal/noise ratio (S/N > 3), the mass-to-charge ratio (*m*/*z*), the peak area, and the migration

time (MT). The peak areas were normalized according to the method (Arif et al., 2023). Putative metabolites were identified from HMT's standard library and Known–Unknown peak library using MT and m/z with tolerances of ± 0.5 min and ± 0.5 ppm, respectively. In instances in which multiple peaks were associated with the same metabolite, branch numbers were assigned to differentiate them.

For the quantification of target metabolites, the calibration curve for the peak areas was adjusted using internal standard concentrations determined through a one-point calibration at 10 μM, with an internal standard concentration of 20 μM. When a compound was undetectable, its abundance was recorded as 0.

Metabolomic data analysis

The effect of the maternal nutrition level on the metabolite concentrations was analyzed using two-sided Student's *t*-tests in SPSS Statistics for Windows, version 25.0 (IBM Corp., Armonk, N.Y., USA). Differences were considered to be statistically significant at $p \leq 0.05$ or to indicate a trend at $p \leq 0.10$. The KEGG pathways were identified using MSEA in the online application MetaboAnalyst v.6.0 (https://www.metaboanalyst.ca/; accessed on 18 January 2024).

Hierarchical clustering analysis

To depict the patterns of gene expression, and metabolite levels, I conducted hierarchical clustering analysis utilizing an online data visualization and graphing platform as a method previously described in section 4.1.

4.2.3. Results

Differentially expressed genes (DEG)

RNA sequencing analysis identified 30,590 unique genes, with 94 DEG ($q < 0.05$). Of these, 66 genes were upregulated, and 28 were downregulated in the LOW group. The gene expression profile is visualized as a heatmap through hierarchical clustering analysis of DEG in Figure 17A.

The DEGs exhibited high prevalences on chromosomes 7, 13, 17, and 29 for the upregulated genes and on chromosomes 19, 4, 1, 3, and 5 for the downregulated genes. Single upregulated genes were identified on chromosomes 7, 13, 11, 18, and 25, and chromosomes 4, 8, 12, and 26 exclusively harbored downregulated genes, as shown in Figure 17B.

Functional enrichment analysis of DEG

The KEGG pathway analysis revealed several significant terms ($q < 0.10$) related to the upregulated genes, encompassing pathways such as the glutathione metabolism, chemical carcinogenesis-reactive oxygen species, oxidative phosphorylation, and metabolic pathways in LOW and CON fetal thymuses. In addition, the downregulated genes were related to pathways including the MAPK signaling pathway, the C-type lectin receptor signaling pathway, and natural killer cell-mediated cytotoxicity in LOW and CON fetal thymuses. Among the upregulated genes, *MIF*, *GPX1*, *GPX4*, *NDUFS8*, *NDUFB10*, *PC*, *IDUA*, *ACAD8*, *CYC1*, and *GGT7* were associated with metabolic pathways. Specifically, *GPX1*, *GPX4*, and *GGT7* were found to be associated with the glutathione metabolism, and the *NDUFS8*, *NDUFB10*, and *CYC1* genes in LOW fetal thymuses were linked to oxidative phosphorylation. The downregulated genes *NLK*, *MAP3K20*, and *PAK1* were associated

with the MAPK signaling pathway in LOW fetal thymuses. Furthermore, *PTPN11* and *PAK1* were associated with natural killer cell-mediated cytotoxicity and the C-type lectin receptor signaling pathway (Table 16).

Immunity-related genes affected by MNR in the fetal thymus

To identify the immunity-related genes that are influenced by MNR, I focused on six genes that are known to be closely linked to the bovine immune response (Knapek et al., 2020; Wakitani et al., 2022): *CD4*, *CD8a*, *CD8b*, *CD205* or *Ly75*, *IFI16*, and *FOXN1*. The RNA-seq of these target genes in the LOW and CON groups revealed a trend towards a higher expression of *CD4* and *CD8b* in the LOW group vs. the CON group, and the opposite trend for *IFI16* ($p < 0.10$). Subsequently, to validate these variations in gene expression, quantitative (q)PCR analysis was performed, which confirmed the differential expression ($p < 0.05$) of *CD4* (Figure 18A and B).

Protein-protein interaction (PPI) network analysis of the target genes

PPI network analysis was conducted using STRING to elucidate the relationships among the six target genes. This identified eleven significant pathway terms ($q < 0.05$) across four categories: biologic processes (BP), two terms; cellular component (CC), one term; KEGG, six terms; and tissue development, two terms.

The genes *IFI16*, *CD8a*, *CD8b*, *CD4*, and *FOXN1* were linked with pathway terms associated with the regulation of the immune system (Figure 19). In addition, the BP T cell differentiation term was linked to *CD8a*, *CD4*, and *FOXN1*. The CC category was the cell surface term, and it was associated with *CD8a*, *CD8b*, *CD4*, and *LY75* (*CD205*). Notably, only *CD4* and *CD8b* were associated with the six pathway terms in KEGG. Within the tissue development category, two pathway terms were identified: the thymic epithelium term was

associated with *CD4* and *FOXN1*, and the thymus term was associated with *CD8a*, *CD4*, and *FOXN1*. Moreover, *CD4* and *CD8* were associated with the primary immunodeficiency pathway in KEGG, which implies a potential link between MNR and defective immunity in the Wagyu fetal thymus (Figure 19 and Figure 20).

Overlapping genes (DMG/DEG) functional analyses

To further evaluate the genomic effects of MNR on fetal thymus development, I investigated the relationship between DNA methylation and genome-wide gene expression. The merging analysis of DMGs and DEGs identified 25 overlapping genes. The genomic distribution of the overlapping genes was consistent with the results of the WGBS analysis, with overlaps being frequently identified in intergenic regions, followed by introns, intron-exon boundaries, and regions within 1-5 kb of genes. However, no overlaps were found in promoter regions (Table 17).

Figure 21 presents the top 16 significant terms ($q < 0.10$) derived from the KEGG pathway analysis. This list includes glutamatergic synapse, cAMP signaling, GABAergic synapse, the cGMP-PKG signaling pathway, and neutrophil extracellular trap formation. Within these pathways, a total of 11 genes were identified, notably including *CACNA1D*, *GRIA1*, and *SLC25A4*, which were upregulated and linked to multiple pathway terms. In addition, the downregulated genes, such as *ATF6*, *PAK1*, and *SLC38A1*, were each associated with two pathway terms.

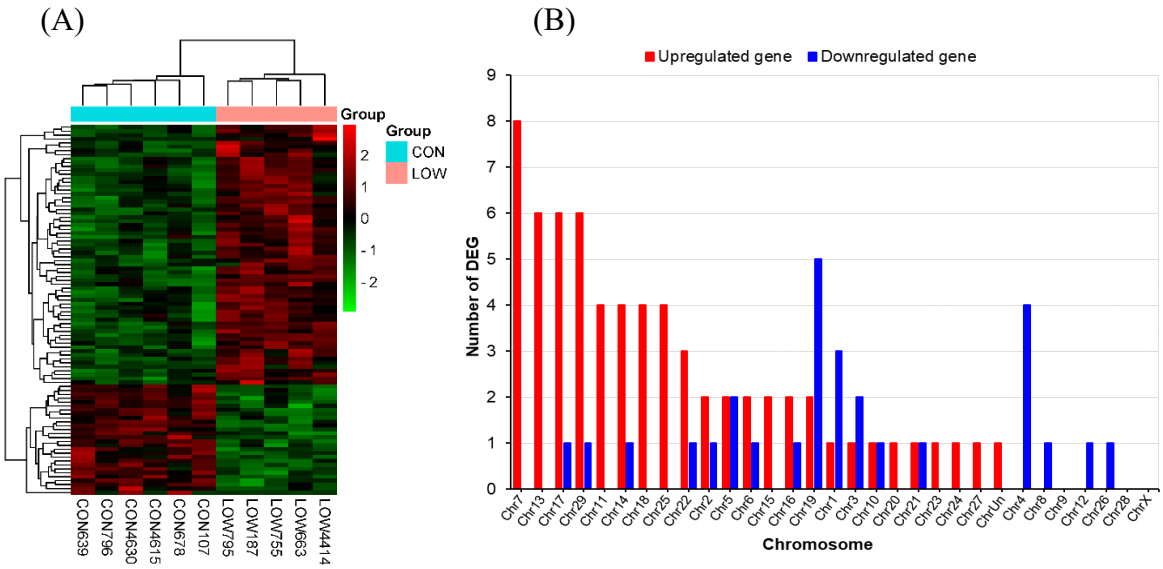

Figure 17. Gene expression profile of the Wagyu fetal thymus. (**A**) Results of the RNA sequencing analysis of the low-nutrition (LOW) and high-nutrition (CON) groups. Heatmap of the hierarchical clustering of the 94 DEGs for LOW (salmon pink) and CON (green blue) fetal thymuses ($q < 0.05$). The row represents the gene, and the column represents the sample. Red: upregulated genes; green: downregulated genes. The darkness of each color corresponds to the magnitude of the difference from the mean value. (**B**) Chromosomal distribution of DEGs in the thymuses of LOW and CON fetuses. ChrUn: unplaced chromosome.

Table 16. Top significant differences ($q < 0.10$) in KEGG pathways, obtained from up- and downregulated genes in LOW and CON fetal thymuses

Direction	KEGG Pathway	*q*-value	Genes
Up regulated			
	Path:bta03010 Ribosome	< 0.0001	*RPS14, RPLP2, RPL37A, MRPS2, RPS15, RPLP1, RPS21, UBA52, RPL38, RPL28, RPL37*
	Path:bta05171 Coronavirus disease-COVID-19	< 0.0001	*RPS14, RPLP2, RPL37A, RPS15, RPLP1, RPS21, UBA52, RPL38, RPL28, RPL37*
	Path:bta05022 Pathways of neurodegeneration-multiple diseases	0.002	*GPX1, SLC25A4, NDUFS8, NDUFB10, CACNA1D, CYC1, GRIA1, UBA52*
	Path:bta05016 Huntington disease	0.005	*GPX1, SLC25A4, NDUFS8, NDUFB10, CYC1, GRIA1*
	Path:bta00480 Glutathione metabolism	0.010	*GPX1, GPX4, GGT7*
	Path:bta04723 Retrograde endocannabinoid signaling	0.011	*NDUFS8, NDUFB10, CACNA1D, GRIA1*
	Path:bta04932 Non-alcoholic fatty liver disease	0.011	*NDUFS8, NDUFB10, CYC1, SREBF1*
	Path:bta05012 Parkinson disease	0.011	*SLC25A4, NDUFS8, NDUFB10, CYC1, UBA52*
	Path:bta05020 Prion disease	0.011	*SLC25A4, NDUFS8, NDUFB10, CACNA1D, CYC1*
	Path:bta05415 Diabetic cardiomyopathy	0.026	*SLC25A4, NDUFS8, NDUFB10, CYC1*
	Path:bta05014 Amyotrophic lateral sclerosis	0.029	*GPX1, NDUFS8, NDUFB10, CYC1, GRIA1*
	Path:bta05208 Chemical carcinogenesis-reactive oxygen species	0.032	*SLC25A4, NDUFS8, NDUFB10, CYC1*
	Path:bta05010 Alzheimer disease	0.032	*SLC25A4, NDUFS8, NDUFB10, CACNA1D, CYC1*
	Path:bta00190 Oxidative phosphorylation	0.047	*NDUFS8, NDUFB10, CYC1*
	Path:bta01100 Metabolic pathways	0.064	*MIF, GPX1, GPX4, NDUFS8, NDUFB10, PC, IDUA, ACAD8, CYC1, GGT7*
	Path:bta05031 Amphetamine addiction	0.078	*CACNA1D, GRIA1*
Down regulated			
	Path:bta04010 MAPK signaling pathway	0.077	*NLK, MAP3K20, PAK1*
	Path:bta04625 C-type lectin receptor signaling pathway	0.077	*PTPN11, PAK1*
	Path:bta05211 Renal cell carcinoma	0.077	*PTPN11, PAK1*
	Path:bta04650 Natural killer cell mediated cytotoxicity	0.094	*PTPN11, PAK1*

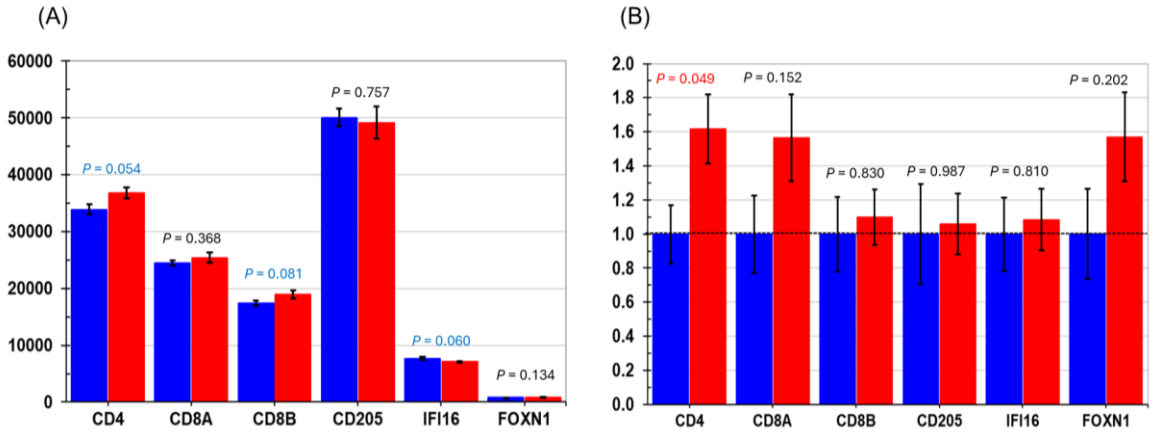

Figure 18. Expression of six target immune-related genes. (**A**) Results of RNA sequencing analysis. (**B**) Comparative expression levels, quantified using qPCR analysis. The y-axis depicts gene expression level and the y-axis shows the list of target genes. Blue bars: CON group (n=6), red bars: LOW group (n=5).

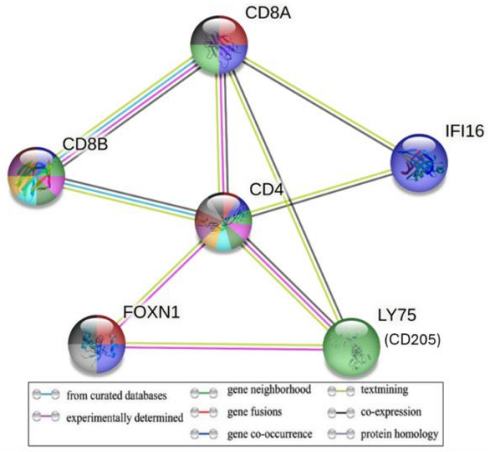

Node color	term description	Genes	Class
Blue	Regulation of immune system process	IFI16, CD8A, CD8B, CD4, FOXN1	BP
Red	T cell differentiation	CD8A, CD4, FOXN1	
Lime green	Cell surface	CD8A, CD8B, CD4, LY75	CC
Magenta	Primary immunodeficiency	CD8B, CD4	KEGG
Dark green	Antigen processing and presentation	CD8B, CD4	
Cyan	T cell receptor signaling pathway	CD8B, CD4	
Orange	Hematopoietic cell lineage	CD8B, CD4	
Purple	Yersinia infection	CD8B, CD4	
Maroon	Cell adhesion molecules	CD8B, CD4	
Grey	Thymic epithelium	CD4, FOXN1	Tissues
Black	Thymus	CD8A, CD4, FOXN1	

BP: Biological process. CC: Cellular component. KEGG: *Kyoto Encyclopedia of Genes and Genomes*

Figure 19. Results of the functional enrichment analysis on the protein-protein interaction (PPI) networks for six target genes. The node colors represent the enrichment of PPI pathways, with each color corresponding to a specific pathway. Significant enriched pathways ($q < 0.05$) are highlighted. BPs: biologic processes; CC: cellular component.

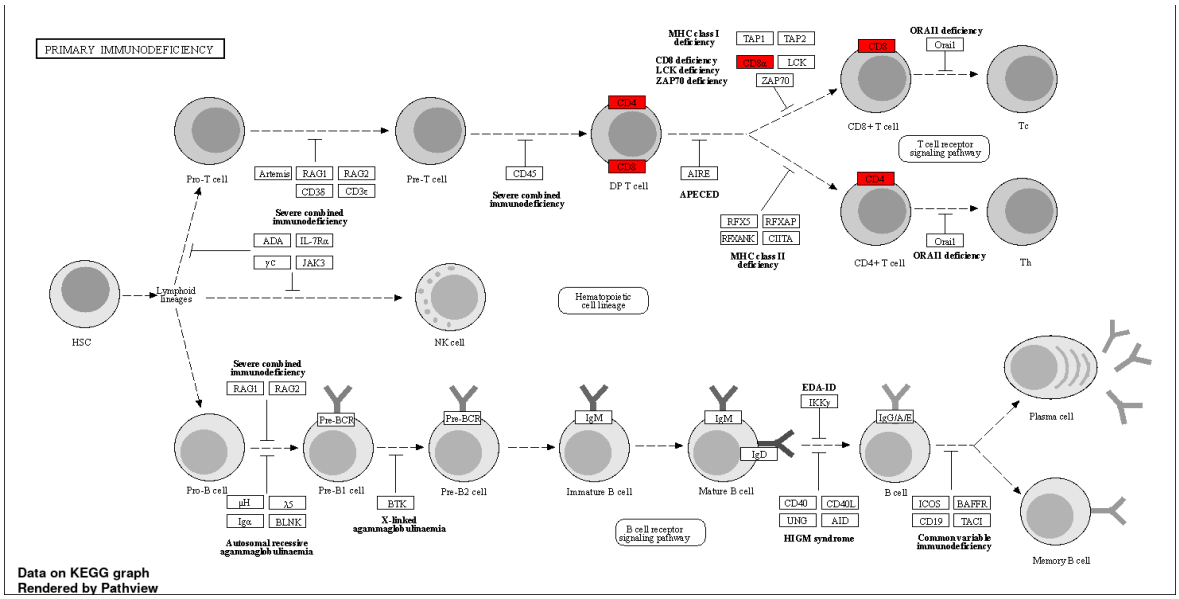

Figure 20. Diagram illustrating the KEGG pathway terms related to primary immunodeficiency associated with the six target genes. Gene names in red were upregulated.

Table 17. List of genes that were both differentially methylated genes (DMGs) and differentially expressed genes (DEGs)

Gene symbol	Entrez	DNA Methylation		Gene Expression			
		Genomic regions	Hypo/Hyper	Up/Down	log2FC	FC	*q*-value
GRIA1	529618	Intron/intergenic	Hypo	Up	3.85	14.42	0.0018
OSR1	539430	Intergenic	Hyper	Up	2.40	5.29	0.0200
TMEM132B	540363	Intronexonboundary	Hypo	Up	1.29	2.46	0.0155
CACNA1D	408013	Intron/Intronexonboundary	Hypo	Up	0.85	1.81	0.0005
ABLIM2	618227	Intron	Hypo	Up	0.59	1.50	<0.0001
MRPS2	505681	Intergenic	Hyper	Up	0.51	1.42	0.0331
DTX1	512873	Intron	Hypo	Up	0.44	1.36	0.0331
PITRM1	513230	Intergenic	Hypo	Up	0.40	1.32	0.0382
LTBP3	532772	Intronexonboundary	Hypo	Up	0.37	1.29	0.0018
BOP1	515056	Intron	Hypo	Up	0.35	1.27	0.0018
RPS14	282050	Intronexonboundary	Hypo	Up	0.29	1.22	0.0342
RPLP1	533285	Intergenic	Hyper	Up	0.26	1.20	0.0157
GYPC	444863	Intergenic	Hypo	Up	0.24	1.18	0.0152
SLC25A4	282478	Intronexonboundary	Hyper	Up	0.23	1.18	0.0432
OTUB1	540984	Intron	Hyper	Up	0.22	1.17	0.0223
H2AFJ	618489	1to5kb	Hyper	Up	0.19	1.14	0.0157
PAFAH1B1	282513	Intergenic	Hyper	Down	-0.16	-1.12	0.0385
ATF6	530610	Intron/Intronexonboundary	Hyper	Down	-0.21	-1.16	0.0160
SLC38A1	527491	Intron	Hyper	Down	-0.25	-1.19	0.0075
HMBOX1	539099	Intron	Hyper	Down	-0.35	-1.27	0.0291
SLC49A3	511117	Intronexonboundary	Hypo	Down	-0.36	-1.28	0.0331
PAK1	533729	Intron/intergenic	Hypo	Down	-0.39	-1.31	0.0166
TFEC	539016	Intron/intergenic	Hypo	Down	-0.56	-1.48	0.0352
LOC101906333	101906333	Intergenic	Hypo	Down	-2.59	-6.26	0.0356
FAIM2	509790	Intergenic	Hypo	Down	-3.55	-11.78	0.0431

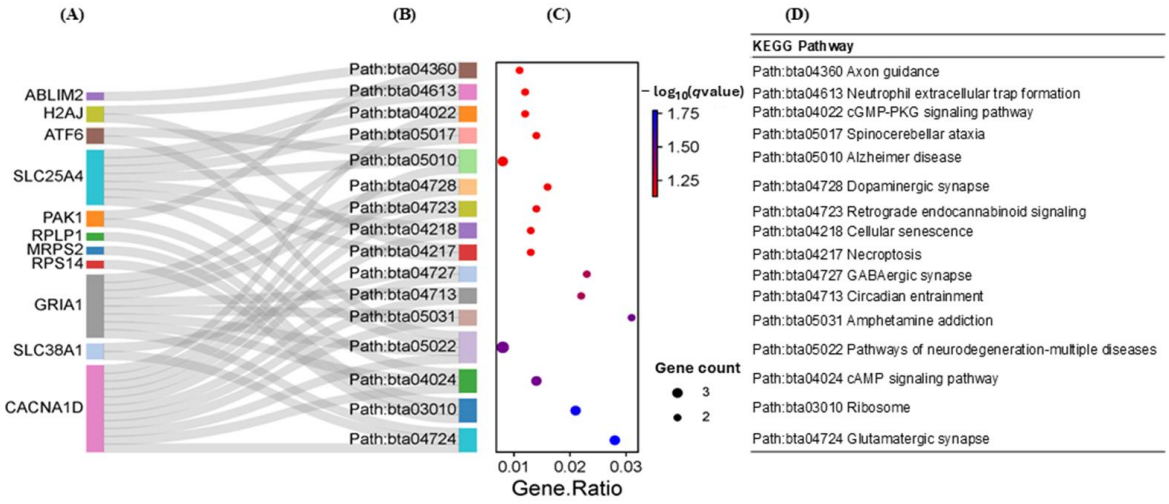

Figure 21. Sankey plot, illustrating the connections of overlapping genes identified using RNA-seq and DNA methylation analysis with the leading KEGG pathways. (**A**) denotes overlapping genes, obtained using DNA methylation and RNA-seq, that are linked to the KEGG pathways in (**B**). (**C**) The y-axis shows the names of genes and pathway terms, and the x-axis shows the ratio of the number of genes associated with terms to the number of genes in the pathway background. The dot size indicates the number of genes, and the color reflects the −log10(*q*-value). (**D**) ID and matched names for the KEGG pathway terms.

Metabolomic profile

To understand the effect of maternal undernutrition on the metabolism of the bovine fetal thymus, a comprehensive metabolomic analysis was conducted using CE–FTMS. A total of 500 peaks detected by mass spectrometry (MS) were identified as metabolites. Lidocaine, 2-deoxyadenosine, ethanolamine phosphate (all $p < 0.01$), histidine, ribulose 5-phosphate, 3-(3,4-dihydroxyphenyl)-2-methylalanine, alanine–alanine, serine, histamine, gluconolactone, 5-hydroxylysine, 1H-imidazole-4-propionic acid, N-acetylglucosamine 1-phosphate, and phenylalanine (all $p < 0.05$), as well as nicotinamide and allo-threonine ($p < 0.10$), were present at higher concentrations in the LOW than in the CON fetal thymus. Conversely, UDP-glucose/UDP-galactose ($p < 0.01$), N-acetylmethionine, terephthalic acid, and deoxycytidine monophosphate (dCMP) ($p < 0.05$) were present at lower concentrations (Table 18).

Figure 22 shows the heatmap generated by hierarchical cluster analysis of the top 50 metabolites. Of these, lidocaine, histidine, histamine, serine, phenylalanine, nicotinamide, ethanolamine phosphate (EAP), ethanolamine, aspartame, and CMP-N-acetylneuraminate were found to be more abundant in the LOW group. Conversely, UDP-glucose/UDP-galactose (UDP-glc/UDP-gal), UDP-N-acetylglucosamine (UDP-GlcNAc), N-acetylmethionine, and dCMP exhibited higher abundance in the CON group. The results of HCA imply that these metabolites contribute to the differences between the thymuses of the two nutrient treatment groups. MSEA was performed using the top 50 metabolites, and this identified significant differences in the metabolic pathways, including the following: amino sugar and nucleotide sugar metabolism ($p < 0.001$); histidine metabolism; glycine, serine, and threonine metabolism; phenylalanine, tyrosine, and tryptophan biosynthesis ($p < 0.01$); pentose and glucuronate interconversion; glycerophospholipid metabolism; phenylalanine metabolism; and ascorbate and aldarate metabolism ($p < 0.05$) (Table 19).

Table 18. Top 20 changed metabolites in fetal thymus between the LOW and CON group

Compound name	CON (N = 6)		LOW (N = 5)		LOW/CON	
	Mean	SEM	Mean	SEM	*p*-value	Ratio
UDP-glucose,UDP-galactose	0.01845	0.00148	0.01190	0.000449	0.004	0.6
2-Deoxyadenosine	0.00001	0.00000	0.00002	0.000001	0.010	1.3
Ethanolamine phosphate	0.22594	0.00462	0.24262	0.002295	0.014	1.1
Histidine	0.03384	0.00152	0.04124	0.002097	0.017	1.2
N-Acetylmethionine	0.00172	0.00010	0.00137	0.000074	0.020	0.8
Ribulose 5-phosphate	0.00150	0.00011	0.00203	0.000173	0.023	1.4
3-(3,4-Dihydroxyphenyl)-2-methylalanine	0.00013	0.00002	0.00024	0.000038	0.023	1.9
Alanine-Alanine	0.00152	0.00010	0.00188	0.000092	0.028	1.2
Serine	0.05118	0.00501	0.07142	0.006726	0.036	1.4
Histamine	0.00112	0.00018	0.00169	0.000143	0.039	1.5
Gluconolactone	0.00050	0.00003	0.00063	0.000046	0.044	1.2
5-Hydroxylysine	0.00099	0.00006	0.00124	0.000084	0.044	1.2
1H-Imidazole-4-propionic acid	0.00004	0.00001	0.00013	0.000041	0.047	2.9
N-Acetylglucosamine 1-phosphate	0.00375	0.00010	0.00465	0.000424	0.050	1.2
Phenylalanine	0.12468	0.00845	0.15371	0.009901	0.051	1.2
Terephthalic acid	0.00016	0.00001	0.00011	0.000017	0.054	0.7
dCMP	0.00153	0.00007	0.00123	0.000124	0.054	0.8
Nicotinamide	0.05056	0.00397	0.06163	0.002909	0.058	1.2
allo-Threonine	0.000227	0.000033	0.000367	0.000041	0.064	1.6
Imidazole-4-acetic acid	0.000016	0.000003	0.000028	0.000005	0.064	1.7

dCMP: deoxycytidine monophosphate.

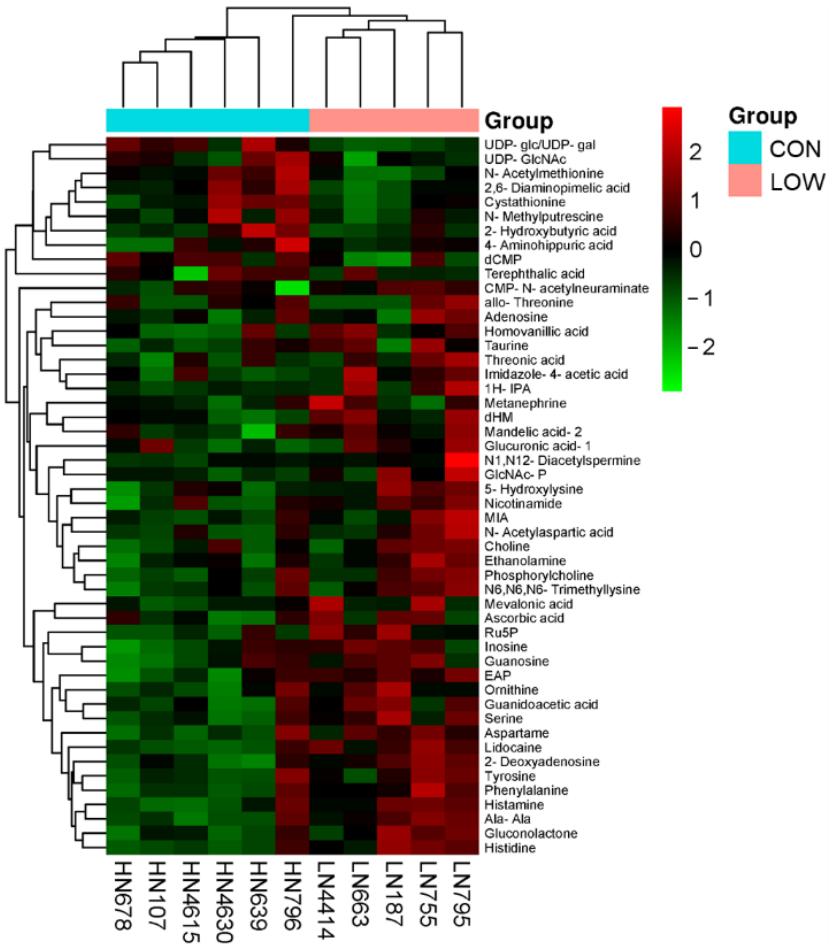

Figure 22. Heatmap of the hierarchical clustering of the top 50 metabolites present at differing concentrations in LOW (salmon pink) and CON (green blue) fetal thymuses. The rows represent the metabolites, and the columns represent the samples. The metabolites present at relatively low concentrations are displayed in green, and those present at relatively high concentrations are displayed in red. The darkness of each color corresponds to the magnitude of the difference vs. the mean value. UDP-glc/UDP-gal, UDP-glucose/UDP-galactose; UDP-GlcNAc, UDP-N-acetylglucosamine; dCMP, deoxycytidine monophosphate; 1H-IPA, 1H-imidazole-4-propionic acid; dHM, 3-(3,4-dihydroxyphenyl)-2-methylalanine; GlcNAc-P, N-acetylglucosamine 1-phosphate; MIA, 1-methyl-4-imidazoleacetic acid; Ru5P, ribulose 5-phosphate; EAP, ethanolamine phosphate; and Ala-Ala, alanine-alanine.

Table 19. Metabolic pathways demonstrating the most significant differences in the thymuses of the LOW and CON fetuses

Pathway	Hits	Total	*p*-value	Increased in LOW group	Decreased in LOW group
Amino sugar and nucleotide sugar metabolism	6	42	<0.001	N-Acetylglucosamine 1-phosphate, CMP-N-acetylneuraminic acid	UDP-N-acetylglucosamine; UDP-glucose; UDP-galactose; UDP-N-acetylgalactosamine
Histidine metabolism	4	16	0.001	His; Histamine; Imidazole-4-acetic acid; 1-Methyl-4-imidazoleacetic acid	
Glycine, serine and threonine metabolism	5	34	0.001	Serine; Choline; Allo-threonine; 4-Guanidinoacetic acid	Cystathionine
Phenylalanine, tyrosine and tryptophan biosynthesis	2	4	0.004	Phenylalanine; tyrosine	
Pentose and glucuronate interconversions	3	19	0.011	Ribulose 5-phosphate; Glucuronic acid	UDP-glucose
Glycerophospholipid metabolism	4	36	0.012	Choline phosphate; Choline; Ethanolamine phosphate; Ethanolamine	
Phenylalanine metabolism	2	10	0.025	Phenylalanine; tyrosine	
Ascorbate and aldarate metabolism	2	10	0.025	Glucuronic acid	UDP-glucose
Tyrosine metabolism	3	42	0.089	Tyrosine; Metanephrine; Homovanillic acid	

4.2.4. Discussion

The nutritional status of mothers has substantial effects on gene expression and thereby affects the tissue metabolism in the offspring pre- and postpartum. In the present study, I focused on measuring the effect of maternal nutrient restriction (MNR) throughout gestation on gene expression and extrapolated the biologic effects of altered expression in the fetal thymus. RNA-seq revealed a 2.4-fold larger number of upregulated rather than downregulated genes (66 vs. 28), and the subsequent KEGG pathway analysis showed a 4.0-fold higher number of dysregulated pathways associated with the upregulated genes compared to the downregulated genes in the LOW group (Table 16). This suggests that MNR tends to upregulate, rather than downregulate, gene expression in the thymus of fetal Wagyu cattle in response to DNA methylation.

The downregulated genes, such as *NLK*, *MAP3K20*, *PTPN11*, and *PAK1*, are involved in several crucial pathways (Table 16). MAPK transduces extracellular signals and orchestrates essential cellular processes, including proliferation, differentiation, survival, and apoptosis. Previous studies have demonstrated that MAPK activation is associated with the upregulation of proinflammatory molecules, such as TNF-α (Vincenzi et al., 2021). Natural killer cell-mediated cytotoxicity plays a key role in immune responses against infections through direct cytotoxic effects (Paul and Lal, 2017). In addition, the C-type lectin receptor pathway recognizes pathogens, triggering immune cell activation and cytokine production, and its dysregulation is implicated in various conditions, including cancer (Drouin et al., 2020). These pathways appear to be attenuated in LOW fetuses, given that the expression of a number of genes expressing the components of these pathways was downregulated.

The functional activities associated with the upregulated genes were identified as nutrient recruitment and stress responses (Table 16). Metabolic pathways form complex networks of biochemical reactions that enable the acquisition, conversion, and utilization of energy from nutrients to support cellular processes. These pathways include genes such as *MIF*, *GPX1*, *GPX4*, *NDUFS8*, *NDUFB10*, *PC*, *IDUA*, *ACAD8*, *CYC1*, and *GGT7*, which are crucial for the glucose, protein, and lipid metabolism and cellular homeostasis. Maternal nutrient deficiency can cause intrauterine stress, leading to excessive reactive oxygen species (ROS) production and fetal oxidative stress, and organs that rely on oxidative phosphorylation (OXPHOS) are particularly affected. Metabolic pathways in the mitochondria are particularly important, such as the Krebs cycle, which oxidizes acetyl-CoA to produce NADH and ATP. OXPHOS is the primary mitochondrial pathway for ATP production, and it links the electron transport chain (ETC) with ATP synthase (Arnold and Finley, 2023). Under nutrient stress, cells undergo metabolic adaptation, using fatty acids and amino acids as alternative substrates for the Krebs cycle and OXPHOS. Thus, the appropriate regulation of OXPHOS is vital for the maintenance of cellular energy homeostasis and redox balance, the stress response, and cellular defense (Koopman et al., 2013). ROS, such as superoxide, hydrogen peroxide, and hydroxyl radicals, can damage DNA, lipids, and proteins, causing pregnancy complications. Nutrient deprivation disrupts mitochondrial function, increases ROS concentrations, triggers stress responses, and impairs cellular defenses. Glutathione (GSH) synthesis, which is crucial to limit the effects of ROS and maintain cellular redox balance as part of immune tolerance and the stress response, relies on amino acid availability (Zhang et al., 2023). Furthermore, antioxidants such as superoxide dismutase, catalase, and GSH peroxidase are important for oxidative balance. These stress response mechanisms help cells adapt to nutrient deprivation by modulating gene expression, reprogramming the metabolism, and enhancing cellular defenses, and

deficiencies in these antioxidants can lead to oxidative stress and DNA damage (Ighodaro and Akinloye, 2018). The present findings imply that there may be abnormal interactions among the metabolic pathways, OXPHOS, ROS generation, and the GSH metabolism in the LOW group, indicative of cellular stress in response to nutrient deprivation. The preservation of normal relationships among these pathways is crucial for cellular adaptation and survival when nutrients are scarce.

Metabolite set enrichment analysis (MSEA) identified defects in several pathways that are linked to cellular defense through the regulation of the immune system in the LOW group (Table 19). UDP-glucose, UDP-galactose, UDP-N-acetylglucosamine, and UDP-N-acetylgalactosamine are vital for immune cell function, enabling the production of glycoproteins and glycolipids. N-acetylglucosamine 1-phosphate is an intermediate in the biosynthesis of UDP-N-acetylglucosamine, and CMP-N-acetylneuraminic acid is the activated form of sialic acid (Ghosh, 2020). These metabolites are linked to the amino sugar and nucleotide sugar metabolism, which is important for immune system regulation. The histidine metabolism generates histamine, a key signaling molecule in immune and inflammatory responses. Furthermore, essential derivatives such as 1-methyl-4-imidazoleacetic acid and imidazole-4-acetic acid are crucial for the regulation of histamine levels and signaling. Histamine plays a central role in inflammation (Holeček, 2020). The metabolism of glycine, serine, and threonine provides precursors and cofactors that are necessary for cellular processes, including immune system regulation. Serine, which is derived from 3-phospho-D-glycerate in the glycolytic pathway, is vital for protein, nucleic acid, and lipid synthesis, via conversion to glycine. Glycine can also be produced in mitochondria from threonine by threonine dehydrogenase and glycine C-acetyltransferase (Ducker and Rabinowitz, 2017). It is vital for the one-carbon metabolism and aids with

cellular processes, including immune responses, through the glycine cleavage system (Tian et al., 2019).

During fetal development, threonine plays a role in metabolic adaptations to optimize nutrient usage and support organ development under conditions of poor maternal nutrition. Such adaptations involve an increase in the threonine concentration to meet fetal demands, which may have beneficial effects in organs such as the thymus. In the immune system, threonine interacts with a nearby amino acid in the FcγRIIB protein, causing a conformational change which affects the innate immune response (Hu et al., 2019). Phenylalanine, tyrosine, and tryptophan are aromatic amino acids that are essential for the biosynthesis of important neurotransmitters and related hormones (Miri et al., 2023). Similarly, tryptophan is a precursor for the synthesis of the neurotransmitter serotonin, the neurohormone melatonin, and the enzyme cofactors NAD and NADP (Richard et al., 2009). This metabolic pathway may affect the immune system through effects on the synthesis of neurotransmitters, hormones, and cofactors. The pentose phosphate pathway and glucuronate interconversion are metabolic pathways that are important for the generation of NADPH and cellular redox homeostasis (Sun et al., 2018). These pathways involve the interconversion of pentose sugars, such as ribulose 5-phosphate, and the production of glucuronic acid, which might be important for detoxification and, therefore, immune tolerance.

The glycerophospholipid metabolism is closely linked to fatty acid transport and the activity of enzymes such as long-chain acyl-CoA synthetase (Prentki and Madiraju, 2008). Nutrient deficiency alters the proportions of fatty acids in cell membrane glycerophospholipids and stimulates the breakdown of intracellular triglycerides, thereby increasing the glycerol and free fatty acid concentrations, which can affect glycerophospholipid synthesis and signaling. Disruptions to this metabolic pathway may

have significant consequences for immune homeostasis (Gimenez et al., 2011). Finally, glucuronic acid is a vital metabolite in the ascorbate and aldarate metabolism pathway, where it is involved in both the synthesis and breakdown of ascorbic acid (vitamin C) (Beyoğlu et al., 2023). Furthermore, glucuronic acid aids in detoxification through glucuronidation reactions, thereby affecting immune responses. Disruptions to these pathways impair the cellular defense by compromising immune cell function and membrane integrity (Peng et al., 2023).

4.2.5. Summary

This section examined the effects of MNR on gene expression and metabolism in the fetal thymus throughout gestation. RNA sequencing analysis revealed 66 upregulated genes and 28 downregulated genes, with 4.0-fold greater pathway enrichment for upregulated genes in the LOW group than in the CON group. MNR induced stress responses, activating pathways related to OXPHOS, ROS, and GSH metabolism. Additionally, it altered pathways linked to immune cell functions, including natural killer cell-mediated cytotoxicity and C-type lectin receptor signaling. Key metabolites, such as histidine, serine, threonine, alanine, and phenylalanine, increased and played crucial roles in immune responses and cellular processes. These findings indicate that MNR affects gene expression, enhancing metabolic and stress response pathways essential for cellular survival and immune function under conditions of nutrient scarcity.

Chapter 5

General discussion

Animal production is vital for food security and economic stability, but currently faces challenges such as rising feed prices, market fluctuations, trade disruptions, and climate change, all of which increase costs, reduce profitability, and harm animal health, productivity, and ecosystems (Godde et al., 2021). Sustainable practices are necessary to minimize the environmental impact while elevating production levels. The Sustainable Development Goals (SDGs) offer a framework for addressing these challenges, focusing on zero hunger, good health, clean water, responsible consumption, and climate action (FAO, 2018). Improving feed efficiency and adopting sustainable practices are key to reducing global poverty and environmental impact. The One Health approach, which connects human, animal, and environmental health, promotes collaboration to enhance health outcomes and cattle production resilience (Douphrate, 2021).

Recently, fetal and neonatal programming has attracted interest owing to its lasting health effects because nutrient exposure during early development can have enduring postnatal consequences. These processes are closely linked to cellular functions and driven by epigenetic modifications, such as DNA methylation and histone modifications, which affect gene expression (Hanley et al., 2010). The immune system plays a pivotal role in maintaining animal health and productivity by acting as the first line of defense against infections, diseases, and environmental stressors. Proper immune regulation is essential for neonatal calf survival (Raboisson et al., 2016). Furthermore, fetal development is vital for the proper formation and function of visceral organs, and body physiology required for survival outside the uterus, which depends on an optimal intrauterine environment. This

study aimed to investigate the mechanistic effects of maternal nutrient restriction (MNR) on physiological alterations and immune system development, focusing on epigenetic modifications, such as DNA methylation, gene expression, and metabolic processes in the fetal thymus, as well as the early growth characteristics of Wagyu cattle offspring.

Changes in hormone secretion and metabolite levels in cows and their offspring

In pregnant animals, there are high demands for the substantial intake of nutrients to maintain maternal tissues, and support placental growth and fetal development. Key nutrients such as glucose, amino acids, and fatty acids are vital for protein synthesis and energy production. Nutrient restriction reduces plasma glucose, signaling less carbohydrate intake and increased reliance on gluconeogenesis and fat metabolism. During pregnancy, nutrient deficiencies can also alter the levels of metabolic hormones such as GH, IGF-1, and insulin, as observed in studies on mice (Liao et al., 2016) and dairy cows (Mohebbi-Fani et al., 2019). The elevation of GH levels acts as an adaptive response to conserve energy and mobilize fat reserves. GH promotes lipolysis, increasing the availability of NEFA as an alternative energy source through enhanced β-adrenergic sensitivity, while inhibiting insulin secretion through systemic action in the somatotropic hormone axis (Alamri et al., 2016). This physiological adjustment helps maintain energy homeostasis during nutrient scarcity by prioritizing fat mobilization over glucose utilization, thereby conserving energy for fetal survival.

Maternal dietary intake, physiological state, and health conditions around the time of conception and during gestation have been shown to influence the phenotypic characteristics of the offspring, including physiological biomarkers (Wells, 2014). Offspring from dams subjected to late-gestational nutrient restriction (LOW group) exhibited significantly higher growth hormone (GH) secretion than offspring from dams receiving adequate nutrition

(CON group), with this disparity persisting until 30 days of age. This phenomenon may be attributable to maternal influence on the calf through intrauterine hormonal transfer and/or early colostrum intake post-parturition. Previous studies have also reported that maternal physiology during late pregnancy can impact offspring characteristics in humans (Moon et al., 2013). Basically, the secretion of IGF-1 is dependent on nutritional status. In the present study, the IGF-1 secretion on the day of parturition was significantly higher in the LOW group than in the CON group, consistent with the observed elevated plasma GH levels. However, these levels converged to similar values by 30 days of age. It has been observed that IGF-1 synthesis differs between fetus and neonate, with GH stimulating IGF-1 synthesis after birth but playing a lesser role in fetal IGF-1 secretion (Hellström et al., 2016). Nevertheless, the relationship between plasma GH and IGF-1 during fetal and early neonatal life in calves remains unclear. Previous studies have reported that plasma IGF-1 levels in calves during the suckling period are positively correlated with the amount of milk replacer intake and increase with age (Takahashi et al., 2016). Additionally, plasma IGF-1 levels promptly increase after weaning (Han et al., 2020). However, in the present study, the secretion of IGF-1 after 2 months of age remained constant, at a lower level in LOW offspring even after weaning than in their CON counterparts. These findings suggest that MNR during late gestation altered metabolic physiology, which subsequently affected the secretion of GH and IGF-1 in the Wagyu offspring.

The MNR influences mitochondrial metabolism via epigenetic modifications linked to immunopoiesis in the fetal thymus of Wagyu cattle

Immunopoiesis refers to the process of generating and maturing immune cells, governed by complex genetic and epigenetic regulatory mechanisms. Nutrient deficiencies can induce epigenetic modifications, including DNA methylation, which modify gene expression and

cellular metabolism, thereby impacting immune system function (Tiffon, 2018). In present study, WGBS analysis indicated alterations in DNA methylation patterns. Concurrently, RNA sequencing identified a 2.4-fold increase in the number of upregulated genes relative to downregulated genes. KEGG pathway analyses of DMG and DEG demonstrated a 5-fold and 4-fold increase, respectively. Furthermore, metabolomic analysis revealed elevated amino acid levels in the LOW group relative to the CON group. The Hippo signaling is critical for embryogenesis, tissue regeneration, wound healing, and maintaining homeostasis in fetal organs (Moya and Halder, 2019). In this study, Hippo signaling is linked to genes exhibiting hypermethylation. Additionally, *SLC38A1*, an amino acid transporter vital for nutrient uptake, energy production, and metabolic processes during fetal development (Vaughan et al., 2021), is connected to the glutamatergic and GABAergic pathways (Table 17, and Figure 21). Its hypermethylation and downregulation may hinder protein synthesis and cell growth, potentially affecting fetal development. These pathways may serve as important indicators of fetal programming influencing the Wagyu fetal thymus phenotype.

The HPA axis, including GnRH, oxytocin, renin, aldosterone, relaxin, and cortisol, is implicated in hypoDMG (Table 14). Basically, HPA hormones are central to mechanisms that regulate fetal preparedness for birth and survival. Stereotypical increases in fetal HPA axis activity near term are critical for preparing the fetus for a successful transition to extrauterine life (Wood and Keller-Wood, 2016). The findings suggest that this hormone axis might be crucial for the thymus, which regulates immune system function, to ensure fetal survival under conditions of nutrient scarcity. The Ras pathway, an upstream pathway crucial for T cell development, and modulates metabolic reprogramming under nutrient deficiency, enhancing mitochondrial activity and the Krebs cycle to meet energy demands (Sadeghi Shaker et al., 2023). Additionally, upregulated genes were associated with

OXPHOS, ROS, and GSH metabolism pathways suggests that these signaling pathways are critical for mitochondrial reprogramming and ATP recruitment.

Pregnancy necessitates greater levels of protein synthesis to maintain pulmonary and systemic circulation and the maternal tissues and for fetal development. Essential nutrients, including glucose, amino acids, proteins, fatty acids, and cholesterol, support fetal processes, such as protein synthesis, substrate conversion, and oxidation. Amino acids are critical for protein synthesis and as precursors for compounds such as nitric oxide, polyamines, and glutathione, which are vital for placental growth, angiogenesis, and conceptus development (Tan et al., 2022). MNR in sheep reduces the total α-amino acid concentrations, particularly those of serine, arginine family amino acids, and branched-chain amino acids, in the maternal and fetal plasma (Kwon et al., 2004). In the bovine fetus, maternal undernutrition alters the amino acid metabolism, resulting in high concentrations of histidine, phenylalanine, and glutamine in fetal muscle and of alanine and serine in the fetal liver (Muroya et al., 2022; Muroya et al., 2023). Consistent with previous findings, in the present study, I identified high concentrations of several amino acids (histidine, serine, alanine, and phenylalanine) in the thymuses of the fetuses of the LOW group. The thymus, a lymphoid organ which is crucial for immune regulation, requires amino acids for functions that are distinct from those in the muscle and liver. Specifically, amino acids are required in the thymus to provide energy for T cell production, which is essential for immune homeostasis and systemic protection.

Maternal nutrient deficiency may cause the fetal thymus to prioritize T cell development, with high amino acid concentrations indicating the presence of metabolic adaptations for ATP production via OXPHOS. This nutrient scarcity induces metabolic reprogramming, involving alterations to mitochondrial dynamics, an increase in oxidative stress, and a reorganization of the Krebs cycle, which is crucial for nutrient oxidation and the

maintenance of cellular bioenergetics(Arnold and Finley, 2023). Mitochondrial OXPHOS is crucial for cellular energy synthesis, and converts ADP to ATP via the ETC, which is closely linked to the oxidative stress induced by excessive ROS production. This relationship is essential for metabolic adaptation, because the mitochondria adjust their function and metabolism in response to nutrient deprivation (Vargas-Mendoza et al., 2021). The amino acid metabolism is crucial for mitochondrial biogenesis, the antioxidant response, and the Krebs cycle. OXPHOS and the Krebs cycle are interconnected through the oxidation of NADH and FADH2 (Martínez-Reyes and Chandel, 2020). In addition, the mitochondria play a key role in the innate immune response by releasing ROS and other danger signals, such as mitochondrial DNA (mtDNA) and cardiolipin (Sokolova, 2018).

In the present study, I identified several hypoDMGs and upregulated genes that play significant roles in the upregulation of mitochondrial activity, secondary to increases in the concentrations of Krebs cycle intermediates. *SLC25A4* encodes the mitochondrial ADP/ATP carrier protein (ANT1), which facilitates ATP transport from the mitochondrial matrix to the cytoplasm and the import of ADP into the mitochondria, which is crucial for the cellular energy metabolism (Thompson et al., 2016). *CYC1* encodes a subunit of mitochondrial complex III that facilitates electron transfer for ATP generation in OXPHOS and the maintenance of the mitochondrial metabolism (Martínez-Reyes and Chandel, 2020). *NDUFS8* is a core subunit of mitochondrial complex I, which is a key component of the ETC, transferring electrons from NADH to ubiquinone for OXPHOS and ATP synthesis. Its role in proton pumping across the inner mitochondrial membrane is vital for ATP synthesis. The Krebs cycle is closely associated with this process, by providing NADH and FADH2 (Xiong et al., 2024). Similarly, *MRPS2* encodes mitochondrial ribosomal protein S2, which is crucial for ATP production via OXPHOS and the synthesis of proteins which are essential for the ETC (Gardeitchik et al., 2018). *ACAD8* encodes an enzyme that is vital for

mitochondrial fatty acid beta-oxidation. This process produces acetyl-CoA for the TCA cycle, which generates NADH and FADH2 (McCammon et al., 2003). Similarly, *PC* is a mitochondrial enzyme that is involved in the energy metabolism, specifically by facilitating the carboxylation of pyruvate, which replenishes oxaloacetate in the Krebs cycle, facilitating the supply of oxaloacetate to the TCA cycle and, thereby, the generation of NADH and FADH2, which are essential for ATP production through OXPHOS (Cappel et al., 2019). *CREB1* is a central regulator of genes that encode proteins involved in mitochondrial biogenesis and function, and it is recruited to the cytochrome c promoter to enhance biogenesis. The study of constitutively active– and dominant–negative *CREB1* variants has demonstrated their crucial role in the control of nuclear-encoded mitochondrial gene expression (Franko et al., 2008). Furthermore, *CACNA1D* encodes Cav1.3, an L-type calcium channel subunit which regulates the calcium influx, including into the mitochondria. An increase in the mitochondrial calcium concentration mediated via Cav1.3 activates Krebs cycle enzymes, thereby enhancing NADH and FADH2 production (Tubert et al., 2023). Finally, *GRIA1* encodes a subunit of the AMPA receptor, a type of ionotropic glutamate receptor which plays a crucial role in synaptic transmission and neuronal excitability (Kim et al., 2021). *GRIA1* interacts with *PGC1α*, a vital regulator of mitochondrial biogenesis. It also regulates PPARα and PPARγ, thereby influencing the glucose and lipid metabolism via the Krebs cycle and ATP production in the neural system (Jadeja et al., 2021).

Genes linked to pathways upstream of mitochondrial function may significantly affect the amino acid concentrations in the fetal thymus, thereby increasing energy generation by the Krebs cycle in the face of nutrient scarcity (Figure 23). Nutrient deprivation hampers the process of mitochondrial fission, reduces mitochondrial biogenesis, and improves survival through the facilitation of substrate sharing (Gomes et al., 2011). The oxidation of amino acids to generate essential metabolites by the Krebs cycle requires specific coenzymes

derived from each type of amino acid. Previous studies have shown that histidine can be metabolized to glutamate by histidine ammonia-lyase and urocanate hydratase (Wang et al., 2013). Glutamate can then be transaminated to form α-ketoglutarate, which is an intermediate in the Krebs cycle (Jochmanova and Pacak, 2016). Serine can be converted to glycine and then to pyruvate through a series of enzymatic reactions (Hara et al., 2021), and pyruvate can be further metabolized to acetyl-CoA, which enters the Krebs cycle (Guda et al., 2007). In addition, alanine can be converted to pyruvate by alanine aminotransferase (Yiew et al., 2023). Furthermore, the hydroxylation of phenylalanine to yield tyrosine is catalyzed by phenylalanine hydroxylase, which requires the cofactor tetrahydrobiopterin and molecular oxygen (Cavalcanti et al., 2014). Moreover, threonine is first converted to α-ketobutyrate by threonine dehydratase. α-ketobutyrate is then converted to propionyl-CoA, which is further metabolized to succinyl-CoA. Succinyl-CoA then enters the Krebs cycle, where it is converted into intermediates used for energy production (Tang et al., 2021).

The cAMP-response element-binding protein (CREB), a key transcription factor, regulates gene expression in response to signals such as hormones, neurotransmitters, and growth factors. CREB-mediated signaling occurs within the mitochondria, as demonstrated by the discovery of a complete cAMP signaling pathway in the mitochondrial matrix (Marquez et al., 2019). Another study showed that CREB links Krebs cycle activity with OXPHOS and thereby regulates critical cellular processes, including glycolysis and immune checkpoint expression, which are essential for immune cell function (Liu et al., 2023). In addition, CREB connects Krebs cycle activity, cellular energy status, and immune cell activation, and, thus, it regulates metabolic pathways and immune responses. CREB activation also induces regulatory T cell expression, thereby affecting proinflammatory responses (Wen et al., 2010). Krebs cycle intermediates such as succinate, citrate, fumarate, and itaconate regulate cellular immunity and immune cell function. These metabolites act as

signaling molecules, thereby modulating macrophage and T cell activity. Succinate and citrate are proinflammatory, and itaconate, α-ketoglutarate, and fumarate have other adverse effects. Specifically, they can affect immune cell epigenetics, thereby influencing polarization and innate immune dynamics (Choi et al., 2021).

In the present study, I identified the hypomethylation of the *CREB1* gene. The interplay between Krebs cycle intermediates, CREB1 signaling, and the regulation of mitochondrial function by calcium appears to fine-tune T cell functionality, thereby influencing the effects of CD4 and CD8 T cells (Figure 23). CD4 and CD8, vital glycoproteins on T cells, directly influence immune responses and form an important link between the cellular metabolism and immune function. CD4 helper T cells initiate primary CD8 T cell activation and guide these effector T cells to antigen-presenting cell (APC) sites through the production of chemokines and also maintain memory cytotoxic T cells (Laidlaw et al., 2016). Both CD4 and CD8 undergo unique developmental programs when activated, generating effector and memory T cell populations. However, the nature of the interaction between CD4 and CD8 cells is controversial. A mouse study demonstrated that low-protein diet-induced IUGR results in high CD4 expression in the fetal thymus (Armengaud et al., 2020). However, high expression of CD4 disrupted the development of thymic epithelial cells, including the CD4 lineages (Yin et al., 2017). CD4 activation is associated with inflammatory responses, which detrimentally affect the coordination of CD8 cells (Duan et al., 2019). In the present study, I identified an upregulation of CD4 in the LOW group, implying that this helper T cell may be involved in the primary immunodeficiency which characterizes nutrient restriction.

It is well established that the methylation of gene promoters is associated with transcriptional repression and the inhibition of gene expression. Conversely, methylation within gene bodies, including intronic regions, can enhance gene expression (de Mendoza et al., 2022). In the present study, I did not identify promoter-related regulation of gene

expression. Instead, I identified complex methylation within gene bodies, including the intronic, intergenic, intron-exon boundary, and 1–5 kb regions. For instance, *GRIA1* was hypermethylated in its intronic and intergenic regions, whereas *SLC25A4* was hypermethylated at the intron–exon boundary, and both of these genes were upregulated. Conversely, *PAK1* displayed hypomethylation in the intronic and intergenic regions, and *SLC49A3* was hypomethylated at the intron-exon boundary, and both of these genes were downregulated. Furthermore, *SLC38A1* was downregulated and hypermethylated at intronic region (Table 17). The KEGG pathway analysis revealed that the Hippo signaling pathway is linked to hyper-DMG, indicating that MNR affects the methylation of gene bodies, which may be responsible for the phenotypic outcomes of MNR identified in the present study. In addition, MNR induced alterations in the DNA methylation, gene expression, and metabolite composition of the fetal thymus. To maintain immune function under these conditions, the expression of genes related to mitochondrial activity, such as *MRPS2* and *SLC25A4*, is critical for the provision of energy with a minimal external nutrient input. Proper functioning of the thymus is essential for correct immune system function, and prolonged CD4 expression under these conditions may result in immune disorders in the affected animals later in life.

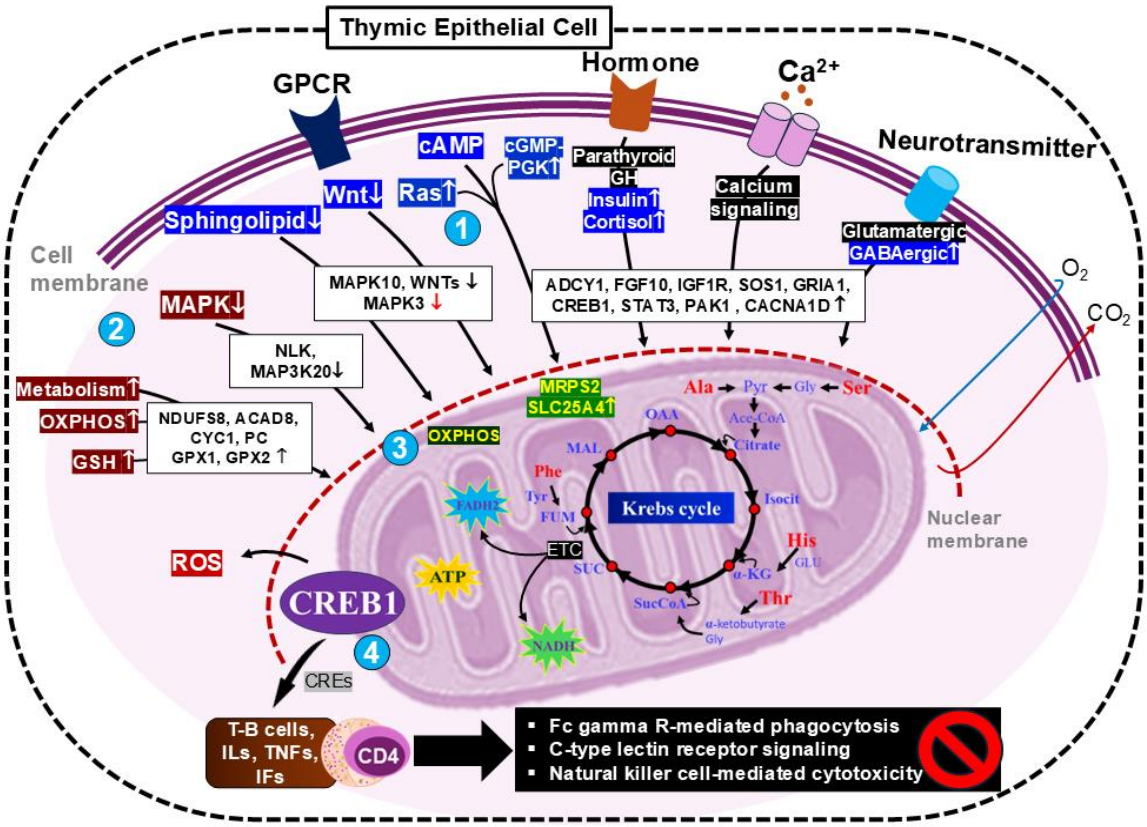

Figure 23. Theoretical framework comprising the pathways associated with the DMGs and DEGs associated with molecular function networks and metabolism in the thymuses of LOW fetuses. (**1**) cAMP, Ras, cGMP–PGK, insulin, cortisol, and GABAergic synapse pathways, which are associated with hypoDMG, and Wnt and sphingolipid signaling pathways, which are associated with hyperDMG. (**2**) Pathways associated with upregulated genes, encompassing metabolic pathways, oxidative phosphorylation (OXPHOS), glutathione (GSH) metabolism, and reactive oxygen species (ROS). (**3**) Reprogramming of the mitochondrial metabolism via OXPHOS may be facilitated by *MRPS2* and *SLC25A4*, with the oxidation of amino acids (His, histidine; Ser, serine; Ala, alanine; Phe, phenylalanine; and Thr, threonine) in the Krebs cycle generating ATP to support immune regulation. (**4**) cAMP-response element-binding protein 1 (CREB1) regulates energy production via mitochondrial OXPHOS and cAMP-response elements (CREs), thereby promoting immune cell development and, in particular, the generation of activated CD4 cells. Prolonged CD4 expression is associated with the suppression of immune pathways, including Fc gamma R-mediated phagocytosis, C-type lectin receptor signaling, and natural killer cell-mediated cytotoxicity. Up and down arrows indicate upregulation/hypomethylation and downregulation/hypermethylation, respectively, and the red arrows represent promoter hypermethylation. Pathways with a black background did not differ between the two groups.

The MNR affects growth characteristics in offspring

Growth represents a coordinated process involving both cell division, leading to the formation of new cells, and cellular enlargement, as existing cells increase in size and undergo specialization towards specific lineages and functions. The growth process is governed by various physiological mechanisms, notably the somatotropic axis, primarily involving GH and IGF-1. These hormones are vital for cell division, expansion, and differentiation, thereby orchestrating overall growth and development (Nijenhuis-Noort et al., 2024). Maternal nutrient perturbation during gestation induces metabolic programming in offspring, impacting long-term growth, physiology, and metabolism, as described by the DOHaD theory (Billah et al., 2022). Early nutrition, growth patterns, immune development, and adipose tissue expansion form a complex system of developmental programming linked to obesity risk. Medical studies suggest that maternal nutrition during critical fetal periods can alter growth, enhancing in utero survival but increasing the risk of postnatal metabolic dysfunctions—a concept known as the "Thrifty Phenotype" hypothesis (Hales and Barker, 2001), which also involves the developmental programming of appetite (Ross and Desai, 2014).

Maternal nutrient deficiency during pregnancy leads to intrauterine growth restriction (IUGR) and low birth weight. This condition often results in postnatal catch-up growth, which is associated with reduced GH mRNA expression and reduced IGF-1 levels (Senna et al., 2015). The phenotype resulting from maternal undernutrition closely resembles GH deficiency, characterized by increased adiposity and lipid abnormalities. In Wistar rats, early nutrient stimulation leads to catch-up growth owing to changes in the expression of genes related to lipid metabolism and immune processes in adipose tissue, contributing to metabolic dysfunction and obesity (Lizarraga-Mollinedo et al., 2022). Furthermore, several studies have revealed that postnatal nutrition can induce epigenetic modifications, such as

change in DNA methylation, facilitating catch-up growth in neonates experiencing IUGR. In murine models, the pharmacological activation of PPARα during the suckling period in IUGR offspring has been shown to further decrease the methylation of *FGF21*, which is associated with an increased propensity for obesity (Yuan et al., 2018). Additionally, treatment with recombinant FGF21 protein has been shown to rescue impairments in fetal thymus organ culture of *FGF21*-knockout mice (Nakayama et al., 2017). Methionine is a precursor to SAM, which influences DNA methylation and gene expression in the liver. A study on maternal methionine supplementation in beef cattle showed lasting epigenetic changes in genes related to muscle contraction, mitochondrial function, ROS homeostasis, and growth signaling, with some effects enduring in offspring up to 200 days old (Amorín et al., 2023). *FGF10* and *IGF1R* are key growth regulators that showed hypomethylation without expression changes in the LOW fetal thymus. Under MNR, the fetus may activate compensatory mechanisms to maintain homeostasis and preserve growth pathways despite epigenetic changes.

Several studies have intriguingly demonstrated that CD4 expression not only influences immune function but also correlates with body growth, fat metabolism, and obesity. In murine models exposed to high-fat diets, there is significant activation of $CD4^+$ adipose tissue-resident T cells (ART), primarily of the Th1 subset. These cells infiltrate adipose tissue and initiate inflammatory responses, which exacerbate insulin resistance and contribute to the development of metabolic syndrome (Deng et al., 2017). Moreover, $CD4^+$ T cells have been identified as markers of metabolic restoration and facilitators of obesity in mice, as their depletion resulted in the elimination of obesity memory (Zou et al., 2018). In the present study, MNR was associated with increased expression of $CD4^+$ in the fetal thymus, a type of adipose tissue, which should be clarified by further study.

In beef cattle production, adipose cells and intramuscular fat (marbling) significantly influence economic value. Marbling, characterized by white streaks of intramuscular fat within muscle fibers, is a major determinant of beef quality grading. Higher marbling levels are associated with improved flavor, juiciness, and tenderness, enhancing palatability and desirability (Hausman et al., 2018). Consumers are willing to pay premiums for well-marbled beef due to its superior eating qualities, such as tenderness, texture, and taste. This high-value product may be related to metabolic regulation during critical developmental windows in ruminants. Studies in sheep have shown that MNR during gestation causes IUGR and low birth weight. Excess nutrition postnatally leads to catch-up growth characterized by rapid weight gain and increased adiposity, compensating for stunted fetal growth. This process involves the programming of stem cell populations, such as satellite and mesenchymal stem cells (Hoffman et al., 2017). Poor maternal nutrition alters gene expression, metabolic pathways, and epigenetic modifications, impairing stem cell function and favoring adipogenesis over myogenesis postnatally. Interestingly, early postnatal high nutrition (ECON), implemented through the administration of a high-nutrient milk replacer and a high-concentrate diet prior to the initiation of roughage feeding at 11 months of age, significantly enhanced body growth and increased IGF-1 secretion during the growing phase before they declined to lower levels at slaughter age. Consequently, this nutritional strategy resulted in superior beef quality in comparison to the traditional milk replacer and roughage feeding regimen employed in cohost Wagyu steers (Khounsaknalath et al., 2021). In the present study, all calves were exposed to the same high-nutrient milk replacer and calf starter after calving. The calves from the LOW group were female, while those from the CON group were male, resulting in a significant birth weight disparity between the two groups (approximately 28%). Typically, birth weight differences between male and female calves in dairy cattle do not exceed 10% (Kertz et al., 1997). The observed birth weight phenotype

in this study likely reflects the combined effects of IUGR and neonatal calf sex differences. Despite the sustained body weight differences between the two groups from birth to 5 months of age, with no observable changes in GH and IGF-1 levels in LOW offspring from 2 months onwards, no discernible differences in body weight ratios were evident. This finding emphasizes the significance of metabolic programming on the physiological development and growth of neonatal calves. This study represents the first examination of MNR during gestation and its consequent sex-based disparities in calves. Considering the significant value attributed to Wagyu cattle, further investigation with a consistent calf sex is warranted, along with additional research on postnatal immune system regulation.

In conclusion, MNR is linked to IUGR, which triggers epigenetic modifications in the fetal thymus, marked by distinct methylation patterns. Specifically, genes associated with the Hippo signaling pathway exhibit hypermethylation, while those involved in the Ras signaling pathway show hypomethylation. These epigenetic changes result in altered gene expression related to metabolic flexibility, thereby affecting stress responses and immune functions, particularly in $CD4^+$ helper T cells. The intricate relationship between DNA methylation and expression of the *GRIA1*, *CACNA1D*, and *SCL25A4* genes is notably linked to the cAMP signaling pathway, which plays a crucial role in cellular and immune system regulation within the thymus. Additionally, MNR disrupts physiological regulation, leading to reduced secretion of GH and IGF-1. These findings pave the way for further research into the complex effects of fetal and neonatal programming, including epigenetic modifications, physiological function, and immune system regulation, on postnatal growth. This research has the potential to lead to advanced strategies for applying these insights to premium-quality beef production from Wagyu cattle.

Acknowledgment

I extend my deepest gratitude to all those who have guided and supported me throughout the journey toward realizing my aspirations. I have witnessed the profound kindness and strength of those around me, akin to a flowering tree that illuminates the path and offers enduring support. I am sincerely appreciative of your unwavering encouragement and generosity.

This dissertation is part of a significant collaborative project on human resource development, made possible through the steadfast cooperation between the governments of Laos and Japan, the support of the Japanese Human Resource Development Scholarship (JDS) program, and the facilitation provided by the Japan International Cooperation Center (JICE).

I am particularly grateful to Dr. Yoichiro Hoshino and Dr. Yutaka Suzuki of the Department of Biosphere Science at Hokkaido University, and Dr. Susumu Muroya of the Department of Animal Science, Kagoshima University, for their valuable help throughout my period of research. My thanks also extend to the staff at the Kuju Agricultural Research Center of Kyushu University and the personnel at the Experimental Farm of Kagoshima University for their meticulous care of animals and technical support during my experiments. I also deeply appreciate the assistance of Mr. Daichi Nishino and Mr. Taketo Haginouchi, Ph.D. students, as well as other labmates and students from the Agro-ecosystem Science Course at the Biological Production Experiment Farm for their generous support throughout my research journey.

Most importantly, I wish to express my profound gratitude to my supervisor, Dr. Takafumi Gotoh of the Laboratory of Meat Science at Hokkaido University. His accommodating nature regarding my study and living conditions in Japan, along with his

sympathetic inspiration and honest support, has been instrumental to the success of my research. I consider myself truly fortunate to have had him as my supervisor. I also extend my sincere thanks to the President of Hokkaido University and the Dean of the Graduate School of Environmental Science at Hokkaido University for their support and facilitation, which have been crucial in me achieving this milestone. I also thank Edanz (https://jp.edanz.com/ac) for editing a draft of this manuscript.

Finally, I am honored to dedicate this dissertation to my family and friends, who have been my steadfast support system throughout this entire process. My heartfelt thanks go to my wife, my beloved daughter, and all my family members for their unwavering support and love. Thank you for always believing in me and providing words of encouragement. I am eternally devoted to my late parents, whose blessings have been with me throughout my life.

References cited

Abuelo, A. 2020. Symposium review: Late-gestation maternal factors affecting the health and development of dairy calves. *Journal of Dairy Science*, 103: 3882-3893.

Abul Abbas, M., A.H. Lichtman, and S. Pillai. 2021. Cellular and Molecular Immunology. 10th edition, *Elsevier Health Sciences,* 587 pp.

Akalin, A., M. Kormaksson, S. Li, F.E. Garrett-Bakelman, M.E. Figueroa, A. Melnick, and C.E. Mason. 2012. methylKit: a comprehensive R package for the analysis of genome-wide DNA methylation profiles. *Genome Biology*, 13: 1-9.

Akbar, M., and M. Jahiruddin. 2010. Utilizing indigenous resources in an integrated approach to improving livestock production while conserving the environment. *Improving Livestock Production Using Indigenous Resources and Conserving the Environment*, 1640: 11-24.

Alamri, B.N., K. Shin, V. Chappe, and Y. Anini. 2016. The role of ghrelin in the regulation of glucose homeostasis. *Hormone Molecular Biology and Clinical Investigation*, 26: 3-11.

Alberts, B., A. Johnson, J. Lewis, M. Raff, K. Roberts, and P. Walter. 2002. Helper T cells and lymphocyte activation. *In* Molecular Biology of the Cell. 4th edition. *Garland Science,* 1463 pp.

Ali, D.S., K. Dandurand, and A.A. Khan. 2021. Hypoparathyroidism in pregnancy and lactation: current approach to diagnosis and management. *Journal of Clinical Medicine*, 10: 1378.

Amorín, R., L. Liu, P. Moriel, N. DiLorenzo, P.A. Lancaster, and F. Peñagaricano. 2023. Maternal diet induces persistent DNA methylation changes in the muscle of beef calves. *Scientific Reports*, 13: 1587.

Arif, M., A. Basu, K.M. Wolf, J.K. Park, L. Pommerolle, M. Behee, B.R. Gochuico, and R. Cinar. 2023. An Integrative Multiomics Framework for Identification of Therapeutic Targets in Pulmonary Fibrosis. *Advanced Science*, 10: 2207454-2207474.

Armengaud, J.-B., Z. Dennebouy, D. Labes, C. Fumey, A. Wilson, F. Candotti, C. Yzydorczyk, and U. Simeoni. 2020. Intra-uterine growth restriction induced by maternal low-protein diet causes long-term alterations of thymic structure and function in adult male rat offspring. *British Journal of Nutrition*, 123: 892-900.

Arnold, P.K., and L.W. Finley. 2023. Regulation and function of the mammalian tricarboxylic acid cycle. *Journal of Biological Chemistry*, 299: 1-21.

Asghar, A., Y.M. Syed, and F.A. Nafis. 2012. Polymorphism of Hassall's corpuscles in thymus of human fetuses. *International Journal of Applied and Basic Medical Research*, 2: 7-10.

Asselman, J. 2019. Bioinformatic analysis of methylation patterns using bisulfite sequencing data. *Insect Genomics: Methods and Protocols*, 1858: 157-175.

Banchero, G.E., R.P. Clariget, R. Bencini, D.R. Lindsay, J.T. Milton, and G.B. Martin. 2006. Endocrine and metabolic factors involved in the effect of nutrition on the production of colostrum in female sheep. *Reproduction Nutrition Development*, 46: 447-460.

Banks, K.L., and T.C. McGuire. 1989. Neonatal immunology. *Veterinary Clinical Immunology*, 1: 193-204.

Baroni, C., P. Pesando, and G. Bertoli. 1971. Effects of hormones on development and function of lymphoid tissues: II. Delayed development of immunological capacity in pituitary dwarf mice. *Immunology*, 21: 455-461.

Barrington, G.M., and S.M. Parish. 2001. Bovine neonatal immunology. *Veterinary Clinics of North America: Food Animal Practice*, 17: 463-476.

Bartol, F., A. Wiley, and C. Bagnell. 2008. Epigenetic programming of porcine endometrial function and the lactocrine hypothesis. *Reproduction in Domestic Animals*, 43: 273-279.

Battaglia, F., and G. Meschia. 1978. Principal substrates of fetal metabolism. *Physiological Reviews*, 58: 499-527.

Bayou, E., A. Haile, S. Gizaw, and Y. Mekasha. 2015. Evaluation of non-genetic factors affecting calf growth, reproductive performance and milk yield of traditionally managed Sheko cattle in southwest Ethiopia. *SpringerPlus*, 4: 1-17.

Beam, D., K.J. Stalder, A.J. Heinrichs, and C.D. Dechow. 2015. Association of calf growth and feed intake traits with mature cow milk yield and body weight. *Iowa State University Animal Industry Report*, 12: 1-2.

Bell, A.W. 1995. Regulation of organic nutrient metabolism during transition from late pregnancy to early lactation. *Journal of Animal Science*, 73: 2804-2819.

Beyoğlu, D., P. Huang, D. Skelton-Badlani, C. Zong, Y.V. Popov, and J.R. Idle. 2023. Metabolic Hijacking of Hexose Metabolism to Ascorbate Synthesis Is the Unifying Biochemical Basis of Murine Liver Fibrosis. *Cells*, 12: 485.

Billah, M.M., S. Khatiwada, M.J. Morris, and C.A. Maloney. 2022. Effects of paternal overnutrition and interventions on future generations. *International Journal of Obesity*, 46: 901-917.

Blum, J. 2006. Nutritional physiology of neonatal calves. *Journal of Animal Physiology and Animal Nutrition*, 90: 1-11.

Blum, J.W., and C.R. Baumrucker. 2008. Insulin-like growth factors (IGFs), IGF binding proteins, and other endocrine factors in milk: role in the newborn. *Bioactive Components of Milk*: 397-422.

Bolger, A.M., M. Lohse, and B. Usadel. 2014. Trimmomatic: a flexible trimmer for Illumina sequence data. *Bioinformatics*, 30: 2114-2120.

Borghetti, P., R. Saleri, E. Mocchegiani, A. Corradi, and P. Martelli. 2009. Infection, immunity and the neuroendocrine response. *Veterinary Immunology and Immunopathology*, 130: 141-162.

Bournazos, S., T.T. Wang, and J.V. Ravetch. 2017. The role and function of Fcγ receptors on myeloid cells. *Myeloid Cells in Health and Disease: A Synthesis*, 4: 405-427.

Breier, B. 1999. Regulation of protein and energy metabolism by the somatotropic axis. *Domestic Animal Endocrinology*, 17: 209-218.

Breier, B., P. Gluckman, and J. Bass. 1988. Influence of nutritional status and oestradiol-17β on plasma growth hormone, insulin-like growth factors-I and-II and the response to exogenous growth hormone in young steers. *Journal of Endocrinology*, 118: 243-250.

Bure, I.V., M.V. Nemtsova, and E.B. Kuznetsova. 2022. Histone modifications and non-coding RNAs: mutual epigenetic regulation and role in pathogenesis. *International Journal of Molecular Sciences*, 23: 5801.

Burke, C., and J. Roche. 2007. Effects of pasture feeding during the periparturient period on postpartum anovulation in grazed dairy cows. *Journal of Dairy Science*, 90: 4304-4312.

Busato, A., D. Faissler, U. Küpfer, and J. Blum. 2002. Body condition scores in dairy cows: associations with metabolic and endocrine changes in healthy dairy cows. *Journal of Veterinary Medicine Series A*, 49: 455-460.

Butler, S.T., A. Marr, S.H. Pelton, R. Radcliff, M.C. Lucy, and W. Butler. 2003. Insulin restores GH responsiveness during lactation-induced negative energy balance in dairy cattle: effects on expression of IGF-I and GH receptor 1A. *Journal of Endocrinology*, 176: 205-217.

Cano, R.L.E., and H.D.E. Lopera. 2013. Introduction to T and B lymphocytes. *In* Autoimmunity: from bench to bedside [Internet]. Bogota (Colombia): El Rosario

University Press; 2013 Jul 18. Chapter 5. Available at https://www.ncbi.nlm.nih.gov/books/NBK459471/. Accessed on 15 August 2024.

Cappel, D.A., S. Deja, J.A. Duarte, B. Kucejova, M. Iñigo, J.A. Fletcher, X. Fu, E.D. Berglund, T. Liu, and J.K. Elmquist. 2019. Pyruvate-carboxylase-mediated anaplerosis promotes antioxidant capacity by sustaining TCA cycle and redox metabolism in liver. *Cell Metabolism*, 29: 1291-1305. e1298.

Casas, E., R. Thallman, and L. Cundiff. 2012. Birth and weaning traits in crossbred cattle from Hereford, Angus, Norwegian Red, Swedish Red and White, Wagyu, and Friesian sires. *Journal of Animal Science*, 90: 2916-2920.

Cavalcanti, J.H.F., A.A. Esteves-Ferreira, C.G. Quinhones, I.A. Pereira-Lima, A. Nunes-Nesi, A.R. Fernie, and W.L. Araujo. 2014. Evolution and functional implications of the tricarboxylic acid cycle as revealed by phylogenetic analysis. *Genome Biology and Evolution*, 6: 2830-2848.

Chen, J.C., A.-L. Frankshun, A.A. Wiley, D.J. Miller, K.A. Welch, T.-Y. Ho, F.F. Bartol, and C.A. Bagnell. 2011. Milk-borne lactocrine-acting factors affect gene expression patterns in the developing neonatal porcine uterus. *Reproduction*, 141: 675.

Choi, I., H. Son, and J.-H. Baek. 2021. Tricarboxylic acid (TCA) cycle intermediates: regulators of immune responses. *Life*, 11: 69.

Christiansen, S., M. Guo, and D. Kjelden. 2010. Chemical composition and nutrient profile of low molecular weight fraction of bovine colostrum. *International Dairy Journal*, 20: 630-636.

Ciofani, M., and J.C. Zúñiga-Pflücker. 2007. The thymus as an inductive site for T lymphopoiesis. *Annual Review of Cell and Developmental Biology*, 23: 463-493.

Cockx, L., L. Colen, and J. De Weerdt. 2018. From corn to popcorn? Urbanization and dietary change: Evidence from rural-urban migrants in Tanzania. *World Development*, 110: 140-159.

Cross, J., D. Baczyk, N. Dobric, M. Hemberger, M. Hughes, D. Simmons, H. Yamamoto, and J. Kingdom. 2003. Genes, development and evolution of the placenta. *Placenta*, 24: 123-130.

Curtis, S.K., R.R. Cowden, and J.W. Nagel. 1979. Ultrastructural and histochemical features of the thymus glands of the adult lungless salamander, Plethodon glutinosus (Caudata: Plethodontidae). *Journal of Morphology*, 160: 241-273.

Danijela, K. 2015. Endocrine and metabolic adaptations of calves to extra-uterine life. *Acta Veterinaria*, 65: 297-318.

de Almeida Brasiel, P.G., and S.C.P.D. Luquetti. 2020. Metabolic Programming and Nutrition. *In* New Insights Into Metabolic Syndrome. IntechOpen. Available online at http://dx.doi.org/10.5772/intechopen.92201. Accessed on 15 August 2024.

de Mendoza, A., T.V. Nguyen, E. Ford, D. Poppe, S. Buckberry, J. Pflueger, M.R. Grimmer, S. Stolzenburg, O. Bogdanovic, and A. Oshlack. 2022. Large-scale manipulation of promoter DNA methylation reveals context-specific transcriptional responses and stability. *Genome Biology*, 23: 163.

Deng, T., J. Liu, Y. Deng, L. Minze, X. Xiao, V. Wright, R. Yu, X.C. Li, A. Blaszczak, and S. Bergin. 2017. Adipocyte adaptive immunity mediates diet-induced adipose inflammation and insulin resistance by decreasing adipose Treg cells. *Nature Communications*, 8: 1-11.

Deodati, A., E. Inzaghi, and S. Cianfarani. 2019. Epigenetics and in utero acquired predisposition to metabolic disease. *Frontiers in Genetics,* 10: 1270.

Dervović, D.D., H.C.-Y. Liang, J.L. Cannons, A.R. Elford, M. Mohtashami, P.S. Ohashi, P.L. Schwartzberg, and J.C. Zúñiga-Pflücker. 2013. Cellular and molecular requirements for the selection of in vitro–generated CD8 T cells reveal a role for Notch. *The Journal of Immunology*, 191: 1704-1715.

Dhakal, K., C. Maltecca, J. Cassady, G. Baloche, C. Williams, and S. Washburn. 2013. Calf birth weight, gestation length, calving ease, and neonatal calf mortality in Holstein, Jersey, and crossbred cows in a pasture system. *Journal of Dairy Science*, 96: 690-698.

Domené, S., and H.M. Domene. 2018. Genetic mutations in the GH/IGF axis. *Pediatric Endocrinology Reviews*, 16 (supplement 1): 82-105.

Douphrate, D.I. 2021. Animal agriculture and the one health approach. *Journal of Agromedicine,* 26: 85-87.

Drouin, M., J. Saenz, and E. Chiffoleau. 2020. C-type lectin-like receptors: head or tail in cell death immunity. *Frontiers in Immunology*, 11: 494473.

Duan, J.E., Z.C. Jiang, F. Alqahtani, I. Mandoiu, H. Dong, X. Zheng, S.L. Marjani, J. Chen, and X.C. Tian. 2019. Methylome dynamics of bovine gametes and in vivo early embryos. *Frontiers in Genetics*, 10: 512.

Ducker, G.S., and J.D. Rabinowitz. 2017. One-carbon metabolism in health and disease. *Cell Metabolism*, 25: 27-42.

Duttaroy, A.K. 2023. Influence of maternal diet and environmental factors on fetal development. Vol. 15. Nutrients. 4094.

Elhage, R., M. Kelly, N. Goudin, A. Legrand, C. Patitucci, V. Quellec, T. Wai, A. Hamaï, and S. Ezine. 2024. Mitochondrial dynamics and metabolic regulation control T cell fate in the thymus. *Frontiers in Immunology*, 14: 1270268.

Ellmeier, W., L. Haust, and R. Tschismarov. 2013. Transcriptional control of CD4 and CD8 coreceptor expression during T cell development. *Cellular and Molecular Life Sciences*, 70: 4537-4553.

Etherton, T.D. 2004. Somatotropic function: the somatomedin hypothesis revisited. *Journal of Animal Science*, 82: E239-E244.

Fairchild, P., and J. Austyn. 1995. Developmental changes predispose the fetal thymus to positive selection of CD4+ CD8-T cells. *Immunology*, 85: 292.

Fall, C., and C. Osmond. 2013. Commentary: the developmental origins of health and disease: an appreciation of the life and work of Professor David JP Barker, 1938–2013. *International Journal of Epidemiology*, 42: 1231-1232.

Fandiño, J., L. Toba, L.C. González-Matías, Y. Diz-Chaves, and F. Mallo. 2019. Perinatal undernutrition, metabolic hormones, and lung development. *Nutrients*, 11: 2870.

FAO. 2018. World livestock: transforming the livestock sector through the sustainable development goals. In brief. Food and Agriculture Organization, UN. *Rome. 12 pp. Licence: CC BY-NC-SA 3.0 IGO.*

Figueiredo, M., R. Zilhão, and H. Neves. 2020. Thymus inception: molecular network in the early stages of thymus organogenesis. *International Journal of Molecular Sciences*, 21: 5765.

Ford, S., B. Hess, M. Schwope, M. Nijland, J. Gilbert, K. Vonnahme, W. Means, H. Han, and P. Nathanielsz. 2007. Maternal undernutrition during early to mid-gestation in the ewe results in altered growth, adiposity, and glucose tolerance in male offspring. *Journal of Animal Science*, 85: 1285-1294.

Ford, S.P. 1995. Control of blood flow to the gravid uterus of domestic livestock species. *Journal of Animal Science*, 73: 1852-1860.

Franko, A., S. Mayer, G. Thiel, L. Mercy, T. Arnould, H.-T. Hornig-Do, R.J. Wiesner, and S. Goffart. 2008. CREB-1α is recruited to and mediates upregulation of the cytochrome c promoter during enhanced mitochondrial biogenesis accompanying skeletal muscle differentiation. *Molecular and Cellular Biology*, 28: 2446-2459.

Garcia-Aragón, J., P.E. Lobie, G.E. Muscat, K.S. Gobius, G. Norstedt, and M.J. Waters. 1992. Prenatal expression of the growth hormone (GH) receptor/binding protein in the rat: a role for GH in embryonic and fetal development? *Development*, 114: 869-876.

Gardeitchik, T., M. Mohamed, B. Ruzzenente, D. Karall, S. Guerrero-Castillo, D. Dalloyaux, M. van den Brand, S. van Kraaij, E. van Asbeck, and Z. Assouline. 2018. Bi-allelic mutations in the mitochondrial ribosomal protein MRPS2 cause sensorineural hearing loss, hypoglycemia, and multiple OXPHOS complex deficiencies. *The American Journal of Human Genetics*, 102: 685-695.

Gauthier, S.F., Y. Pouliot, and J.-L. Maubois. 2006. Growth factors from bovine milk and colostrum: composition, extraction and biological activities. *Le Lait*, 86: 99-125.

Ge, S.X., D. Jung, and R. Yao. 2020. ShinyGO: a graphical gene-set enrichment tool for animals and plants. *Bioinformatics*, 36: 2628-2629.

Gemuh, A. 2020. Birth Weight and Growth Rate of Bali Cattle Calf. *Technium: Romanian Journal of Applied Sciences and Technology*, 2: 436-441.

Ghorbani, A., H. Sadri, A. Alizadeh, and R. Bruckmaier. 2012. Performance and metabolic responses of Holstein calves to supplemental chromium in colostrum and milk. *Journal of Dairy Science*, 95: 5760-5769.

Ghosh, S. 2020. Sialic acid and biology of life: An introduction. Sialic acids and sialoglycoconjugates in the biology of life, health and disease. *Epub 2020 Jan 17. PMCID: PMC7153325. Elsevier*: p 1-61.

Gimenez, M.S., L.B. Oliveros, and N.N. Gomez. 2011. Nutritional deficiencies and phospholipid metabolism. *International Journal of Molecular Sciences*, 12: 2408-2433.

Gluckman, P., B. Breier, and S. Davis. 1987. Physiology of the somatotropic axis with particular reference to the ruminant. *Journal of Dairy Science*, 70: 442-466.

Gluckman, P.D., and C.S. Pinal. 2003. Regulation of fetal growth by the somatotrophic axis. *The Journal of Nutrition*, 133: 1741S-1746S.

Godde, C.M., D. Mason-D'Croz, D. Mayberry, P.K. Thornton, and M. Herrero. 2021. Impacts of climate change on the livestock food supply chain; a review of the evidence. *Global Food Security*, 28: 100488.

Gomes, L.C., G.D. Benedetto, and L. Scorrano. 2011. During autophagy mitochondria elongate, are spared from degradation and sustain cell viability. *Nature Cell Biology*, 13: 589-598.

Gotardo, A.T., V.V. Dipe, I.M. Hueza, and S.L. Górniak. 2017. Maternal feed restriction during pregnancy in Wistar rats: Evaluation of offspring using classical and immunoteratology protocols. *Human & Experimental Toxicology*, 36: 603-615.

Gotoh, T. 2014. Potential of the application of epigenetics in animal production. *Animal Production Science*, 55: 145-158.

Gotoh, T., T. Nishimura, K. Kuchida, and H. Mannen. 2018. The Japanese Wagyu beef industry: Current situation and future prospects—A review. *Asian-Australasian Journal of Animal Sciences*, 31: 933.

Gotoh, T., H. Takahashi, T. Nishimura, K. Kuchida, and H. Mannen. 2014. Meat produced by Japanese Black cattle and Wagyu. *Animal Frontiers*, 4: 46-54.

Grandin, T. 2018. Welfare problems in cattle, pigs, and sheep that persist even though scientific research clearly shows how to prevent them. *Animals*, 8: 124.

Guda, P., C. Guda, and S. Subramaniam. 2007. Reconstruction of pathways associated with amino acid metabolism in human mitochondria. *Genomics, Proteomics and Bioinformatics*, 5: 166-176.

Hales, C.N., and D.J. Barker. 2001. The thrifty phenotype hypothesis: Type 2 diabetes. *British Medical Bulletin*, 60: 5-20.

Hammon, H., and J. Blum. 1999. Free amino acids in plasma of neonatal calves are influenced by feeding colostrum for different durations or by feeding only milk replacer1. *Journal of Animal Physiology and Animal Nutrition*, 82: 193-204.

Han, T., S. Björkman, N. Soede, C. Oliviero, and O.T. Peltoniemi. 2020. IGF-1 concentration patterns and their relationship with follicle development after weaning in young sows fed different pre-mating diets. *Animal*, 14: 1493-1501.

Hanley, B., J. Dijane, M. Fewtrell, A. Grynberg, S. Hummel, C. Junien, B. Koletzko, S. Lewis, H. Renz, and M. Symonds. 2010. Metabolic imprinting, programming and epigenetics–a review of present priorities and future opportunities. *British Journal of Nutrition*, 104: S1-S25.

Hara, Y., S. Kume, Y. Kataoka, and N. Watanabe. 2021. Changes in TCA cycle and TCA cycle-related metabolites in plasma upon citric acid administration in rats. *Heliyon*, 7: e08501.

Hausman, G.J., W.G. Bergen, T.D. Etherton, and S.B. Smith. 2018. The history of adipocyte and adipose tissue research in meat animals. *Journal of Animal Science*, 96: 473-486.

Hellström, A., D. Ley, I. Hansen-Pupp, B. Hallberg, L.A. Ramenghi, C. Löfqvist, L.E. Smith, and A.-L. Hård. 2016. Role of insulinlike growth factor 1 in fetal development and in the early postnatal life of premature infants. *American Journal of Perinatology*, 33: 1067-1071.

Heppolette, C.A., J.-H. Chen, S.K. Carr, D.B. Palmer, and S.E. Ozanne. 2016. The effects of aging and maternal protein restriction during lactation on thymic involution and peripheral immunosenescence in adult mice. *Oncotarget*, 7: 6398.

Hirahara, K., and T. Nakayama. 2016. CD4+ T-cell subsets in inflammatory diseases: beyond the T h 1/T h 2 paradigm. *International Immunology*, 28: 163-171.

Hoffman, M., S. Reed, S. Pillai, A. Jones, K. McFadden, S. Zinn, and K. Govoni. 2017. Physiology and endocrinology symposium: the effects of poor maternal nutrition during gestation on offspring postnatal growth and metabolism. *Journal of Animal Science*, 95: 2222-2232.

Holeček, M. 2020. Histidine in health and disease: metabolism, physiological importance, and use as a supplement. *Nutrients*, 12: 848.

Hollmann, M., K. Knowlton, and M. Hanigan. 2008. Evaluation of solids, nitrogen, and phosphorus excretion models for lactating dairy cows. *Journal of Dairy Science*, 91: 1245-1257.

Hough, R., F. McCarthy, H. Kent, D. Eversole, and M. Wahlberg. 1990. Influence of nutritional restriction during late gestation on production measures and passive immunity in beef cattle. *Journal of Animal Science*, 68: 2622-2627.

Hu, W., Y. Zhang, X. Sun, T. Zhang, L. Xu, H. Xie, Z. Li, W. Liu, J. Lou, and W. Chen. 2019. FcγRIIB-I232T polymorphic change allosterically suppresses ligand binding. *Elife*, 8: e46689.

Iborra, S., M. Soto, L. Stark-Aroeira, E. Castellano, B. Alarcón, C. Alonso, E. Santos, and E. Fernández-Malavé. 2011. H-ras and N-ras are dispensable for T-cell development and activation but critical for protective Th1 immunity. *Blood, The Journal of the American Society of Hematology*, 117: 5102-5111.

Ighodaro, O., and O. Akinloye. 2018. First line defence antioxidants-superoxide dismutase (SOD), catalase (CAT) and glutathione peroxidase (GPX): Their fundamental role in the entire antioxidant defence grid. *Alexandria Journal of Medicine*, 54: 287-293.

Imakawa, K., R. Bai, H. Fujiwara, and K. Kusama. 2016. Conceptus implantation and placentation: molecules related to epithelial–mesenchymal transition, lymphocyte homing, endogenous retroviruses, and exosomes. *Reproductive Medicine and Biology*, 15: 1-11.

Jadeja, R.N., P.M. Martin, and W. Chen. 2021. Mitochondrial oxidative stress and energy metabolism: impact on aging and longevity. *Oxidative Medicine and Cellular Longevity*, 2021: 1-3.

Janeway Jr, C.A. 1997. Immunobiology the immune system in health and disease. *New York: Garland Pub. Artes Medicas*, 2: 54.

Jia, J., I. Ahmed, L. Liu, Y. Liu, Z. Xu, X. Duan, Q. Li, T. Dou, D. Gu, and H. Rong. 2018. Selection for growth rate and body size have altered the expression profiles of somatotropic axis genes in chickens. *PloS One*, 13: e0195378.

Jochmanova, I., and K. Pacak. 2016. Pheochromocytoma: the first metabolic endocrine cancer. *Clinical Cancer Research*, 22: 5001-5011.

Johnston, C.S., C.S. Day, and P.D. Swan. 2002. Postprandial thermogenesis is increased 100% on a high-protein, low-fat diet versus a high-carbohydrate, low-fat diet in healthy, young women. *Journal of the American College of Nutrition*, 21: 55-61.

Jun, J.E., I. Rubio, and J.P. Roose. 2013. Regulation of ras exchange factors and cellular localization of ras activation by lipid messengers in T cells. *Frontiers in Immunology*, 4: 57883.

Kato, A., A. Takaori-Kondo, N. Minato, and Y. Hamazaki. 2018. CXCR3high CD8+ T cells with naïve phenotype and high capacity for IFN-γ production are generated during homeostatic T-cell proliferation. *European Journal of Immunology*, 48: 1663-1678.

Kertz, A., and H. Chester-Jones. 2004. Invited review: Guidelines for measuring and reporting calf and heifer experimental data. *Journal of Dairy Science*, 87: 3577-3580.

Kertz, A., L. Reutzel, B. Barton, and R. Ely. 1997. Body weight, body condition score, and wither height of prepartum Holstein cows and birth weight and sex of calves by parity: A database and summary. *Journal of Dairy Science*, 80: 525-529.

Khounsaknalath, S., K. Etoh, K. Sakuma, K. Saito, A. Saito, T. Abe, F. Ebara, T. Sugiyama, E. Kobayashi, and T. Gotoh. 2021. Effects of early high nutrition related to metabolic imprinting events on growth, carcass characteristics, and meat quality of grass-fed Wagyu (Japanese Black cattle). *Journal of Animal Science*, 99: skab123.

Kim, J.-E., D.-S. Lee, H. Park, T.-H. Kim, and T.-C. Kang. 2021. Inhibition of AKT/GSK3β/CREB pathway improves the responsiveness to AMPA receptor antagonists by regulating GRIA1 surface expression in chronic epilepsy rats. *Biomedicines*, 9: 425.

Kim, J.W. 2014. Modulation of the somatotropic axis in periparturient dairy cows. *Asian-Australasian Journal of Animal Sciences*, 27: 147.

Knapek, K.J., H.M. Georges, H. Van Campen, J.V. Bishop, H. Bielefeldt-Ohmann, N.P. Smirnova, and T.R. Hansen. 2020. Fetal lymphoid organ immune responses to transient and persistent infection with bovine viral diarrhea virus. *Viruses*, 12: 816.

Koopman, W.J., F. Distelmaier, J.A. Smeitink, and P.H. Willems. 2013. OXPHOS mutations and neurodegeneration. *The EMBO Journal*, 32: 9-29.

Kopchick, J.J., E.O. List, B. Kelder, E.S. Gosney, and D.E. Berryman. 2014. Evaluation of growth hormone (GH) action in mice: discovery of GH receptor antagonists and clinical indications. *Molecular and Cellular Endocrinology*, 386: 34-45.

Kwon, H., S.P. Ford, F.W. Bazer, T.E. Spencer, P.W. Nathanielsz, M.J. Nijland, B.W. Hess, and G. Wu. 2004. Maternal nutrient restriction reduces concentrations of amino acids and polyamines in ovine maternal and fetal plasma and fetal fluids. *Biology of Reproduction*, 71: 901-908.

Laarman, A., A. Ruiz-Sanchez, T. Sugino, L. Guan, and M. Oba. 2012. Effects of feeding a calf starter on molecular adaptations in the ruminal epithelium and liver of Holstein dairy calves. *Journal of Dairy Science*, 95: 2585-2594.

Laidlaw, B.J., J.E. Craft, and S.M. Kaech. 2016. The multifaceted role of CD4+ T cells in CD8+ T cell memory. *Nature Reviews Immunology*, 16: 102-111.

Lan, X., E. Cretney, J. Kropp, K. Khateeb, M. Berg, F. Peñagaricano, R. Magness, A. Radunz, and H. Khatib. 2013. Maternal diet during pregnancy induces gene expression and DNA methylation changes in fetal tissues in sheep. *Frontiers in Genetics,* 4: 49.

Leach, J.L., D.D. Sedmak, J.M. Osborne, B. Rahill, M.D. Lairmore, and C.L. Anderson. 1996. Isolation from human placenta of the IgG transporter, FcRn, and localization to the syncytiotrophoblast: implications for maternal-fetal antibody transport. *Journal of Immunology (Baltimore, Md.: 1950)*, 157: 3317-3322.

Li, A., and R.F. Barber. 2019. Multiple testing with the structure-adaptive Benjamini–Hochberg algorithm. *Journal of the Royal Statistical Society Series B: Statistical Methodology*, 81: 45-74.

Li, H., B. Handsaker, A. Wysoker, T. Fennell, J. Ruan, N. Homer, G. Marth, G. Abecasis, R. Durbin, and G.P.D.P. Subgroup. 2009. The sequence alignment/map format and SAMtools. *Bioinformatics*, 25: 2078-2079.

Li, N., N. Lu, and C. Xie. 2019. The Hippo and Wnt signalling pathways: crosstalk during neoplastic progression in gastrointestinal tissue. *The FEBS Journal*, 286: 3745-3756.

Liao, S., M.H. Vickers, J.L. Stanley, A.P. Ponnampalam, P.N. Baker, and J.K. Perry. 2016. The placental variant of human growth hormone reduces maternal insulin sensitivity in a dose-dependent manner in C57BL/6J mice. *Endocrinology*, 157: 1175-1186.

Littell, R.C., P. Henry, and C.B. Ammerman. 1998. Statistical analysis of repeated measures data using SAS procedures. *Journal of Animal Science*, 76: 1216-1231.

Liu, N., M. Yan, Q. Tao, J. Wu, J. Chen, X. Chen, and C. Peng. 2023. Inhibition of TCA cycle improves the anti-PD-1 immunotherapy efficacy in melanoma cells via ATF3-

mediated PD-L1 expression and glycolysis. *Journal for Immunotherapy of Cancer*, 11: e007146.

Liu, Y., S. He, Y. Zhang, W. Xia, M. Li, C. Zhang, and F. Gao. 2015. Effects of Intrauterine Growth Restriction During Late Pregnancy on the Development of the Ovine Fetal Thymus and the T-Lymphocyte Subpopulation. *American Journal of Reproductive Immunology*, 74: 26-37.

Livak, K.J., and T.D. Schmittgen. 2001. Analysis of relative gene expression data using real-time quantitative PCR and the 2− ΔΔCT method. *Methods*, 25: 402-408.

Lizarraga-Mollinedo, E., G. Carreras-Badosa, S. Xargay-Torrent, X. Remesar, B. Mas-Pares, A. Prats-Puig, F. de Zegher, L. Ibáñez, A. López-Bermejo, and J. Bassols. 2022. Catch-up growth in juvenile rats, fat expansion, and dysregulation of visceral adipose tissue. *Pediatric Research*, 91: 107-115.

Long, N., R. Collier, and J. Smith. 2012. Comparison of 2 methods of assessing calf birth weights in dairy calves. *Journal of Dairy Science*, 95: 7206-7209.

Lorincz, M.C., D.R. Dickerson, M. Schmitt, and M. Groudine. 2004. Intragenic DNA methylation alters chromatin structure and elongation efficiency in mammalian cells. *Nature Structural & Molecular Biology*, 11: 1068-1075.

Love, M.I., W. Huber, and S. Anders. 2014. Moderated estimation of fold change and dispersion for RNA-seq data with DESeq2. *Genome Biology*, 15: 1-21.

Lucy, M., G. Verkerk, B. Whyte, K. Macdonald, L. Burton, R. Cursons, J. Roche, and C. Holmes. 2009. Somatotropic axis components and nutrient partitioning in genetically diverse dairy cows managed under different feed allowances in a pasture system. *Journal of Dairy Science*, 92: 526-539.

Luque, R.M., M.D. Gahete, R.J. Valentine, and R.D. Kineman. 2006. Examination of the direct effects of metabolic factors on somatotrope function in a non-human primate model, Papio anubis. *Journal of Molecular Endocrinology*, 37: 25-38.

Lutes, L.K., Z. Steier, L.L. McIntyre, S. Pandey, J. Kaminski, A.R. Hoover, S. Ariotti, A. Streets, N. Yosef, and E.A. Robey. 2021. T cell self-reactivity during thymic development dictates the timing of positive selection. *Elife*, 10: e65435.

Manna, P.R., Z.C. Gray, and P.H. Reddy. 2022. Healthy immunity on preventive medicine for combating COVID-19. *Nutrients*, 14: 1004.

Marquez, S., J.J. Fernández, C. Mancebo, C. Herrero-Sanchez, S. Alonso, T.A. Sandoval, M.R. Prados, J.R. Cubillos-Ruiz, O. Montero, and N. Fernandez. 2019. Tricarboxylic

acid cycle activity and remodeling of glycerophosphocholine lipids support cytokine induction in response to fungal patterns. *Cell Reports*, 27: 525-536. e524.

Marshall, J.S., R. Warrington, W. Watson, and H.L. Kim. 2018. An introduction to immunology and immunopathology. *Allergy, Asthma & Clinical Immunology*, 14: 1-10.

Martínez-Reyes, I., and N.S. Chandel. 2020. Mitochondrial TCA cycle metabolites control physiology and disease. *Nature Communications*, 11: 102.

McCammon, M.T., C.B. Epstein, B. Przybyla-Zawislak, L. McAlister-Henn, and R.A. Butow. 2003. Global transcription analysis of Krebs tricarboxylic acid cycle mutants reveals an alternating pattern of gene expression and effects on hypoxic and oxidative genes. *Molecular Biology of the Cell*, 14: 958-972.

McMahon, C., R. Radcliff, K. Lookingland, and H. Tucker. 2001. Neuroregulation of growth hormone secretion in domestic animals. *Domestic Animal Endocrinology*, 20: 65-87.

Medina, K.L. 2016. Overview of the immune system. *In* Handbook of clinical neurology. *Elsevier,* 133: 61-76.

Meikle, A., M. Kulcsar, Y. Chilliard, H. Febel, C. Delavaud, D. Cavestany, and P. Chilibroste. 2004. Effects of parity and body condition at parturition on endocrine and reproductive parameters of the cow. *Reproduction*, 127: 727-737.

Mejia-Naranjo, W., S. Yakar, R. Bernal, D. LeRoith, and M. Sanchez-Gomez. 2003. Regulation of the splenic somatotropic axis by dietary protein and insulin-like growth factor-I in the rat. *Growth Hormone & IGF Research*, 13: 254-263.

Miri, S., J. Yeo, S. Abubaker, and R. Hammami. 2023. Neuromicrobiology, an emerging neurometabolic facet of the gut microbiome? *Frontiers in Microbiology*, 14: 1098412.

Mirzaei, H.R., H. Mirzaei, S.Y. Lee, J. Hadjati, and B.G. Till. 2016. Prospects for chimeric antigen receptor (CAR) γδ T cells: A potential game changer for adoptive T cell cancer immunotherapy. *Cancer Letters*, 380: 413-423.

Mitra, S., A. Bhattacharya, and S. Roy. 2019. The history of livestock farming and future perspective. *United States: Biotechnological Advances for Precision Feeding. Available online at https://www.researchgate.net/publication/347513829. Accessed on 20 August 2024*.

Mocchegiani, E., L. Santarelli, L. Costarelli, C. Cipriano, E. Muti, R. Giacconi, and M. Malavolta. 2006. Plasticity of neuroendocrine–thymus interactions during ontogeny and ageing: role of zinc and arginine. *Ageing Research Reviews*, 5: 281-309.

Moen, E.L., C.J. Mariani, H. Zullow, M. Jeff-Eke, E. Litwin, J.N. Nikitas, and L.A. Godley. 2015. New themes in the biological functions of 5-methylcytosine and 5-hydroxymethylcytosine. *Immunological Reviews*, 263: 36-49.

Mogi, K., T. Yonezawa, D.-S. Chen, J.-Y. Li, M. Suzuki, K. Yamanouchi, T. Sawasaki, and M. Nishihara. 2004. Relationship between growth hormone (GH) pulses in the peripheral circulation and GH-releasing hormone and somatostatin profiles in the cerebrospinal fluid of goats. *Journal of Veterinary Medical Science*, 66: 1071-1078.

Mohammed, A.H., A. Al-Saffar, and K. Allehibi. 2022. The relation between insulin resistance and both growth hormone and insulin-like growth factor (IGF-1) levels in a sample of Iraqi patients with type 2 diabetes. *In* Endocrine Abstracts. Vol. 81. *Bioscientifica*. 107.

Mohebbi-Fani, M., A. Omidi, A. Mirzaei, S. Nazifi, and K. Nowroozi. 2019. A field study on glucose, non-esterified fatty acids, beta-hydroxybutyrate and thyroid hormones in dairy cows during the breeding period in Fars province, Iran. *Iranian Journal of Veterinary Research*, 20: 55.

Mohsen, A.H.A., S. Sallam, M.M. Ramzy, and E.K. Hamed. 2016. Investigating the Relationship between Insulin-like Growth Factor-1 (IGF-1) in diabetic mother's breast milk and the blood serum of their babies. *Electronic Physician*, 8: 2546.

Moon, R., N. Harvey, S. Robinson, G. Ntani, J. Davies, H. Inskip, K. Godfrey, E. Dennison, P. Calder, and C. Cooper. 2013. Maternal plasma polyunsaturated fatty acid status in late pregnancy is associated with offspring body composition in childhood. *The Journal of Clinical Endocrinology & Metabolism*, 98: 299-307.

Moore, L.D., T. Le, and G. Fan. 2013. DNA methylation and its basic function. *Neuropsychopharmacology*, 38: 23-38.

Morimoto, R., J. Swann, A. Nusser, I. Trancoso, M. Schorpp, and T. Boehm. 2021. Evolution of thymopoietic microenvironments. *Open Biology*, 11: 200383.

Morton, S.U., and D. Brodsky. 2016. Fetal physiology and the transition to extrauterine life. *Clinics in Perinatology*, 43: 395-407.

Moya, I.M., and G. Halder. 2019. Hippo–YAP/TAZ signalling in organ regeneration and regenerative medicine. *Nature Reviews Molecular Cell Biology*, 20: 211-226.

Mullen, M.P., D.P. Berry, D.J. Howard, M.G. Diskin, C.O. Lynch, L. Giblin, D.A. Kenny, D.A. Magee, K.G. Meade, and S.M. Waters. 2011. Single nucleotide polymorphisms in the insulin-like growth factor 1 (IGF-1) gene are associated with performance in Holstein-Friesian dairy cattle. *Frontiers in Genetics*, 2: 3.

Muroya, S., K. Otomaru, K. Oshima, I. Oshima, K. Ojima, and T. Gotoh. 2023. DNA Methylation of Genes Participating in Hepatic Metabolisms and Function in Fetal Calf Liver Is Altered by Maternal Undernutrition during Gestation. *International Journal of Molecular Sciences*, 24: 10682.

Muroya, S., Y. Zhang, A. Kinoshita, K. Otomaru, K. Oshima, Y. Gotoh, I. Oshima, M. Sano, S. Roh, M. Oe, K. Ojima, and T. Gotoh. 2021. Maternal undernutrition during pregnancy alters amino acid metabolism and gene expression associated with energy metabolism and angiogenesis in fetal calf muscle. *Metabolites*, 11: 582.

Muroya, S., Y. Zhang, K. Otomaru, K. Oshima, I. Oshima, M. Sano, S. Roh, K. Ojima, and T. Gotoh. 2022. Maternal nutrient restriction disrupts gene expression and metabolites associated with urea cycle, steroid synthesis, glucose homeostasis, and glucuronidation in fetal calf liver. *Metabolites*, 12: 203.

Murphy, K., and C. Weaver. 2016. Janeway's immunobiology. Taylor & Francis Group, LLC., An Informa Business. New York, USA. 9th Edition. *Garland science,* 924 pp.

Muscogiuri, G., L. Barrea, D. Laudisio, C. Di Somma, G. Pugliese, C. Salzano, A. Colao, and S. Savastano. 2019. Somatotropic axis and obesity: is there any role for the Mediterranean diet? *Nutrients*, 11: 2228.

Nakayama, Y., Y. Masuda, H. Ohta, T. Tanaka, M. Washida, Y.-i. Nabeshima, A. Miyake, N. Itoh, and M. Konishi. 2017. Fgf21 regulates T-cell development in the neonatal and juvenile thymus. *Scientific Reports*, 7: 330.

NARO. 2008. Japanese feeding standard for beef cattle. National Agrocultural Research Organization. Japan Livestock Industry Association Tokyo, (In Japanese).

Nijenhuis-Noort, E.C., K.A. Berk, S.J. Neggers, and A.J. van der Lely. 2024. The Fascinating Interplay between Growth Hormone, Insulin-Like Growth Factor-1, and Insulin. *Endocrinology and Metabolism*, 39: 83-89.

Nowak, W., R. Mikuła, A. Zachwieja, K. Paczyńska, E. Pecka, K. Drzazga, and P. Ślósarz. 2012. The impact of cow nutrition in the dry period on colostrum quality and immune status of calves. *Polish Journal of Veterinary Sciences*, 15: 77-82.

Oda, S., H. Satoh, T. Sugawara, N. Matsunaga, T. Kuhara, K. Katoh, Y. Shoji, A. Nihei, M. Ohta, and Y. Sasaki. 1989. Insulin-like growth factor-I, GH, insulin and glucagon concentrations in bovine colostrum and in plasma of dairy cows and neonatal calves around parturition. *Comparative Biochemistry and Physiology. A, Comparative Physiology*, 94: 805-808.

Oh, S., X. Liu, S. Tomei, M. Luo, J.P. Skinner, S.P. Berzins, S.H. Naik, D.H. Gray, and M.M. Chong. 2023. Distinct subpopulations of DN1 thymocytes exhibit preferential γδ T lineage potential. *Frontiers in Immunology*, 14: 1106652.

Oka, A., F. Iwaki, E. Iwamoto, and K. Tatsuda. 2007. Effects of growth rate during the early fattening period on growth, carcass characteristics and circulating hormones in the different growth hormone genotypes of Japanese black steers. *Animal Science Journal*, 78: 142-150.

Osburn, B., N. MacLachlan, and T. Terrell. 1982. Ontogeny of the immune system. *Journal of the American Veterinary Medical Association*, 181: 1049-1052.

Osgerby, J., D. Wathes, D. Howard, and T. Gadd. 2002. The effect of maternal undernutrition on ovine fetal growth. *Journal of Endocrinology*, 173: 131-142.

Østrup, E., P. Hyttel, and O. Østrup. 2011. Embryo–maternal communication: signalling before and during placentation in cattle and pig. *Reproduction, Fertility and Development*, 23: 964-975.

Padgett, D.A., and R. Glaser. 2003. How stress influences the immune response. *Trends in Immunology*, 24: 444-448.

Palmer, A.C. 2011. Nutritionally mediated programming of the developing immune system. *Advances in Nutrition*, 2: 377-395.

Paul, S., and G. Lal. 2017. The molecular mechanism of natural killer cells function and its importance in cancer immunotherapy. *Frontiers in Immunology*, 8: 290728.

Peng, L., L. Chen, J. Wan, W. Liu, S. Lou, and Z. Shen. 2023. Single-cell transcriptomic landscape of immunometabolism reveals intervention candidates of ascorbate and aldarate metabolism, fatty-acid degradation and PUFA metabolism of T-cell subsets in healthy controls, psoriasis and psoriatic arthritis. *Frontiers in Immunology*, 14: 1179877.

Pertea, M., D. Kim, G.M. Pertea, J.T. Leek, and S.L. Salzberg. 2016. Transcript-level expression analysis of RNA-seq experiments with HISAT, StringTie and Ballgown. *Nature Protocols*, 11: 1650-1667.

Prabavathy, G. 2014. Histogenesis of human fetal thymus in different gestational age groups. *National Journal of Clinical Anatomy*, 3: 117-121.

Prentki, M., and S.M. Madiraju. 2008. Glycerolipid metabolism and signaling in health and disease. *Endocrine Reviews*, 29: 647-676.

Puche, J.E., and I. Castilla-Cortázar. 2012. Human conditions of insulin-like growth factor-I (IGF-I) deficiency. *Journal of Translational Medicine*, 10: 1-29.

Quilter, C.R., K.M. Harvey, J. Bauer, B.M. Skinner, M. Gomez, M. Shrivastava, A.M. Doel, S. Drammeh, D.B. Dunger, and S.E. Moore. 2021. Identification of methylation changes associated with positive and negative growth deviance in Gambian infants using a targeted methyl sequencing approach of genomic DNA. *FASEB BioAdvances*, 3: 205.

Raboisson, D., P. Trillat, and C. Cahuzac. 2016. Failure of passive immune transfer in calves: A meta-analysis on the consequences and assessment of the economic impact. *PloS One*, 11: e0150452.

Radcliff, R., B. McCormack, B. Crooker, and M. Lucy. 2003. Plasma hormones and expression of growth hormone receptor and insulin-like growth factor-I mRNA in hepatic tissue of periparturient dairy cows. *Journal of Dairy Science*, 86: 3920-3926.

Randunu, R.S., and R.F. Bertolo. 2020. The effects of maternal and postnatal dietary methyl nutrients on epigenetic changes that lead to non-communicable diseases in adulthood. *International Journal of Molecular Sciences*, 21: 3290.

Reddy, K.E., J. Jeong, Y.-C. Baek, Y.K. Oh, M. Kim, K.M. So, M.J. Kim, D.W. Kim, S.K. Park, and H.-J. Lee. 2017. Early weaning of calves after different dietary regimens affects later rumen development, growth, and carcass traits in Hanwoo cattle. *Asian-Australasian Journal of Animal Sciences*, 30: 1425.

Redifer, C.A., L.G. Wichman, A.R. Rathert-Williams, H.C. Freetly, and A.M. Meyer. 2023. Late gestational nutrient restriction in primiparous beef females: nutrient partitioning among the dam, fetus, and colostrum during gestation. *Journal of Animal Science*, 101: skad195.

Rehfeldt, C., G. Kuhn, G. Nürnberg, E. Kanitz, F. Schneider, M. Beyer, K. Nürnberg, and K. Ender. 2001. Effects of exogenous somatotropin during early gestation on maternal performance, fetal growth, and compositional traits in pigs. *Journal of Animal Science*, 79: 1789-1799.

Reis, M.D.d.S., L.P. Veneziani, F.L. Porto, M.P. Lins, D.A. Mendes-da-Cruz, and W. Savino. 2023. Intrathymic somatotropic circuitry: consequences upon thymus involution. *Frontiers in Immunology*, 14: 1108630.

Reynolds, C.M., J.K. Perry, and M.H. Vickers. 2017. Manipulation of the growth hormone-insulin-like growth factor (GH-IGF) axis: A treatment strategy to reverse the effects of early life developmental programming. *International Journal of Molecular Sciences*, 18: 1729.

Richard, D.M., M.A. Dawes, C.W. Mathias, A. Acheson, N. Hill-Kapturczak, and D.M. Dougherty. 2009. L-tryptophan: basic metabolic functions, behavioral research and therapeutic indications. *International Journal of Tryptophan Research*, 2: IJTR. S2129.

Robinson, I., E. Gevers, and P. Bennett. 1998. Sex differences in growth hormone secretion and action in the rat. *Growth Hormone & IGF Research*, 8: 39-47.

Roche, J., L. Turner, J. Lee, D. Edmeades, D. Donaghy, K. Macdonald, J. Penno, and D. Berry. 2009. Weather, herbage quality and milk production in pastoral systems. 4. Effects on dairy cattle production. *Animal Production Science*, 49: 222-232.

Roche, J.R., D.P. Berry, and E.S. Kolver. 2006. Holstein-Friesian strain and feed effects on milk production, body weight, and body condition score profiles in grazing dairy cows. *Journal of Dairy Science*, 89: 3532-3543.

Rolink, A.G., S. Massa, G. Balciunaite, and R. Ceredig. 2006. Early lymphocyte development in bone marrow and thymus. *Swiss Medical Weekly*, 136: 679-679.

Romano, R., L. Palamaro, A. Fusco, G. Giardino, V. Gallo, L. Del Vecchio, and C. Pignata. 2013. FOXN1: a master regulator gene of thymic epithelial development program. *Frontiers in Immunology*, 4: 187.

Ross, M.G., and M. Desai. 2014. Developmental programming of appetite/satiety. *Annals of Nutrition and Metabolism*, 64: 36-44.

Rothenberg, E.V., J.E. Moore, and M.A. Yui. 2008. Launching the T-cell-lineage developmental programme. *Nature Reviews Immunology*, 8: 9-21.

Roy, A., A. Tolone, R. Hilhorst, J. Groten, T. Tomar, and F. Paquet-Durand. 2022. Kinase activity profiling identifies putative downstream targets of cGMP/PKG signaling in inherited retinal neurodegeneration. *Cell Death Discovery*, 8: 93.

Sadeghi Shaker, M., M. Rokni, M. Mahmoudi, and E. Farhadi. 2023. Ras family signaling pathway in immunopathogenesis of inflammatory rheumatic diseases. *Frontiers in Immunology*, 14: 1151246.

Sadri, H., R. Bruckmaier, H. Rahmani, G. Ghorbani, I. Morel, and H.A. Van Dorland. 2010. Gene expression of tumour necrosis factor and insulin signalling-related factors in subcutaneous adipose tissue during the dry period and in early lactation in dairy cows. *Journal of Animal Physiology and Animal Nutrition*, 94: e194-e202.

Sano, H., S. Narahara, T. Kondo, A. Takahashi, and Y. Terashima. 1993. Insulin responsiveness to glucose and tissue responsiveness to insulin during lactation in dairy cows. *Domestic Animal Endocrinology*, 10: 191-197.

Sartin, J., R. Kemppainen, K. Cummins, and J. Williams. 1988. Plasma concentrations of metabolic hormones in high and low producing dairy cows. *Journal of Dairy Science*, 71: 650-657.

Sauter, S.N., E. Ontsouka, B. Roffler, Y. Zbinden, C. Philipona, M. Pfaffl, B.H. Breier, J.W. Blum, and H.M. Hammon. 2003. Effects of dexamethasone and colostrum intake on the somatotropic axis in neonatal calves. *American Journal of Physiology-Endocrinology and Metabolism*, 285: E252-E261.

Savino, W., and M. Dardenne. 2000. Neuroendocrine control of thymus physiology. *Endocrine Reviews*, 21: 412-443.

Scacchi, M., A.I. Pincelli, and F. Cavagnini. 2003. Nutritional status in the neuroendocrine control of growth hormone secretion: the model of anorexia nervosa. *Frontiers in Neuroendocrinology*, 24: 200-224.

Schaarschmidt, S., A. Fischer, E. Zuther, and D.K. Hincha. 2020. Evaluation of seven different RNA-seq alignment tools based on experimental data from the model plant Arabidopsis thaliana. *International Journal of Molecular Sciences*, 21: 1720.

Scheffler, J., M. McCann, S. Greiner, H. Jiang, M. Hanigan, G. Bridges, S. Lake, and D. Gerrard. 2014. Early metabolic imprinting events increase marbling scores in fed cattle. *Journal of Animal Science*, 92: 320-324.

Schoenberg, K., R. Ehrhardt, and T. Overton. 2012. Effects of plane of nutrition and feed deprivation on insulin responses in dairy cattle during late gestation. *Journal of Dairy Science*, 95: 670-682.

Schultz, M.D., Y. He, J.W. Whitaker, M. Hariharan, E.A. Mukamel, D. Leung, N. Rajagopal, J.R. Nery, M.A. Urich, and H. Chen. 2015. Human body epigenome maps reveal noncanonical DNA methylation variation. *Nature*, 523: 212-216.

Senna, S.M., J.C. Ferraz Jr, and C.G. Leandro. 2015. Perinatal malnutrition and the protective role of the physical training on the immune system. *Nutrición Hospitalaria*, 32: 967-976.

Shah, K., A. Al-Haidari, J. Sun, and J.U. Kazi. 2021. T cell receptor (TCR) signaling in health and disease. *Signal Transduction and Targeted Therapy*, 6: 412.

Shahoha, M., R. Cohen, Y. Ben-Simon, and U. Ashery. 2022. cAMP-dependent synaptic plasticity at the hippocampal mossy fiber terminal. *Frontiers in Synaptic Neuroscience*, 14: 861215.

Sibuh, B.Z., S. Quazi, H. Panday, R. Parashar, N.K. Jha, R. Mathur, S.K. Jha, P. Taneja, and A.K. Jha. 2023. The emerging role of epigenetics in metabolism and endocrinology. *Biology*, 12: 256.

Smaniotto, S., V. de Mello-Coelho, D.M.S. Villa-Verde, J.-M. Pléau, M.-C. Postel-Vinay, M. Dardenne, and W. Savino. 2005. Growth hormone modulates thymocyte development in vivo through a combined action of laminin and CXC chemokine ligand 12. *Endocrinology*, 146: 3005-3017.

Smith, P.E. 1930. The effect of hypophysectomy upon the involution of the thymus in the rat. *The Anatomical Record*, 47: 119-129.

Soberon, F., E. Raffrenato, R. Everett, and M. Van Amburgh. 2012. Preweaning milk replacer intake and effects on long-term productivity of dairy calves. *Journal of Dairy Science*, 95: 783-793.

Sohlstrom, A., A. Katsman, K. Kind, C. Roberts, P. Owens, J. Robinson, and J. Owens. 1998. Food restriction alters pregnancy-associated changes in IGF and IGFBP in the guinea pig. *American Journal of Physiology-Endocrinology and Metabolism*, 274: E410-E416.

Sokolova, I. 2018. Mitochondrial adaptations to variable environments and their role in animals' stress tolerance. *Integrative and Comparative Biology*, 58: 519-531.

Sugino, T., Y. Hasegawa, Y. Kurose, M. Kojima, K. Kangawa, and Y. Terashima. 2004. Effects of ghrelin on food intake and neuroendocrine function in sheep. *Animal Reproduction Science*, 82: 183-194.

Sun, H., A.-h. Zhang, Q. Song, H. Fang, X.-y. Liu, J. Su, L. Yang, M.-d. Yu, and X.-j. Wang. 2018. Functional metabolomics discover pentose and glucuronate interconversion pathways as promising targets for Yang Huang syndrome treatment with Yinchenhao Tang. *RSC Advances*, 8: 36831-36839.

Swaney, K.F., and R. Li. 2016. Function and regulation of the Arp2/3 complex during cell migration in diverse environments. *Current Opinion in Cell Biology*, 42: 63-72.

Szondy, Z., É. Garabuczi, K. Tóth, B. Kiss, and K. Köröskényi. 2012. Thymocyte death by neglect: contribution of engulfing macrophages. *European Journal of Immunology*, 42: 1662-1667.

Tabilas, C., N.L. Smith, and B.D. Rudd. 2023. Shaping immunity for life: Layered development of CD8+ T cells. *Immunological Reviews*, 315: 108-125.

Takahashi, H., Y. Kurose, Y. Suzuki, M. Kojima, T. Yamaguchi, Y. Yoshida, M. Ogino, K. Hodate, Y. Azuma, and T. Sugino. 2009. Ghrelin differentially modulates the GH

secretory response to GHRH between the fed and fasted states in sheep. *Domestic Animal Endocrinology*, 37: 55-60.

Takahashi, H., A. Matsubara, A. Saito, O. Phomvisith, A. Shiga, H.T. Mai, T. Sugino, C.D. McMahon, T. Etoh, Y. Shiotsuka, R. Fujino, M. Furuse, and T. Gotoh. 2016. Higher intake of milk-replacer pre-weaning enhances post-weaning insulin-like growth factor 1 levels in Japanese black cattle. *Veterinary Science & Technology*, 8: 2.

Takeno, M.A., and R.M.Y. Nomura. 2023. Fetal thymus in growth-restricted fetuses due to placental insufficiency. *Revista da Associação Médica Brasileira*, 69: 136-141.

Takizawa, T., C.L. Anderson, and J.M. Robinson. 2005. A novel FcγR-defined, IgG-containing organelle in placental endothelium. *The Journal of Immunology*, 175: 2331-2339.

Tamboli, R.A., J. Antoun, R.M. Sidani, A. Clements, E.E. Harmata, P. Marks-Shulman, B.D. Gaylinn, B. Williams, R.H. Clements, and V.L. Albaugh. 2017. Metabolic responses to exogenous ghrelin in obesity and early after R oux-en-Y gastric bypass in humans. *Diabetes, Obesity and Metabolism*, 19: 1267-1275.

Tan, C., Z. Huang, W. Xiong, H. Ye, J. Deng, and Y. Yin. 2022. A review of the amino acid metabolism in placental function response to fetal loss and low birth weight in pigs. *Journal of Animal Science and Biotechnology*, 13: 28.

Tang, D., M. Chen, X. Huang, G. Zhang, L. Zeng, G. Zhang, S. Wu, and Y. Wang. 2023. SRplot: A free online platform for data visualization and graphing. *PLoS One*, 18: e0294236.

Tang, Q., P. Tan, N. Ma, and X. Ma. 2021. Physiological functions of threonine in animals: beyond nutrition metabolism. *Nutrients*, 13: 2592.

Tekola-Ayele, F., X. Zeng, M. Ouidir, T. Workalemahu, C. Zhang, F. Delahaye, and R. Wapner. 2020. DNA methylation loci in placenta associated with birthweight and expression of genes relevant for early development and adult diseases. *Clinical Epigenetics*, 12: 1-14.

Thapa, P., and D.L. Farber. 2019. The role of the thymus in the immune response. *Thoracic Surgery Clinics*, 29: 123-131.

Thompson, K., H. Majd, C. Dallabona, K. Reinson, M.S. King, C.L. Alston, L. He, T. Lodi, S.A. Jones, and A. Fattal-Valevski. 2016. Recurrent de novo dominant mutations in SLC25A4 cause severe early-onset mitochondrial disease and loss of mitochondrial DNA copy number. *The American Journal of Human Genetics*, 99: 860-876.

Thornton, P.K. 2010. Livestock production: recent trends, future prospects. *Philosophical Transactions of the Royal Society B: Biological Sciences*, 365: 2853-2867.

Tian, S., J. Feng, Y. Cao, S. Shen, Y. Cai, D. Yang, R. Yan, L. Wang, H. Zhang, and X. Zhong. 2019. Glycine cleavage system determines the fate of pluripotent stem cells via the regulation of senescence and epigenetic modifications. *Life Science Alliance*, 2: e201900413.

Tiffon, C. 2018. The impact of nutrition and environmental epigenetics on human health and disease. *International Journal of Molecular Sciences*, 19: 3425.

Tortora, G.J., and B.H. Derrickson. 2018. Principles of anatomy and physiology. 15th Edition. *John Wiley & Sons*. 1240 pp.

Trotta, R.J., M.A. Vasquez-Hidalgo, K.A. Vonnahme, and K.C. Swanson. 2020. Effects of nutrient restriction during midgestation to late gestation on maternal and fetal postruminal carbohydrase activities in sheep. *Journal of Animal Science*, 98: skz393.

Tubert, C., E. Zampese, T. Pancani, T. Tkatch, and D.J. Surmeier. 2023. Feed-forward metabotropic signaling by Cav1 $Ca2^{+}$ channels supports pacemaking in pedunculo-pontine cholinergic neurons. *Neurobiology of Disease*, 188: 106328.

Tudor, G., and P. O'rourke. 1980. The effect of pre-and post-natal nutrition on the growth of beef cattle. 2. The effect of severe restriction in early post-natal life on growth and feed efficiency during recovery. *Australian Journal of Agricultural Research*, 31: 179-189.

Tuersunjiang, N., J.F. Odhiambo, D.R. Shasa, A.M. Smith, P.W. Nathanielsz, and S.P. Ford. 2017. Maternal obesity programs reduced leptin signaling in the pituitary and altered GH/IGF1 axis function leading to increased adiposity in adult sheep offspring. *PloS One*, 12: e0181795.

Turvey, S.E., and D.H. Broide. 2010. Innate immunity. *Journal of Allergy and Clinical Immunology*, 125: S24-S32.

Valadão, L., H.M. da Silva, and F.M. da Silva. 2018. Bovine embryonic development to implantation. *In* Embryology-Theory and Practice. *IntechOpen*. Available online at https://www.intechopen.com/chapters/64133. Accessed on 15 August 2024.

Valdivia-Silva, J., J. Medina-Tamayo, and E.A. Garcia-Zepeda. 2015. Chemokine-derived peptides: novel antimicrobial and antineoplasic agents. *International Journal of Molecular Sciences*, 16: 12958-12985.

Valiente, S.L., A.M. Rodriguez, N.M. Long, I.M. Lacau-Mengido, S. Maresca, and D. Pacheco. 2021. The degree of maternal nutrient restriction during late gestation

influences the growth and endocrine profiles of offspring from beef cows. *Animal Production Science*, 62: 163-172.

Vargas-Mendoza, N., M. Angeles-Valencia, Á. Morales-González, E.O. Madrigal-Santillán, M. Morales-Martínez, E. Madrigal-Bujaidar, I. Álvarez-González, J. Gutiérrez-Salinas, C. Esquivel-Chirino, and G. Chamorro-Cevallos. 2021. Oxidative stress, mitochondrial function and adaptation to exercise: new perspectives in nutrition. *Life*, 11: 1269.

Vaughan, O.R., K. Maksym, E. Silva, K. Barentsen, R.V. Anthony, T.L. Brown, S.L. Hillman, R. Spencer, A.L. David, and F.J. Rosario. 2021. Placenta-specific Slc38a2/SNAT2 knockdown causes fetal growth restriction in mice. *Clinical Science*, 135: 2049-2066.

Vincenzi, A., M.I. Goettert, and C.F.V. de Souza. 2021. An evaluation of the effects of probiotics on tumoral necrosis factor (TNF-α) signaling and gene expression. *Cytokine & Growth Factor Reviews*, 57: 27-38.

Volzhenin, K., L. Bittner, and A. Carbone. 2023. SENSE-PPI reconstructs protein-protein interactions of various complexities, within, across, and between species, with sequence-based evolutionary scale modeling and deep learning. *bioRxiv*: 2023-2009.

Vonnahme, K., M. Zhu, P. Borowicz, T. Geary, B. Hess, L. Reynolds, J. Caton, W. Means, and S. Ford. 2007. Effect of early gestational undernutrition on angiogenic factor expression and vascularity in the bovine placentome. *Journal of Animal Science*, 85: 2464-2472.

Vonnahme, K.A., A.R. Tanner, and M.A.V. Hildago. 2018. Effect of maternal diet on placental development, uteroplacental blood flow, and offspring development in beef cattle. *Animal Reproduction*, 15: 912.

Wakitani, S., R. Kawabata, and M. Yasuda. 2022. Insufficiency of CD205-positive cortical thymic epithelial cells in immature Japanese Black cattle with severe thymic abnormalities and poor prognosis. *Veterinary Immunology and Immunopathology*, 245: 110379.

Wallace, J., P. Da Silva, R. Aitken, and M. Cruickshank. 1997. Maternal endocrine status in relation to pregnancy outcome in rapidly growing adolescent sheep. *Journal of Endocrinology*, 155: 359-368.

Wallace, J.M., J.S. Milne, and R.P. Aitken. 2004. Maternal growth hormone treatment from day 35 to 80 of gestation alters nutrient partitioning in favor of uteroplacental growth in the overnourished adolescent sheep. *Biology of Reproduction*, 70: 1277-1285.

Wang, J., M. Sekai, T. Matsui, Y. Fujii, M. Matsumoto, O. Takeuchi, N. Minato, and Y. Hamazaki. 2019. Hassall's corpuscles with cellular-senescence features maintain IFNα production through neutrophils and pDC activation in the thymus. *International Immunology*, 31: 127-139.

Wang, R.Y., W.R. Wilcox, and S.D. Cederbaum. 2013. Amino acid metabolism. *Emery and Rimoin's Essential Medical Genetics*, 372: 1-42.

Wells, H.G., and T.B. Osborne. 1921. Anaphylaxis reactions with purified proteins from milk. *The Journal of Infectious Diseases*, 29: 200-216.

Wells, J.C. 2014. Commentary: paternal and maternal influences on offspring phenotype: the same, only different. *International Journal of Epidemiology*, 43: 772-774.

Wen, A.Y., K.M. Sakamoto, and L.S. Miller. 2010. The role of the transcription factor CREB in immune function. *The Journal of Immunology*, 185: 6413-6419.

Wichman, L.G., C.A. Redifer, and A.M. Meyer. 2023. Maternal nutrient restriction during late gestation reduces vigor and alters blood chemistry and hematology in neonatal beef calves. *Journal of Animal Science*, 101: skad342.

Wilson, D.F. 2017. Oxidative phosphorylation: regulation and role in cellular and tissue metabolism. *The Journal of Physiology*, 595: 7023-7038.

Wood, C.E., and M. Keller-Wood. 2016. The critical importance of the fetal hypothalamus-pituitary-adrenal axis. *F1000Research*, 5: 115.

Woodall, S., B. Breier, B. Johnston, and P. Gluckman. 1996a. A model of intrauterine growth retardation caused by chronic maternal undernutrition in the rat: effects on the somatotrophic axis and postnatal growth. *Journal of Endocrinology*, 150: 231-242.

Woodall, S., B. Johnston, B. Breier, and P. Gluckman. 1996b. Chronic maternal undernutrition in the rat leads to delayed postnatal growth and elevated blood pressure of offspring. *Pediatric Research*, 40: 438-443.

Wu, G., F.W. Bazer, T.A. Cudd, C.J. Meininger, and T.E. Spencer. 2004. Maternal nutrition and fetal development. *The Journal of Nutrition*, 134: 2169-2172.

Xiong, Q.-w., K. Jiang, X.-w. Shen, Z.-r. Ma, X.-m. Yan, H. Xia, and X. Cao. 2024. The requirement of the mitochondrial protein NDUFS8 for angiogenesis. *Cell Death & Disease*, 15: 253.

Xu, X., and Q. Ge. 2014. Maturation and migration of murine CD4 single positive thymocytes and thymic emigrants. *Computational and Structural Biotechnology Journal*, 9: e201403003.

Yiew, N.K., J.H. Vazquez, M.R. Martino, S. Kennon-McGill, J.R. Price, F.D. Allard, E.U. Yee, A.J. Layman, L.P. James, and K.S. McCommis. 2023. Hepatic pyruvate and alanine metabolism are critical and complementary for maintenance of antioxidant capacity and resistance to oxidative insult. *Molecular Metabolism*, 77: 101808.

Yin, C., X.-Y. Pei, H. Shen, Y.-N. Gao, X.-Y. Sun, W. Wang, Q. Ge, and Y. Zhang. 2017. Thymic homing of activated $CD4^+$ T cells induces degeneration of the thymic epithelium through excessive RANK signaling. *Scientific Reports*, 7: 2421.

Yuan, X., K. Tsujimoto, K. Hashimoto, K. Kawahori, N. Hanzawa, M. Hamaguchi, T. Seki, M. Nawa, T. Ehara, and Y. Kitamura. 2018. Epigenetic modulation of *Fgf21* in the perinatal mouse liver ameliorates diet-induced obesity in adulthood. *Nature Communications*, 9: 636.

Yumani, D.F., A.K. Calor, and M.M. van Weissenbruch. 2020. The course of IGF-1 levels and nutrient intake in extremely and very preterm infants during hospitalisation. *Nutrients*, 12: 675.

Yvon, M., D. Levieux, M.-C. Valluy, J.-P. Pélissier, and P.P. Mirand. 1993. Colostrum protein digestion in newborn lambs. *The Journal of Nutrition*, 123: 586-596.

Zhang, L., Y. Wei, S. Yuan, and L. Sun. 2023. Targeting mitochondrial metabolic reprogramming as a potential approach for cancer therapy. *International Journal of Molecular Sciences*, 24: 4954.

Zhang, Y., K. Otomaru, K. Oshima, Y. Goto, I. Oshima, S. Muroya, M. Sano, R. Saneshima, Y. Nagao, A. Kinoshita, Y. Okamura, S. Roh, A. Ohtsuka, and T. Gotoh. 2021. Effects of low and high levels of maternal nutrition consumed for the entirety of gestation on the development of muscle, adipose tissue, bone, and the organs of Wagyu cattle fetuses. *Animal Science Journal*, 92: e13600.

Zou, J., B. Lai, M. Zheng, Q. Chen, S. Jiang, A. Song, Z. Huang, P. Shi, X. Tu, and D. Wang. 2018. CD4+ T cells memorize obesity and promote weight regain. *Cellular & Molecular Immunology*, 15: 630-639.

Zulu, V.C., T. Nakao, and Y. Sawamukai. 2002. Insulin-like growth factor-I as a possible hormonal mediator of nutritional regulation of reproduction in cattle. *Journal of Veterinary Medical Science*, 64: 657-665.